



**Manchester  
Metropolitan  
University**

**Human Mesenchymal Stem Cell Loading as  
a Novel Targeting and Drug Delivery System  
for Stroke.**

**Alexander M Andrews**

**MSc by Research**

**October 2015**

**Human Mesenchymal Stem Cell Loading as  
a Novel Targeting and Drug Delivery System  
for Stroke.**

**Alexander M Andrews**

**A thesis submitted in fulfilment of the  
requirements of the Manchester  
Metropolitan University for the degree of  
MSc (by Research)**

**School of Healthcare Science,  
The Manchester Metropolitan University,  
October 2015**

# Table of Contents

|   |    |
|---|----|
| Title Page .....  | 1  |
| Table of Contents .....   | 2  |
| List of Figures .....   | 5  |
| List of Tables .....  | 6  |
| Abbreviations .....   | 7  |
| Abstract.....   | 9  |
| Declaration.....  | 10 |
| Copyright Statement.....  | 11 |
| Acknowledgements.....   | 12 |
| Chapter 1: Introduction .....   | 13 |
| 1.1 Ischemic Stroke .....   | 13 |
| 1.1.1 Stroke Overview .....   | 13 |
| 1.1.2 Pathophysiology of Ischemic Stroke .....  | 13 |
| 1.2 The Blood-Brain Barrier .....   | 16 |
| 1.3 Inflammatory Response .....   | 17 |
| 1.4 Stroke Prognosis and Therapy .....  | 18 |
| 1.5 Angiogenesis .....  | 18 |
| 1.5.1 Fibroblast Growth Factor 2 .....  | 19 |
| 1.6 Cyclin-dependant Kinases .....  | 19 |
| 1.6.1 Cyclin-dependant Kinase 5.....  | 20 |
| 1.7 Cyclin-dependant Kinase 5 Inhibitory Peptide.....                                       | 21 |
| 1.7.1 The p5 Peptide .....  | 22 |
| 1.8 Limitations of Current Stroke Therapy.....  | 23 |
| 1.9 Stem Cells.....   | 24 |
| 1.9.1 Mesenchymal Stem Cells .....  | 25 |
| 1.10 Migration of Mesenchymal Stem Cells .....  | 26 |
| 1.10.1 Superparamagnetic Iron Oxide Nanoparticles.....                                      | 27 |
| 1.10.2 Superparamagnetic Iron Oxide Nanoparticles as a Novel Magnetic Targeted Therapy..... | 27 |

|  |    |
|--|----|
| 1.11 Summary and Aims .....  | 27 |
| 1.12 Objectives.....   | 28 |
| Chapter 2: Materials and Methods.....  | 29 |
| 2.1 Cell Culture.....  | 29 |
| 2.1.1 Bovine Aortic Endothelial Cell Culture .....                               | 29 |
| 2.1.2 Human Brain Microvascular Endothelial Cell Culture .....                   | 29 |
| 2.1.3 Human Mesenchymal Stem Cell Culture .....                                  | 29 |
| 2.1.4 Cryopreservation of Cells .....  | 30 |
| 2.1.5 Cell Counting .....  | 30 |
| 2.2 Enzyme-Linked Immunosorbent Assay (ELISA).....                               | 30 |
| 2.2.1 FGF-2 Quantitation by ELISA .....  | 30 |
| 2.2.2 Colour-metric Biotin Quantitation by ELISA.....                            | 31 |
| 2.2.3 Fluorescent Biotin Quantitation by ELISA .....                             | 31 |
| 2.3 Immunofluorescence .....   | 32 |
| 2.3.1 Immunofluorescence of the Internalisation of p5 by HMSCs.....              | 32 |
| 2.3.2 Immunofluorescence of the Internalisation of SPIOs by HMSCs and BAECs..... | 32 |
| 2.4 Immunohistochemistry .....   | 33 |
| 2.4.1 Immunohistochemistry of the Internalisation of SPIOs by HMSCs.....         | 33 |
| 2.5 SDS-PAGE and Western Blotting .....  | 33 |
| 2.5.1 Protein extraction .....   | 33 |
| 2.5.2 SDS-PAGE and Western Blot Analysis .....                                   | 34 |
| 2.6 HPLC-MS/MS.....  | 35 |
| 2.6.1 Cell Treatment.....  | 35 |
| 2.6.2 Cartridge Extraction .....   | 35 |
| 2.6.3 HPLC-MS/MS Analysis .....  | 35 |
| 2.7 MACS Cell Sorting.....   | 36 |
| 2.8 Transwell Migration Assay .....  | 36 |
| 2.8.1 Chemotactic Migration .....  | 36 |
| 2.8.2 SPIO Facilitated Cell Migration.....                                       | 36 |

|   |    |
|---|----|
| 2.8.3 Determining Cell Migration.....   | 37 |
| 2.9 Statistical Analysis.....   | 37 |
| Chapter 3: Results.....   | 38 |
| 3.1 Uptake and Release of FGF-2 by HMSCs.....   | 38 |
| 3.2 Uptake and Release of p5 by HMSCs.....  | 39 |
| 3.2.1 ELISA Analysis of the Uptake and Release of p5 by HMSCs.....                        | 39 |
| 3.2.2 Immuno-fluorescent Analysis of p5 Internalisation by HMSCs.....                     | 43 |
| 3.2.3 Analysis of p5 Using HPLC-MS/MS.....  | 47 |
| 3.3 <i>In vitro</i> Activity of p5 in an Experimental Apoptotic Model.....                | 50 |
| 3.3 Cellular internalisation of Superparamagnetic Iron Oxide Nanoparticles.....           | 53 |
| 3.3.1 Internalisation of SPIOs by Bovine Aortic Endothelial Cells.....                    | 53 |
| 3.3.2 Internalisation of Biotin Functionalised SPIOs by Human Mesenchymal Stem Cells..... | 53 |
| 3.3.3 Internalisation of PEG Functionalised SPIOs by Human Mesenchymal Stem Cells.....    | 56 |
| 3.4 HMSC Transwell Migration Assay.....   | 59 |
| 3.4.1 Chemotactic Migration.....  | 59 |
| 3.4.2 Magnetic Facilitated HMSC Transwell Migration.....                                  | 59 |
| Chapter 4: Discussion.....  | 64 |
| 4.1 Uptake and Release of FGF-2 by Human Mesenchymal Stem Cells.....                      | 64 |
| 4.2 Uptake and Release of p5 by Human Mesenchymal Stem Cells.....                         | 65 |
| 4.3 Effects of p5 in Apoptotic Stroke Model.....  | 67 |
| 4.4 Internalisation of SPIOs by Bovine Aortic Endothelial Cells.....                      | 69 |
| 4.5 Internalisation of SPIOs by Human Mesenchymal Stem Cells.....                         | 69 |
| 4.6 Magnetic Facilitated Human Mesenchymal Stem Cell Migration.....                       | 70 |
| 4.6 Future Work.....  | 71 |
| 4.7 Conclusions.....  | 76 |
| References.....   | 78 |
| Appendix 1- HPLC-MS/MS Acquisition Report.....  | 90 |

# List of Figures

|   |    |
|---|----|
| Figure 1: Ischemic Cell Death. ....   | 15 |
| Figure 2: Structure of the blood-brain barrier .....  | 17 |
| Figure 3: Hyperactivation of Cdk5 by cleaved p35 .....  | 21 |
| Figure 4: Cdk5/p25 inhibited by p5. ....  | 23 |
| Figure 5: Cdk5 inhibitory peptides derived from p25.....  | 23 |
| Figure 6: Magnetic facilitated transwell migration .....  | 37 |
| Figure 7: The correlation of FGF-2 concentration and absorbance at 490nm.....   | 38 |
| Figure 8: The uptake, release and residual amount of FGF-2 in HMSCs when treated with varying concentrations (5-20ng) over a period of 48 hours ..... | 39 |
| Figure 9: The correlation of biotin concentration and absorbance at both 494nm and 520nm.....   | 40 |
| Figure 10: Commercial Biotinylated p5 standard curve. ....  | 40 |
| Figure 11: Biotinylated p5 standard curve. The correlation between biotinylated p5 and emission at 520nm .....  | 41 |
| Figure 12: Uptake of p5 by HMSCs. Lysates produced of HMSCs comparing uptake of p5 (2.5µg/ml) in treated and untreated cells over 24 hours .....      | 41 |
| Figure 13: Biotinylated p5 standard curve .....   | 42 |
| Figure 14: Internalisation of p5 by HMSC analysed using fluorescent microscopy.....   | 44 |
| Figure 15: Analysis of timed p5 treatment using fluorescent microscopy.....   | 45 |
| Figure 16: Threshold analysis of p5 uptake by HMSCs .....   | 46 |
| Figure 17: HPLC-MS/MS of p5. ....   | 47 |
| Figure 18: HPLC-MS/MS of p5 extracted from cell media. ....   | 48 |
| Figure 19: Extracted-ion chromatograms of p5 extracted from cell media .....  | 49 |
| Figure 20: Analysis of 30 minute CaCl <sub>2</sub> and p5 treatment of HMSCs by Western blot. ....  | 51 |
| Figure 21: Analysis of 10 minute CaCl <sub>2</sub> and p5 treatment of HMSCs by Western blot. ....  | 52 |
| Figure 22: Internalisation of biotin functionalised SPIOs by BAECs was analysed using fluorescent microscopy. ....                                    | 54 |
| Figure 23: Internalisation of biotin functionalised SPIOs by HMSCs was analysed using fluorescent microscopy. ....                                    | 55 |
| Figure 24: Internalisation of PEG functionalised SPIOs was analysed using bright-field microscopy.....  | 57 |
| Figure 25: Threshold analysis of Prussian blue staining. ....   | 58 |
| Figure 26: Chemotactic migration of 5x10 <sup>5</sup> HMSCs through PET-membrane.. ....   | 60 |
| Figure 27: Magnetic facilitated migration of 5x10 <sup>5</sup> HMSCs through PET-membrane .....   | 61 |
| Figure 28: Magnetic facilitated migration of 5x10 <sup>5</sup> HMSCs through PET-membrane. ....   | 62 |
| Figure 29: Magnetic facilitated migration of 2x10 <sup>5</sup> HMSCs through PET-membrane. ....   | 63 |
| Figure 30: Wound Healing Models. ....   | 73 |

# List of Tables

Table 1: Primary antibodies for western blotting. .... 34

## Abbreviations

|                   |  |
|-------------------|--|
| ATP               | Adenosine Triphosphate   |
| BAEC              | Bovine Aortic Endothelial Cell                                 |
| BBB               | Blood-Brain Barrier  |
| Bis-Tris          | 2-[Bis(2-hydroxyethyl)amino]-2-(hydroxymethyl)propane-1,3-diol |
| BSA               | Bovine Serum Albumin   |
| Ca <sub>2+</sub>  | Calcium  |
| CaCl <sub>2</sub> | Calcium Chloride   |
| Cdk               | Cyclin-dependant Kinase  |
| Cdk5              | Cyclin-dependant Kinase 5                                      |
| CIP               | Cyclin-dependant Kinase 5 Inhibitory Peptide                   |
| CNS               | Central Nervous System   |
| CO <sub>2</sub>   | Carbon Dioxide   |
| DAPI              | 4',6-diamidino-2-phenylindole                                  |
| DMEM              | Dulbecco's Modified Eagle's Medium                             |
| DMSO              | Dimethyl Sulfoxide   |
| DTT               | Dithiothreitol   |
| EBM               | Endothelial Basal Medium                                       |
| EC                | Endothelial Cell   |
| EDTA              | Ethylenediaminetetraacetic Acid                                |
| EGM               | Endothelial Growth Medium                                      |
| ELISA             | Enzyme-linked Immunosorbent Assay                              |
| ERK               | Extracellular-signal-regulated Kinase 1/2                      |
| ESI               | Electrospray Ionization  |
| FBS               | Foetal Bovine Serum  |
| FGF-2             | Fibroblast Growth Factor 2                                     |
| HABA              | 4'-hydroxyazobenzene-2-carboxylic Acid                         |
| HBMEC             | Human Brain Microvascular Endothelial Cell                     |
| HMSC              | Human Mesenchymal Stem Cell                                    |
| HPLC              | High Performance Liquid Chromatography                         |
| IMDM              | Iscove's Modified Dulbecco's Medium                            |
| K <sup>+</sup>    | Potassium  |
| kDa               | Kilodaltons  |
| MAPK              | Mitogen-activated Protein Kinase                               |
| mRNA              | Messenger Ribonucleic Acid                                     |

|                 |  |
|-----------------|--|
| MS              | Mass Spectrometry  |
| MS/MS           | Tandem Mass Spectrometry                                   |
| MSC             | Mesenchymal Stem Cell                                      |
| Na <sup>+</sup> | Sodium   |
| NaCl            | Sodium Chloride  |
| pAKT            | Phosphorylated Protein Kinase B                            |
| PBST            | Phosphate Buffered Saline with Tween 20                    |
| pCDK5           | Phosphorylated Cyclin-dependant Kinase 5                   |
| PEG             | Polyethylene Glycol  |
| pERK            | Phosphorylated Extracellular-signal-regulated Kinase 1/2   |
| PET-Membrane    | Polyethylene Terephthalate Membrane                        |
| pMAPK           | Phosphorylated Mitogen-activated Protein Kinase            |
| PVDF            | Polyvinylidene Fluoride                                    |
| Q-TOF           | Quadrupole Time-of-flight                                  |
| SDS-PAGE        | Sodium Dodecyl Sulphate Polyacrylamide Gel Electrophoresis |
| SEM             | Standard Error of the Mean                                 |
| SPIO            | Superparamagnetic Iron Oxide Nanoparticles                 |
| Tof             | Time-of-flight   |
| tpA             | Tissue Plasminogen Activator                               |
| Tris            | 2-Amino-2-hydroxymethyl-propane-1,3-diol                   |
| VEGF            | Vascular Endothelial Growth Factor                         |

## Abstract

Stroke is the second most common cause of death globally and yet there have been no new developments towards a therapy in the last 25 years. The main issue that surrounds developing therapeutic options for stroke, is the task of overcoming the blood brain barrier (BBB) and delivering an effective treatment to the brain itself. The complications of effectively delivering treatment after stroke are so monumental, that the efficiency of a new therapeutic drug is directly related to the efficiency of the delivery method. Previous methods of drug delivery such as intravenous injection have proved highly ineffective or gravely invasive for the patient. Human mesenchymal stem cells (HMSCs) provide a unique opportunity for developing a novel targeting and drug delivery system, which could effectively deliver therapeutics to specific regions of infarct following stroke. This work aimed to evaluate and quantify the potential of HMSCs to uptake and release various therapeutics, whilst also investigating whether superparamagnetic iron oxide nanoparticles (SPIOs) could be combined with a fixed magnetic field in order to facilitate HMSC migration.

In order to investigate the uptake and release of therapeutics, HMSCs were primed with both fibroblast growth factor 2 (FGF-2) and a cyclin-dependent kinase 5 inhibitory peptide (p5). The uptake and release of these potential therapeutics was investigated using developed enzyme-linked immunosorbent assays, fluorescent microscopy and HPLC-MS/MS. The *in vitro* effects of p5 were investigated using an experimental stroke model and Western blotting.

HMSCs were also primed with SPIOs, to determine whether they could be successfully internalized by the cells and if the magnetic properties of the nanoparticles could be also used to facilitate cellular migration. This was completed by using both fluorescent and bright-field microscopy, combined with a transwell migration assay.

The data provided shows the potential of HMSCs both as a drug delivery method and for cellular manipulation *in vitro*. HMSCs have not only been shown to successfully internalize both potential therapeutics and SPIOs but that this could be directly applied to the development of new treatment options following stroke. Furthermore, these results show that the p5 peptide also provides a leading new development for targeted therapy following stroke and that it could pose a useful candidate for future studies within neurodegenerative diseases.

## **Declaration**

I declare that no portion of the work referred to in this thesis has been submitted in support of an application for another degree or qualification of this or any other university or institute of learning.

## Copyright Statement

i. The author of this thesis (including any appendices and/or schedules to this thesis) owns certain copyright or related rights in it (the “Copyright”) and s/he has given The Manchester Metropolitan University certain rights to use such Copyright, including for administrative purposes.

ii. Copies of this thesis, either in full or in extracts and whether in hard or electronic copy, may be made **only** in accordance with the Copyright, Designs and Patents Act 1988 (as amended) and regulations issued under it or, where appropriate, in accordance with licensing agreements which the University has from time to time. This page must form part of any such copies made.

iii. The ownership of certain Copyright, patents, designs, trademarks and other intellectual property (the “Intellectual Property”) and any reproductions of copyright works in the thesis, for example graphs and tables (“Reproductions”), which may be described in this thesis, may not be owned by the author and may be owned by third parties. Such Intellectual Property and Reproductions cannot and must not be made available for use without the prior written permission of the owner(s) of the relevant Intellectual Property and/or Reproductions.

## Acknowledgements

First of all, I think it's important to say I cannot believe how quickly this year has flown and that it's now come to the point for me to thank everyone who has helped and guided me through it.

I would initially like to thank my supervisors, Mark Slevin who provided me with the amazing opportunity to complete my MRes and Ria Weston, because without her continued guidance and endless support I doubt any of this would have been possible.

I would also like to mention all the other students that I've had the pleasure of spending that last year with, including everyone who has answered one of my stupid questions, offered me some form of food/ drink, contributed to foot-long Fridays or tutored me in the art of conference chiselling (I would name you all but there's just too many!). This gratitude also extends to everyone else within MMU who I've had the pleasure of meeting, especially Glenn who has provided me with everything anyone could possibly need!

It also wouldn't be fair not to mention my family, who have continued to support me throughout another year of university, even if they don't really understand it and the fact that it's definitely not a proper job!

Finally I'd like to thank Lucy, because without her in twisting my arm, I doubt I ever would have applied for my masters. I'm immensely proud to have completed this year and without her I couldn't have done it.

# Chapter 1: Introduction

## 1.1 Ischemic Stroke

### 1.1.1 Stroke Overview

Stroke is the second most common cause of death globally, accounting for approximately 9% of all deaths and is a major cause of disability (Donnan, *et al.*, 2008). A stroke is termed medically as a cardiovascular accident and is defined as a disturbance in the blood supply to the brain, of which 80% are ischemic compared to 20% that are caused by cerebral haemorrhage (Dewey, *et al.*, 2001).

Stroke prognosis is also quite adverse, with a quarter of patients dying after the first month, with this rising to around 50% by the first year (Hankey, *et al.*, 1998). The major cause of this early stage death is the implications of the neurological deterioration and further contributions from factors such as secondary infections and aspiration (White, *et al.*, 2000). Ischemia is defined as a reduction in blood flow that is significant enough to alter cellular function. Brain tissue is exceedingly sensitive to ischemia, with only brief periods of ischemia required to severely alter the cellular activity of neurons, ultimately resulting in cell death (Mattson, *et al.*, 2001). Despite stroke being such a common cause of death, there is very little available in terms of treatment, with the main focus being on restoring blood flow, in order to limit the damage caused to the brain. This therapeutic intervention, is often the application of thrombolytic therapy or intravenous tissue plasminogen activator (tpA), which can break down fibrin clots by converting plasminogen into active plasmin (Vassalli, *et al.*, 1991 and Uyttenboogaart, *et al.*, 2009). This form of therapy is however very limited as it can only be safely applied to patients within 4.5 hours after insult due to the increased risk of bleeding into the brain tissue (Saqqur, *et al.*, 2008).

### 1.1.2 Pathophysiology of Ischemic Stroke

The pathophysiology of an ischemic stroke, can be referred to as the ischemic cascade (figure 1), which refers to the sequence of events that follow the starvation of oxygen that the brain sustains

following an arterial blockage (Xing, *et al.*, 2012). Understanding this chain of events is essential for the development of future therapies and is the focus of numerous research groups. The main issues that surround understanding the ischemic cascade, is its inherent complexity but it can be summarised as cellular bioenergetic failure due to focal cerebral hypoperfusion, followed by excitotoxicity, oxidative stress, blood–brain barrier dysfunction, microvascular injury, haemostatic activation, post-ischemic inflammation and finally cell death of neurons, glia and endothelial cells (Brouns & De Deyn, 2009). During an acute ischemic stroke, the areas affected by the reduction of blood flow can be split into two main areas; the first is the infarct core, which denotes the area of the brain, that regardless of re-perfusion, is destined to go on to infarct (Hossmann, 1994). The second is the region that borders the infarct core that is defined as the ischemic penumbra. Although less severe ischemia occurs within the penumbra region, over time, without treatment the penumbra can either develop into further infarction due to the increasing levels of excitotoxicity or can progress into further depolarization, post ischemic inflammation and apoptosis (Dirnagl, *et al.*, 1999). However because of this time delay, the penumbra region provides an ideal goal for neuroprotection after an ischemic event. It is also important to note that areas of the brain that are affected by the ischemia display a non-selective loss of all cells, including neurons, endothelial cells and astrocytes (Sims & Muyderman, 2010).

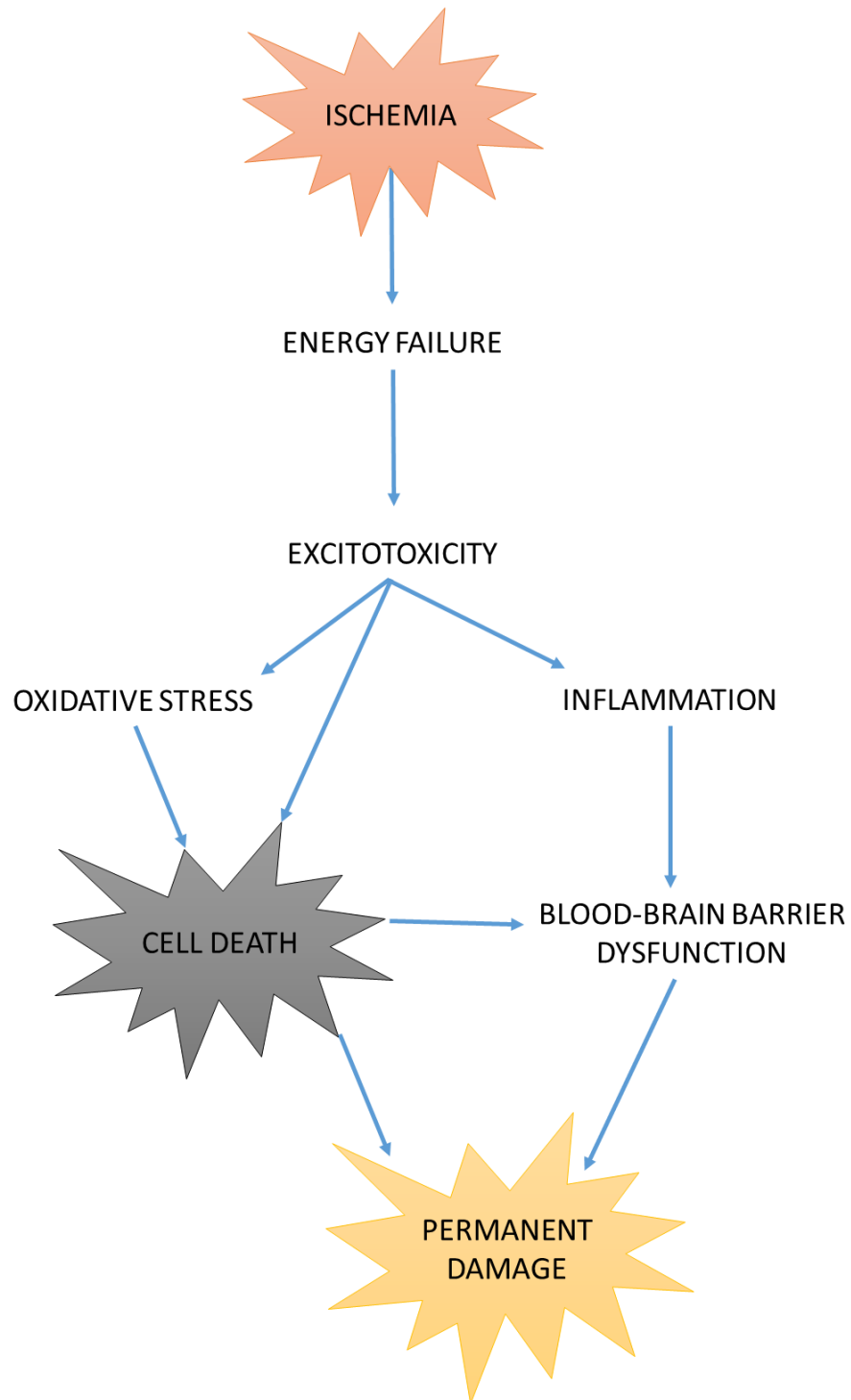
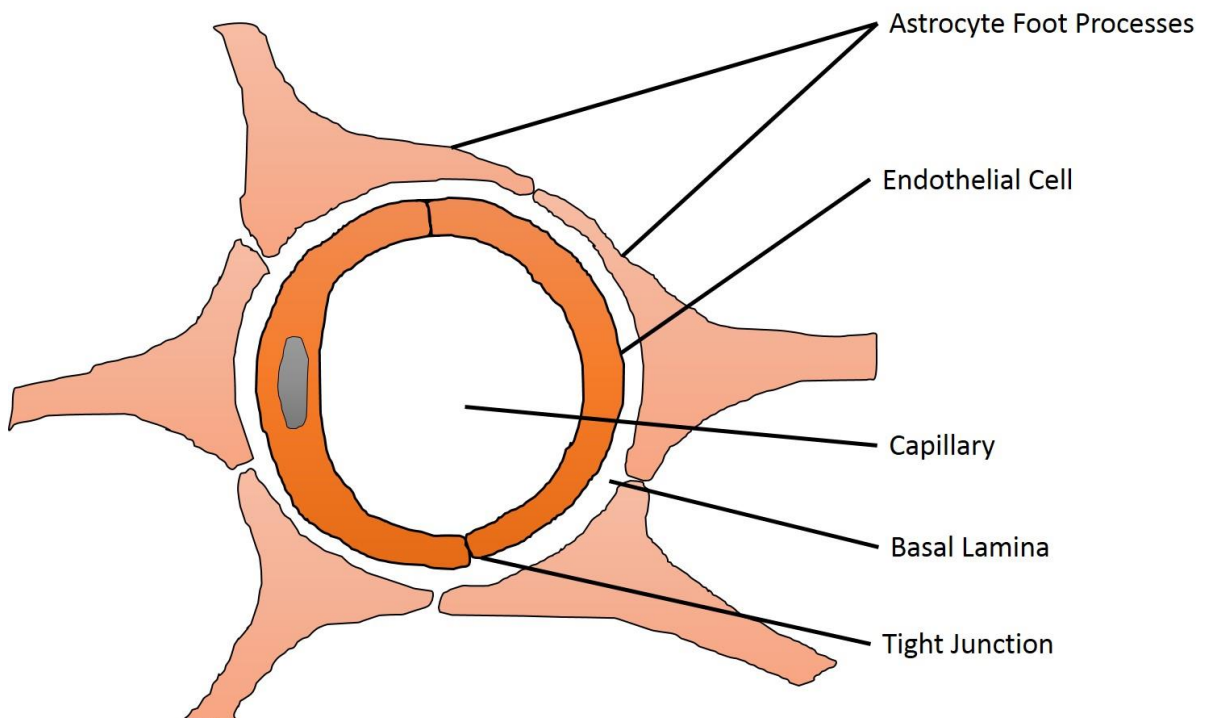


**Figure 1: Ischemic Cell Death.** The ischemic induced energy failure induces multiple pathways that result in neurotoxicity. During these processes there is a dramatic increase in extracellular  $\text{Ca}^{2+}$ ,  $\text{Na}^{+}$  and  $\text{K}^{+}$  as well as an increase in intracellular messenger  $\text{Ca}^{2+}$  that activates proteases, lipases and endonucleases. The resulting cell death, culminates in pro-inflammatory cytokine and chemokine secretion responses in glial cells, endothelial cells and infiltrating leukocytes (Woodruff, *et al.*, 2011).

## 1.2 The Blood-Brain Barrier

The blood-brain barrier (BBB) has historically been described as the gatekeeper of the central nervous system (CNS) and is a highly selective barrier that is able to separate circulating blood from the delicate homeostasis of the brain. Although the BBB consists primarily of endothelial cells (ECs), it is the interaction and formation of astrocytes, neurons, pericytes and ECs that produce the overall function of the BBB (Banerjee & Bhat, 2007). The BBB acts in three distinct ways; initially it acts as a physical barrier because of the tight junctions that form between adjacent endothelial cells, prevent most of the transport of cells, proteins and soluble agents. Secondly, it is able to act as a transport barrier by selectively allowing the transport of required nutrients and waste through specific systems. Finally, using a combination of both intracellular and extracellular enzymes, the BBB is also able to provide a metabolic barrier by metabolising peptides, adenosine triphosphate (ATP), nucleotides and many other neuroactive or toxic compounds (Abbott, *et al.*, 2006). It is also important to note that the BBB is not a fixed system but is able to respond to a variety of signals from both the circulatory blood and the brain and it is for this reason that is significantly disturbed during neurodegenerative events, such as stroke



(Abbott & Friedman, 2012).

Figure 2: Structure of the blood-brain barrier. The key features of the blood-brain barrier, showing the tight junctions formed by endothelial cells preventing a physical barrier to cells, proteins and soluble agents.

### 1.3 Inflammatory Response

Inflammation plays a key role in the pathophysiology of stroke, with both an acute and prolonged inflammatory response following an ischemic incident. Following ischemia and rapid neuronal death, resident microglia become activated and take up a phagocytic role to engulf dead cells and produce pro-inflammatory cytokines (Faustino, *et al.*, 2011). In addition to activated microglial cells, astrocytes also produce pro-inflammatory cytokines and neuroprotective factors. This production by both microglial cells and astrocytes also varies at different time points following stroke, meaning that they could be responsible for both protective and regenerative aspects (Jin, *et al.*, 2010). However, this production of cytokines and the production of reactive oxygen species by resident immune cells causes a disruption to the BBB allowing the invasion of circulatory immune cells such as lymphocytes, neutrophils and monocytes, exacerbating the inflammatory response (Benakis, *et al.*, 2014). This invasion of immune cells also varies both depending on the severity of the ischemia and the amount of time that has elapsed from the initial infarction. For example, in experimental models with permanent ischemia, immune cells can begin to accumulate as early as three hours following the attack, whereas with transient ischemic attack immune cells begin to accumulate 48 hours after normal blood flow is regained (Gelderblom, *et al.*, 2009 and Zhou, *et al.*, 2013). Because of both the protective and regenerative aspects to the immune response, it adds a further complexity to the pathology of stroke and the development of possible therapies. It is also important to note that the increased permeability of the BBB caused by this described influx of immune response, facilitates the leaking of fluid onto the brain and it is this oedema that is responsible for a large proportion of deaths following a stroke (Balami, *et al.*, 2011).

## 1.4 Stroke Prognosis and Therapy

Due to the complexity of stroke and the cascade of events that follow cerebral ischemia, the prognosis of stroke can only be described as adverse. As previously stated, there is a high rate of early mortality due to neurological deterioration and secondary infections following the initial ischemia but even the later deaths of patients are commonly caused by the complications that follow stroke (Hankey, *et al.*, 2000). Despite this complexity, the application of treating stroke by targeting the mechanisms that are involved in cell death are not difficult. The main issues that surround treatment is that the therapeutic time windows are relatively small and require an effective method of delivery to the brain itself. It is also noted that due to the variance of the ischemic cascade, a combinational therapy is hypothesised to be more effective than a stand-alone neuroprotective treatment (Xing, *et al.*, 2012). It will be the development of these possible therapies that will be discussed further.

## 1.5 Angiogenesis

One area of interest in the development of possible therapies in stroke is the application of angiogenesis. Angiogenesis is defined as the development of new blood vessels from existing vessels, with this process having a central role in multiple ischemic and inflammatory diseases (Birbrair, *et al.*, 2014). It is also apparent that angiogenesis is not only the method in which the brain is vascularised but angiogenesis can also be stimulated by the central nervous system following hypoxic or ischemic attack (Greenburg, 1998). This natural recovery from ischemic stroke relies heavily on the angiogenic response and the delivery of oxygen and nutrients that the restoration of blood flow provides (Yin, *et al.*, 2015). This upregulation of angiogenesis following stroke is thought to be responsible for neuronal re-organisation, stem cell differentiation, functional recovery and for the development of new micro-vessel environments (Slevin, *et al.*, 2006). When induced *in vivo*, treatment by angiogenesis has also been shown to significantly

improve motor functions long and short-term, within animal models (Avraham, *et al.*, 2011 and Avraham, *et al.*, 2013). For this reason, the application of pro-angiogenic factors could be beneficial as a therapeutic option in stroke.

### 1.5.1 Fibroblast Growth Factor 2

One possible pro-angiogenic agent that could possibly be applied to stroke therapy is fibroblast growth factor 2 (FGF-2). Not only is FGF-2 involved in the regulation and survival of neuronal cells (Chao, 2000), it is also thought to be responsible for the regeneration of function within pathological situations such as brain ischemia by protecting against oxidative stress within the ischemic cascade (Font, *et al.*, 2010). FGF-2 has been shown to be upregulated within the penumbra region of stroke within human brains and it is within these highly angiogenic areas that neurons tend to have a better survival rate (Krupinski, *et al.*, 1997). Due to all these factors, effective application of FGF-2 to restore local micro-circulation, along with a combinational therapy to reduce apoptosis could generate neuronal survival, promote reorganisation and improve patient recovery (Shin, *et al.*, 2006).

### 1.6 Cyclin-dependant Kinases

In addition to angiogenesis, another area that provides a possible therapeutic opportunity for ischemic stroke is the cyclin-dependant kinases family of proteins. In general, cyclin-dependant kinases (Cdk5), have a well-established role in the eukaryotic cell cycle, regulating transcription, messenger ribonucleic acid (mRNA) processing and other processes such as cellular differentiation (Morgan, 1997). The deregulation of Cdk5 has also been implemented in a variety of diseases such as cancer (Fabbro, *et al.*, 2002) and neurodegenerative disorders such as stroke (Geschwind, 2003). Within this study, the member of the Cdk family that provides the biggest area of interest is cyclin-dependant kinase 5 (Cdk5) that is exclusively active within the nervous system (Paglini & Caceres, 2001).

### 1.6.1 Cyclin-dependant Kinase 5

Although Cdk5 is categorised amongst other members of the Cdk family, it is unique in the fact that it is not regulated by cyclins as the name suggests, but it is in fact activated by the molecule p35 and its homolog p39. Due to these two molecules only being expressed by neurons, despite Cdk5 being produced by multiple cell types, Cdk5 activity is only observed within neurons (Sridhar, *et al.*, 2006). Compared to other Cdk enzymes, Cdk5 also differs in the aspect that it is not responsible for cell cycle regulation. It is in fact responsible for pivotal roles within the development of the central nervous system, such as the migration of neurons and aspects of normal brain function such as cell adhesion and neurite growth (Dhavan & Tsai, 2001 and Ko, *et al.*, 2001). From a pathological perspective, the most interesting characteristic of Cdk5 is the events that occur when it becomes deregulated. The deregulation of Cdk5 is directly associated with the cleavage of its trigger molecule, p35, to a more stable, truncated molecule of p25 (figure 3), with upregulation of Cdk5 and p35/p25 both being associated with multiple neurodegenerative diseases (Weishaupt, *et al.*, 2003). This cleavage of p35 to p25 is caused by calpains at the time of neuronal cell death and when studied *in vivo* this Cdk5/p25 complex causes cytoskeletal disruption and apoptosis (Patrick, *et al.*, 1999 and Hisanaga & Saito, 2003). Further evidence shows that the deregulation of Cdk5 may contribute to a number of neurological degenerative diseases, with further links to hallmarks of neurological death and the decline of cognitive function (Sundaram, *et al.*, 2013). This also draws a direct relationship to the hypoxic regions of stroke, where there is also an increased expression of both Cdk5 and its activators p35 and p25 (Bosutti, *et al.*, 2013). Due to these pathological hallmarks, there has been development of inhibitory molecules that could target this increase of both Cdk5 and its activators as a potential therapeutic option. One area of this research is discussed below.

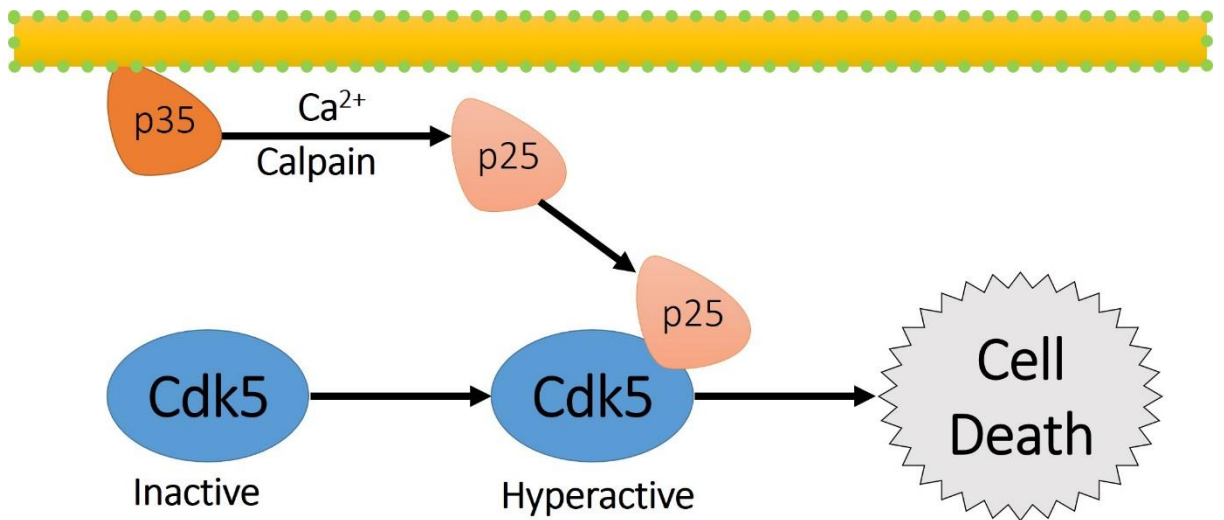


**Figure 3: Hyperactivation of Cdk5 by cleaved p35.** Cdk5 become hyperactive when p35 is cleaved to p25 by calpains. This process ultimately leads to neuronal cell death.

### 1.7 Cyclin-dependant Kinase 5 Inhibitory Peptide

As previously discussed, the cleavage of p35 to p25 by calpains and calcium causes the disruption of Cdk5 activity, which ultimately leads to cytoskeletal disruption and neuronal cell death (Chen, *et al.*, 2008). When p35 is cleaved to p25 by activated calpains, it allows the release of free soluble Cdk5 beginning the phosphorylation of surrounding proteins and the detrimental effects to neurons (Kusakawa, *et al.*, 2000). This pathway is therefore an ideal candidate for a targeted therapy, due to the fact, regulated Cdk5 activity is still required for normal brain activity and controlled cell death (Zhang, *et al.*, 2008). Previous research has identified that the use of calpain inhibitors and other compounds such as tanishinone IIA, reduce levels of apoptosis and show neuroprotective qualities by disrupting the Cdk5/p35-Cdk5/p25 pathway (Verdaguer, *et al.*, 2005 and Shi, *et al.*, 2012). Further research has also shown a possible therapeutic approach to combat this increase of both Cdk5 and its activators, by the development of a truncated fragment of p35, named the Cdk5 inhibitory peptide or CIP. CIP has been shown to successfully inhibit the binding of p25 to Cdk5 both *in vivo* and *in vitro* without affecting regular binding of p35 or other members of the Cdk protein family (Zheng, *et al.*, 2002). Further work with CIP has not only shown that,

when treated *in vitro*, there is a reduction of cleaved p35 to p25, but also that under hypoxic conditions CIP protects endothelial cells whilst also promoting both angiogenesis and cellular remodelling (Bosutti, *et al.*, 2013). When studied *in vivo*, using a mouse model, CIP is observed to be responsible for extensive reductions in neuroinflammation and an increase in neuroprotection (Sundaram, *et al.*, 2013). From the work covered, CIP provides excellent therapeutic options but for it to be used as a therapy, it must be able to cross the BBB and due to the fact that CIP is constructed of 125 amino acids this could prove to be extremely problematic. One development that overcomes this issue is a derivative peptide of CIP, named p5 that is discussed below.

### 1.7.1 The p5 Peptide

A 24-residue peptide, p5, which is derived from CIP, provides the unique quality that it inhibits Cdk5/p25 activity (figure 4) and yet it is small enough to cross the BBB. When studied *in vitro* p5 offers more effective inhibition of Cdk5/p25 activity when compared with CIP and has been shown to protect against neuronal cell death (Zheng, *et al.*, 2010). Further *in vivo* studies using a neonatal rat model of severe hypoxic ischemia, observed that p5 treatment promoted recovery after ischemic/hypoxic injury by reducing infarct volume and attenuating neuronal apoptosis (Tan, *et al.*, 2015).

Cdk5 activity is dependent on the binding of neuron specific, cyclin-related activators p25, p35 and p39, with p5 being derived from the 138-291 region of p25 (figure 5), which is responsible for Cdk5 activation (Amin, *et al.*, 2002). Following a neurotoxic insult, there is an elevation of cellular calpain levels, p25 production and hyperactivity of Cdk5, leading to hyperphosphorylation of cytoskeletal components such as tau, resulting in cellular death (Kesavapany, *et al.*, 2003). The mechanism and specificity of which p5 is able to inhibit Cdk5/p25 interaction is not yet fully understood but it is hypothesised that the p35 N-terminal, which is absent in p25, obstructs the binding of p5. This absence of this N-terminal in p25 may explain the specificity of p5 but further research is required to fully understand the mechanisms underlying this pathway (Zheng, *et al.*, 2004).

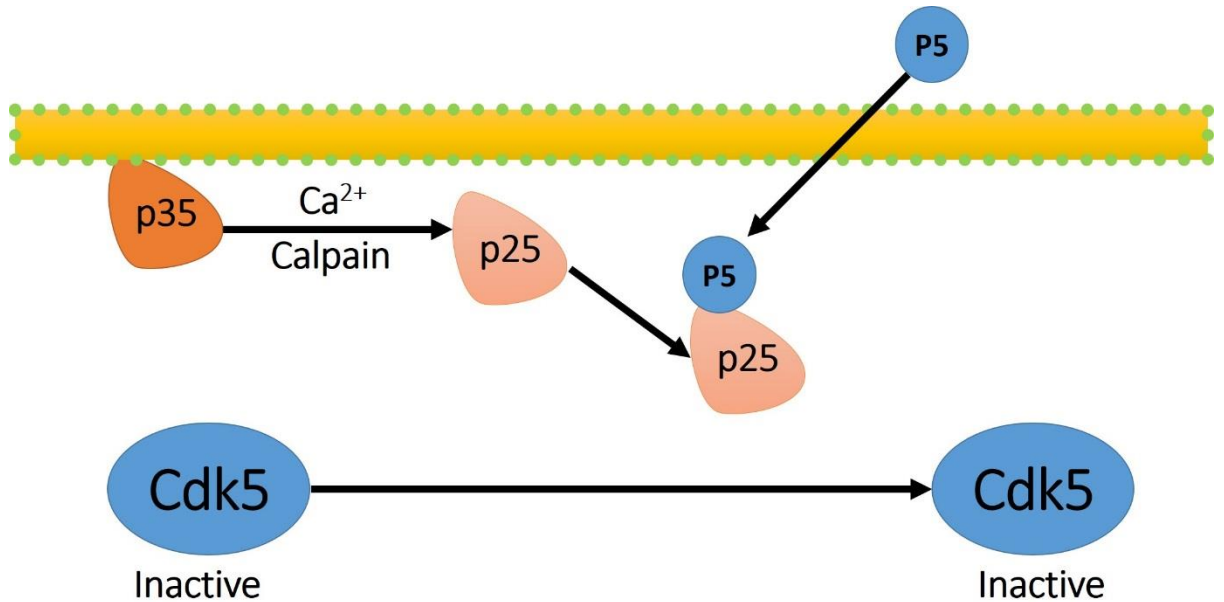


**Figure 4: Cdk5/p25 inhibited by p5.** The p5 peptide inhibits the Cdk5/p25 complex, preventing Cdk5 becoming hyperactive and the subsequent neuronal cell death.

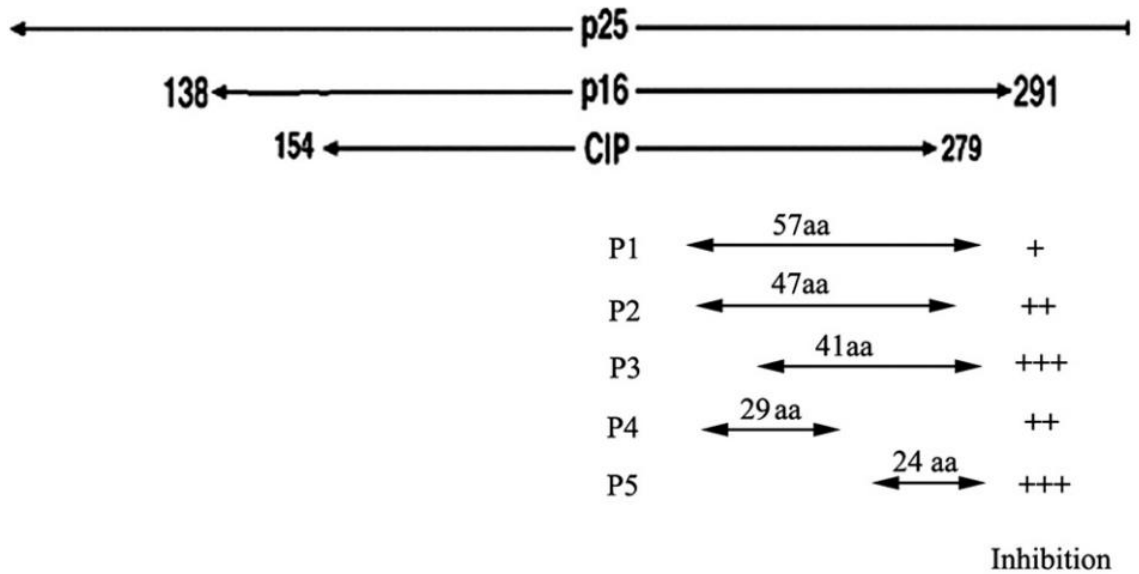


**Figure 5: Cdk5 inhibitory peptides derived from p25.** The above schematic shows the truncated p25 peptides including CIP, from which a further 5 further peptides were derived (p1-5). From these peptides, p5 had the greatest inhibitory properties and is short enough to be an effective therapeutic candidate (Zheng, et al., 2010).

## 1.8 Limitations of Current Stroke Therapy

As previously stated stroke is globally the second most common cause of death and therefore the only logical step can be towards the development of new therapeutic methods to both prevent and treat the condition. Despite this, there have been no major developments towards a new stroke therapy in the last 25 years. The main issues that surround developing therapeutic options for the treatment of stroke is the monumental hurdle of delivering therapies effectively across the blood brain barrier (BBB) (Hu, *et al.*, 2012). Therefore, in relation to the brain, the efficiency of a drug is directly related to the efficiency of the delivery method. Previous methods of drug delivery such as intravenous injection or specific brain targeting ligands have proved ineffective and although administering the drugs directly to the brain is more efficient, the procedures are gravely invasive and can further damage the brain (Taiyoun, *et al.*, 2013). Current treatment methods, such as the use of thrombolytic agents, are also limited by small time windows despite areas of ischemia being active for weeks after the initial attack (Thored, *et al.*, 2006 and Goldstein, 2007). One development that may overcome these limitations of current treatment options, is the use of cell based therapies, more specifically the application of stem cells.

## 1.9 Stem Cells

As a cell type, stem cells are classically defined as cells that possess both of the following properties; potency, meaning that they can differentiate into multiple cell types and that they can maintain their undifferentiated state throughout numerous cycles of cell division (Preynat-Seauve & Krause, 2011). In general, stem cells are also broadly termed either embryonic or somatic (adult) stem cells, dependant on their level of potency. Embryonic stem cells are a unique self-renewing, pluripotent cell type, that generate the ectodermal, endodermal and mesodermal lineages during embryogenesis (Lee, *et al.*, 2006). Whereas somatic stem cells are a multipotent, self-renewing cell type, that are restricted to differentiation of specific lineages such as hematopoietic stem cells or neural crest cells (Gonzalez & Bernad, 2012). Due to specific cell characteristics, stem cells provide unique opportunities within the field of stroke research and the

application of various stem cells types has been explored. As an example, embryonic, neuronal and umbilical cord blood stem cells have all being applied to stroke research, either in attempt at replacing lost cells or other cellular applications such as recruiting progenitor cells (Luo, 2011). However, the type of stem cells that provide the biggest interest for a combinational therapy are mesenchymal stem cells, which are discussed below.

### 1.9.1 Mesenchymal Stem Cells

Mesenchymal stem cells (MSCs) also termed as marrow stromal cells or stromal precursor cells (stromal cells), were originally described by (Friedenstein, *et al.*, 1976) as clonogenic fibroblast precursor cells that had the defining characteristics of being clonogenic, plastic adherent and are found within the bone marrow. MSCs are a heterogeneous mix of progenitor cells that have the capability of differentiating into multiple cell lineages of mesodermal, ectodermal and endodermal origins (Menicanin, *et al.*, 2009). MSCs also possess a high growth capacity and are highly accessible from multiple sources including adipose tissue, bone marrow, placenta and umbilical cord blood making them an ideal candidate for clinical applications (Sinden & Muir, 2012).

#### 1.9.1.2 Mesenchymal Stem Cells as a Therapy for Stroke

MSCs provide enormous potential in the development for new therapies in order to combat stroke. When applied in general to neurodegenerative diseases, MSCs have been shown not only to target and hone into areas of damaged tissue but also secrete anti-apoptotic, pro-angiogenic and neurotrophic factors (Chopp & Li, 2002 and Kurozumi, *et al.*, 2005). Similar results have also been observed when stromal cells were transplanted into areas of cerebral ischemia reducing infarct volume and levels of inflammation (Ikegame, *et al.*, 2011). MSCs also offer a possible method of drug delivery to the brain as an experimental therapeutic possibility that could also overcome the restrictions of the BBB.

MSC's have been shown to cross the BBB and express chemokine receptors, which provide them with the ability to home in on areas of tissue damage with high levels of chemokines, such as in stroke tissue (Aleynik, *et al.*, 2014). MSC's also display the ability to increase; angiogenesis, anti-

apoptotic factors, mitogenic factors and neurogenic factors (Quittet, *et al.*, 2015) as well as having been shown to uptake and release drugs through endocytosis facilitated by micro and nano-vesicles (Baglio, *et al.*, 2012). Although the use of stem cells as a method for drug delivery is quite novel, there has been recent research showing the effectiveness of MSC's in the uptake and release of various drugs. MSC's have been primed with an anti-cancer drug, Paclitaxel, where it has been shown that the cells not only effectively uptake and release the drug (Pessina, *et al.*, 2011) but also attract and kill tumour cells, inhibit angiogenesis and improve the survival of leukaemia-bearing mice (Pessina, *et al.*, 2013). Similar research has demonstrated that MSC's can uptake and release the antibiotic, ciprofloxacin, with the antibiotic remaining effective after the process (Sisto, *et al.*, 2014) Further work has also found that MSC's primed with valproate and lithium, migrate to and facilitate recovery in infarcted regions within an *in-vivo* rat stroke model (Tsai, *et al.*, 2011).

### 1.10 Migration of Mesenchymal Stem Cells

Although MSCs provide promising cell therapeutic possibilities for ischemic stroke, there are still issues that surround that rate of cell migration towards the infarct areas. Upon administration, MSC migration has been tracked using immunohistological analysis, magnetic resonance imaging (MRI) using magnetic cells labelling and nuclear imaging using <sup>99m</sup>Tc-labeled graft. (Ikegame, *et al.*, 2014). Using these imaging techniques, MSCs have been shown to not only migrate to areas of damaged tissue but also accumulate in various organs with the highest volumes seen in the liver and the lungs. It was also shown that MSCs also migrated into areas of undamaged cerebral tissue as opposed to being solely attracted to infarct regions (Detante, *et al.*, 2009; Vasconcelos-dos-Santos, *et al.*, 2012). One method that may hold a potential to increase the cell transplantation efficiency of MSCs is the use of ferumoxides or superparamagnetic iron oxide nanoparticles (SPIOs).

### 1.10.1 Superparamagnetic Iron Oxide Nanoparticles

SPIOs are a development within nanotechnology, which are classed as iron oxide molecules encased within synthetic polymers, polysaccharide or monomer coatings that have been applied to MRI as a contrast agent for the last two decades (Weissleder, *et al.*, 1990 and Weinstein, *et al.*, 2009). When this technique is applied to MSCs, it exploits similar mechanisms within the stem cells as with the drug loading, where the cells are able to engulf the SPIOs and then localise them within secondary lysosomes without affecting any of the key characteristics of the cells themselves (Landázuri, *et al.*, 2013). The magnetic properties of the nanoparticles are then used to manipulate the MSCs by using an external magnetic field, providing a novel opportunity for targeted therapies.

### 1.10.2 Superparamagnetic Iron Oxide Nanoparticles as a Novel Magnetic Targeted Therapy

When this technique has been applied to both *in vitro* and *in vivo* studies it has been shown to trap magnetised MSCs effectively at areas of interest both in animal and *in vitro* models (Oshima, *et al.*, 2014 and El Haj, *et al.*, 2015). Further studies have also shown that in animal models, SPIO loaded MSCs can increase migration efficiency, 6-fold within a vascular injury rabbit model (Riegler, *et al.*, 2013) and a 10-fold increase when applied to retinal targeting (Yanai, *et al.*, 2012). This targeting method has also been shown to successfully target MSCs near lesion sites in rat spinal cord injuries (Vaněček, *et al.*, 2012) and although it has not been directly applied to a stroke model, SPIOs have been used to effectively identify MSCs *in vivo* without effecting cell viability, phenotype or differentiation potential (Detante, *et al.*, 2012).

## 1.11 Summary and Aims

Due to the limitations and lack of developments towards treatment options for stroke, the use of mesenchymal stem cells may provide a unique opportunity towards the development of new therapeutic options. The broad aim of this thesis is to investigate the potential of human

mesenchymal stem cells (HMSCs) as a novel drug delivery system by exploring the uptake and release of FGF-2 and p5, whilst also exploring the potential of internalisation and cellular manipulation by SPIOs.

### 1.12 Objectives

1. To investigate the uptake and release of FGF-2 and p5 by HMSCs.
2. To investigate the *in vitro* effect of p5 in an induced apoptotic model.
3. To investigate the internalisation of SPIOs by HMSCs and the potential of magnetic facilitated migration.

## Chapter 2: Materials and Methods

### 2.1 Cell Culture

#### 2.1.1 Bovine Aortic Endothelial Cell Culture

Laboratory stocks of bovine aortic endothelial cells (BAECs), were revived from liquid nitrogen and cultured in Dulbecco's Modified Eagles Medium (DMEM) supplemented with, 10% foetal bovine serum (FBS), 100 µg/ml penicillin, 100 µg/ml streptomycin and 2mM L-glutamine in T75 flasks.

BAECs were maintained at 37°C in a humidified incubator with 5% CO<sub>2</sub>, until 80% confluent. Cells were seeded in 24-well plates at 200,000 cells well and allowed to reach confluency 24 hours before treatment.

#### 2.1.2 Human Brain Microvascular Endothelial Cell Culture

Laboratory stocks of Human brain microvascular endothelial cells (HBMECs), were revived from liquid nitrogen and cultured in endothelial basal medium 2 (EBM-2) Basal medium (Lonza) supplemented with endothelial growth medium 2 (EGM-2) SingleQuot kit (Lonza) in T75 flasks coated with poly-L-lysine (Sigma-Aldrich), until 80% confluent. HBMECs were maintained at 37°C in a humidified incubator with 5% carbon dioxide (CO<sub>2</sub>). Cells were seeded in 6 well plates at 800,000 cells per well and allowed to reach confluency before calcium chloride (CaCl<sub>2</sub>) treatment.

#### 2.1.3 Human Mesenchymal Stem Cell Culture

Human mesenchymal stem cells (HMSCs) were generously donated by Dr Valentina Ceserani and her team at the Istituto Neurologico "Carlo Besta". The HMSCs were cultured in 80% Iscove's Modified Dulbecco's Medium (Lonza) supplemented with 5% FBS, 2mM L-glutamine and 20% Endo PM in T75 flasks. Endo PM consisted of 50% complete Neurocult (Stem Cell Technologies, Neurocult NS-A Basal Medium (human) supplemented with Stem Cell Technologies, Neurocult NS-A Proliferation Supplement (human)) and 50% complete endothelial basal medium (EBM) (Lonza, EBM Basal Medium supplemented with Lonza, EGM SingleQuot Kit Supplement & Growth Factors). HMSCs were maintained at 37°C in a humidified incubator with 5% CO<sub>2</sub>.

#### 2.1.4 Cryopreservation of Cells

Viable cell stores were produced by cryopreservation. Cells at confluency in a T75 flask, were washed with phosphate-buffered saline (PBS), detached with trypsin and then centrifuged at 300g for 10 minutes at 4°C. BAECs and HBMECs were then re-suspended in freezing media (50% cell media, 50% FBS containing 10 % dimethyl sulfoxide (DMSO)). HMSCs were re-suspended in FBS containing 10 % DMSO. The cell suspensions were then transferred into cryopreservation tubes before being placed into a Mr Frosty (ThermoFisher Scientific) for 24 hours at -80°C. After this 24 hour period, the cells were then placed in liquid nitrogen. When needed, cells were revived by incubating at 37°C in a water bath. Cells were then transferred to T25 flasks in 5ml of fresh cell media and cultured for 6 hours until viable cells attached. After this time period, the cell media was replaced in order to remove the DMSO and normal cell culture protocol was then followed.

#### 2.1.5 Cell Counting

Cell media was removed, the cells were washed in PBS and detached using trypsin. After the cells had detached, they were centrifuged at 300g for 8 minutes and the cell pellet was re-suspended in fresh cell media. The cell suspension was then removed and mixed with an equal volume of trypan blue. Cells were then counted using a TC20 automated cell counter (Bio-Rad).

### 2.2 Enzyme-Linked Immunosorbent Assay (ELISA)

#### 2.2.1 FGF-2 Quantitation by ELISA

24 hours before treatment HMSCs were seeded into 12 well plates and allowed to reach 80% confluency. The cells were then washed twice in PBS and then treated for 24 hours in FGF-2 loaded cell media at varying concentrations (5, 10, 15 and 20 ng/ml). At the end of the incubation period, the cell media was collected, the cells were washed twice with PBS, detached with trypsin and then seeded into a fresh 12 well plate. After 24 hours of culture the cell media was collected and replaced. This process was then repeated after 48 hours of culture. The collected media samples were then tested, against samples collected from untreated HMSCs as a negative control.

For analysis, commercial ELISA kits were purchased from R&D Systems UK and the manufacturer's protocol was followed. The plate was then read at 490nm and the absorbance recorded on a plate reader (Biotech).

### 2.2.2 Colour-metric Biotin Quantitation by ELISA

A 4'-hydroxyazobenzene-2-carboxylic acid (HABA) commercial ELISA kit was purchased from ThermoFisher Scientific and the manufacturer's protocol was followed. A serial dilution of standards was produced in HMSC cell media using biotin (SigmaAldrich). The absorbance of each well was then recorded at 494 and 520nm using a plate reader (Biotech).

### 2.2.3 Fluorescent Biotin Quantitation by ELISA

To optimise this methodology, multiple experimental approaches were trialled but all standards and samples were analysed using the commercial ELISA kit purchased from ThermoFisher Scientific and the protocol provided.

Initially, 24 hours before treatment  $5 \times 10^5$  HMSCs were seeded into 6 well plates and allowed to reach 80% confluency. The cells were then washed twice in PBS and then treated for 24 hours in p5 loaded cell media (2.5  $\mu\text{g}/\text{ml}$ ). At the end of the incubation period, the cell media was collected, the cells were washed twice with PBS, detached with trypsin and then seeded into a fresh 6 well plate. After 24 hours of culture the cell media was collected and replaced. This process was then repeated after 48 hours of culture.

Further  $5 \times 10^5$  HMSCs were seeded into 6 well plates and allowed to reach 80% confluency over 24 hours. The cells were then washed twice in PBS and then treated for 24 hours in p5 loaded cell media (2.5  $\mu\text{g}/\text{ml}$ ). At the end of the incubation period, the HMSC media was removed and the cells were lysed in lysis buffer (50 mM Tris(hydroxymethyl)aminomethane (Tris) (pH 8.0), 150 mM sodium chloride (NaCl), 1% TritonX-100, 1M Dithiothreitol (DTT), containing a mixture of protease inhibitors (Sigma-Aldrich) and phosphatase inhibitors (Sigma-Aldrich)). To increase lysis efficiency, each sample was incubated on ice for 20 minutes vortexing every 2 minutes during the incubation

period. Each sample was then centrifuged at 2100g for 4 minutes at 4°C before the supernatant was collected into and the pellet discarded.

Three sets of standards were then produced by serial dilution; the manufacturers provided Biocytin standards in PBS, p5 in PBS and p5 in HMSC media. Each standard or sample was mixed with the DyLight Reporter Working Reagent and then added to each well of a black opaque 96-well microplate. The plate was then incubated for 5 minutes at room temperature before the excitation/emission was read at 494/520 nm on a plate reader (Biotech).

## 2.3 Immunofluorescence

### 2.3.1 Immunofluorescence of the Internalisation of p5 by HMSCs

13 mm coverslips were added to each well of a 24 well plate.  $2 \times 10^5$  HMSCs were seeded into each well and allowed to reach 70% confluency over 24 hours. The cells were then washed twice in PBS and then treated with p5 loaded cell media (2.5  $\mu\text{g}/\text{ml}$ ). At the end of the appropriate incubation period (4, 8, 24 or 48 hours), the cell media was removed and the cells were fixed in 4% paraformaldehyde in PBS for 10 minutes. The cells were then washed 3 times in PBS, permeabilised using 0.5% TritonX-100 in PBS for 8 minutes and then washed a further 3 times. The cells were blocked in 3% bovine serum albumin (BSA) in PBS for 1 hour at room temperature before incubating for 1 hour at room temperature with anti-fluorescein (biotin) antibody (Abcam) in 5% skimmed milk. The wash stage was then repeated 3 times with PBS before each coverslip was mounted using VECTASHEILD mounting medium with 4',6-diamidino-2-phenylindole (DAPI) and sealed using nail varnish. Each image was then taken using a fluorescent microscope (Zeiss, Imager Z1).

### 2.3.2 Immunofluorescence of the Internalisation of SPIOs by HMSCs and BAECs

13 mm coverslips were added to each well of a 24 well plate.  $2 \times 10^5$  HMSCs or  $5 \times 10^5$  BAECs were seeded into each well and allowed to reach 70% confluency over 24 hours. The cells were washed twice in PBS and then treated with biotin functionalised SPIOs (Sigma-Aldrich) loaded cell media

(2.5 µg/ml). Each plate was then incubated for 90 minutes before the cell media was removed and the cells were fixed in 4% paraformaldehyde. The cells were then washed 3 times in PBS, permeabilised and then washed as above. The cells were blocked in 3% BSA in PBS for 1 hour at room temperature before incubating for 1 hour at room temperature with anti-fluorescein (biotin) antibody (Abcam) in BSA. The wash stage was then repeated three times with PBS before each coverslip was mounted using VECTASHEILD mounting medium with DAPI and sealed using nail varnish. Each image was then taken using a fluorescent microscope (Zeiss Imager Z1).

## 2.4 Immunohistochemistry

### 2.4.1 Immunohistochemistry of the Internalisation of SPIOs by HMSCs

13 mm untreated coverslips were added to each well of a 24 well plate.  $2 \times 10^5$  HMSCs were seeded into each well and allowed to reach 70% confluency over 24 hours. The cells were then washed twice in PBS and then treated with polyethylene glycol (PEG) functionalised SPIOs (Sigma-Aldrich) loaded cell media (2.5 µg/ml). Each plate was then incubated for 90 minutes before the cell media was removed and the cells were fixed in 4% paraformaldehyde. Each coverslip was then stained with 5% Prussian blue for 20 minutes, rinsed with PBS and then mounted on glass slides using glycerol gelatine. Images were captured using a bright field microscope (Zeiss, Imager M1).

## 2.5 SDS-PAGE and Western Blotting

### 2.5.1 Protein extraction

$1 \times 10^5$  cells were transferred into 6 well plates, treated with 5mM CaCl<sub>2</sub>, 5mM CaCl<sub>2</sub> and p5 (2.5µg/ml) or FGF-2 (10ng/ml) and then lysed in lysis buffer as in 2.2.3. To increase lysis efficiency, each sample was incubated on ice for 20 minutes vortexing every 2 minutes during the incubation period. Each sample was then centrifuged at 2100g for 4 minutes at 4°C before the supernatant was collected and the pellet discarded.

## 2.5.2 SDS-PAGE and Western Blot Analysis

Samples were added to 5X loading dye (ThermoFisher Scientific) before boiling at 99°C for 2 minutes. Protein ladder (ThermoFisher Scientific) or sample was added to each well of a 4-12% Bis-Tris Gel (ThermoFisher Scientific) and the gel was run in MOPS running buffer (ThermoFisher Scientific) at 200v for 45 minutes.

A polyvinylidene difluoride PVDF membrane (GE Healthcare) was soaked in 100% methanol for 5 minutes before being transferred to soak in transfer buffer for a further 5 minutes. The Western blot cassette was assembled as follows; two sponges, two pieces of blotting paper, 4-12% Bis-Tris gel, PVDF membrane, two pieces of blotting paper followed by two sponges. The transfer was run for 1 hour at 35v. After the transfer, the membrane was blocked for 1 hour at room temperature in PBS 0.1 % Tween-20 (PBST) with 5% skimmed milk before incubating for 1 hour in primary antibodies again at room temperature in PBST with 5% skimmed milk. The primary antibodies are shown in table 1. The secondary antibodies were either peroxidase-conjugated goat anti-rabbit IgG or goat anti-mouse IgG (Daco). The membrane was washed 3 times in PBST for 10 minutes before incubating at room temperature for another hour in secondary antibodies in PBST with 5% milk. The membrane was then washed a further 3 times with PBST for 10 minutes before developing with the ECL reagent (Pierce). Images were captured on the Chemidoc Touch gel documentation system (Biorad).

| <b>Antibody</b>                    | <b>Species</b> | <b>Dilution</b> | <b>Supplier</b>                   | <b>Product Code</b> |
|------------------------------------|----------------|-----------------|-----------------------------------|---------------------|
| <b>pERK 1/2</b>                    | Rabbit         | 1:2000          | Cell Signalling Technologies      | 3192                |
| <b>ERK 1/2</b>                     | Rabbit         | 1:2000          | Cell Signalling Technologies      | 4370                |
| <b>Active Caspase 3</b>            | Rabbit         | 1:200           | SigmaAldrich                      | C8487               |
| <b>pCDK5</b>                       | Rabbit         | 1:1000          | SigmaAldrich                      | SAB4504276          |
| <b>pAKT</b>                        | Rabbit         | 1:2000          | Upstate Cell Signalling Solutions | 07-310              |
| <b><math>\alpha</math>-tubulin</b> | Mouse          | 1:5000          | Abcam                             | Ab7291              |

**Table 1: Primary antibodies for Western blotting.**

## 2.6 HPLC-MS/MS

### 2.6.1 Cell Treatment

$3 \times 10^5$  HMSCs were treated for 24 hours with p5 (2.5 $\mu$ g/ml). At the end of the incubation period the cells were washed twice with PBS, detached with trypsin and seeded into a new T25 flask. After a further 24 hours of culture, the cell media was collected and replaced. This process was then repeated at 48 and 72 hours.

### 2.6.2 Cartridge Extraction

For sample extraction, a vacuum manifold was used with solid phase extraction c18 HPLC columns (Agilent Technologies). At each stage, the solutions were drawn through the cartridge using the vacuum but the cartridge was never allowed to run dry. Initially the vacuum manifold was cleaned with 70% ethanol before loading with c18 cartridges. The cartridge was then primed with methanol, followed by deionised water before the samples were added to each. The cartridges were then washed with water before elution. Each sample was eluted from the cartridge in acetonitrile with 1% ammonia. Each cartridge was then removed and each manifold entry was washed twice with acetonitrile containing 1% ammonia to ensure that all the elution was collected. Each sample was then dried under a flow of nitrogen gas before being re-suspended in acetonitrile-water-sodium acetate. The samples were then individually passed through a 15 $\mu$ m filter before being pipetted into micro-vials.

### 2.6.3 HPLC-MS/MS Analysis

Sample analysis was conducted using a time-of-flight/quadrupole-time-of-flight (TOF/Q-TOF) mass spectrometer using dual electron spray ionisation (ESI) as an ion source. For detailed parameters see *Appendix 1*.

## 2.7 MACS Cell Sorting

$1 \times 10^5$  HMSCs were seeded into 6 well plates and allowed to reach confluency. The cells were then washed twice in PBS and then treated with PEG functionalised SPIOs (Sigma-Aldrich) loaded cell media ( $2.5 \mu\text{g}/\text{ml}$ ). Each plate was incubated for 90 minutes before the cells were washed a further 3 times with PBS, detached with trypsin and then centrifuged at 300g for 8 minutes. The cells were then re-suspended in buffer (PBS, 0.5% BSA and 2 mM ethylenediaminetetraacetic acid (EDTA) diluted 1:20 in autoMACS Rinsing Solution). The cells were initially counted using an automated cell counter. The magnetic cell sorting was conducted using a MidiMACS separator with LS columns (Miltenyibiotec) and the manufacturer's protocol was followed. The two effluents collected represent the non-magnetised and the magnetised cells. Each effluent was then analysed using the automated cell counter (Biorad).

## 2.8 Transwell Migration Assay

### 2.8.1 Chemotactic Migration

Chemotactic migration of stem cells was used as a positive control.  $5 \times 10^4$  HMSCS were harvested using trypsin, centrifuged at 300g for 10 minutes and re-suspended in basal cell media containing no growth factors. This cell suspension was then seeded into the upper compartment of the transwell insert, while the lower compartment either contained complete media with 10% FBS or complete media containing 10% FBS plus FGF-2 ( $20\text{ng}/\text{ml}$ ). The cells were then incubated for 22 hours under normal growth conditions.

### 2.8.2 SPIO Facilitated Cell Migration

$5 \times 10^4$  or  $2 \times 10^4$  HMSCS were washed twice in PBS and then treated with PEG functionalised SPIOs (Sigma-Aldrich) loaded cell media ( $2.5 \mu\text{g}/\text{ml}$ ). The cells were then incubated at  $37^\circ\text{C}$  for 90 minutes, before being washed a further 2 times with PBS, detached with trypsin and centrifuged at 300g for 10 minutes. The cells were then re-suspended in complete cell media containing 10% FBS and placed in the top compartment of the transwell insert, whilst the bottom compartment

also contain complete medium containing 10% FBS. The cells were then incubated under normal growth conditions for 22 hours under a fixed magnetic field (**Figure 6**).

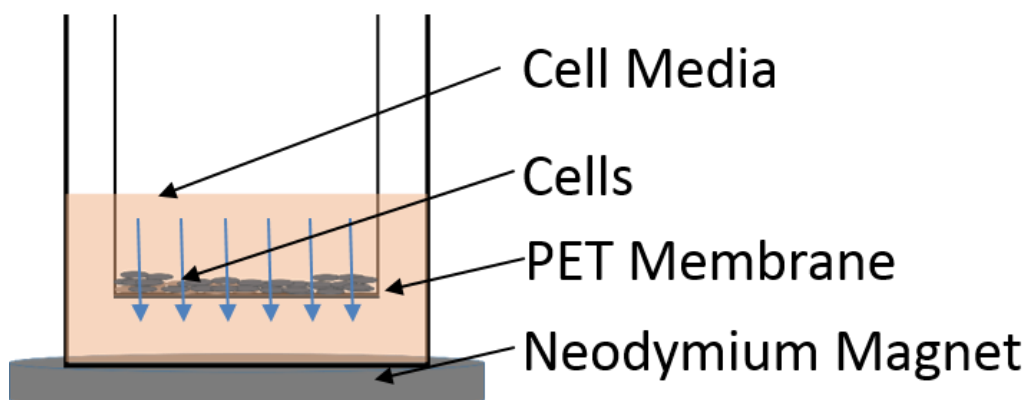


**Figure 6: Magnetic facilitated transwell migration.** Blue arrows show the direction of cell migration towards the neodymium magnet.

### 2.8.3 Determining Cell Migration

To determine the number of migrated cells, the non-migrating cells were removed by gently wiping the top of the membrane using a cotton swab. The membrane was then fixed for 10 minutes in 4% paraformaldehyde. Once fixed, the cells were stained in 0.5% crystal violet for 20 minutes washed 3 times in PBS, before images were taken using a bright-field microscope (Zeiss, Imager M1).

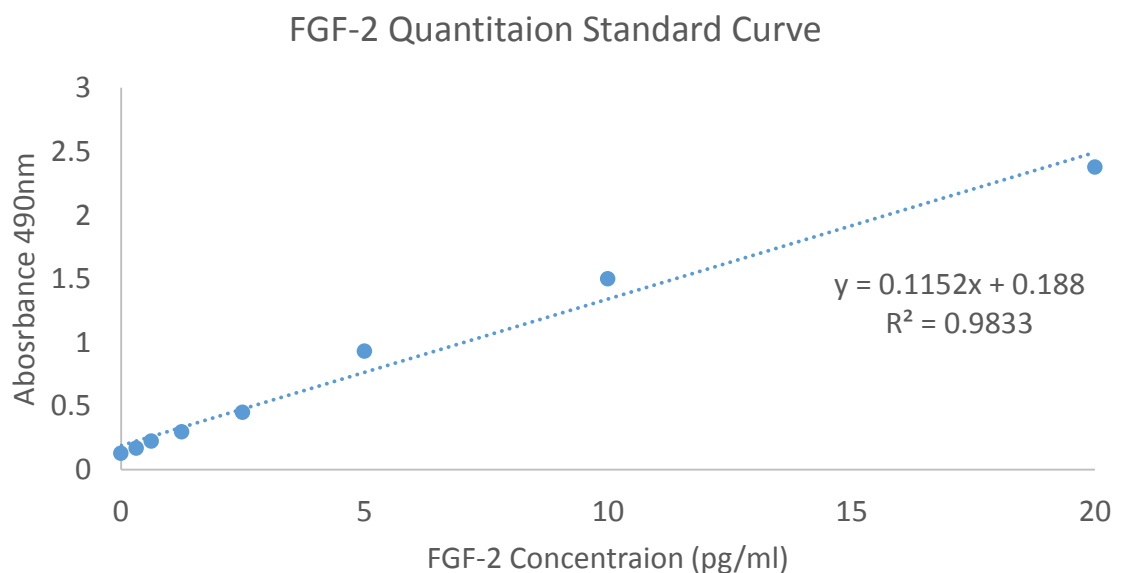
### 2.9 Statistical Analysis

Throughout this project, all graphical representation and statistical analysis was completed using Microsoft Excel. Microsoft Excel was also used to calculate all the mean, standard error of the mean, student T-test values and One-way Anova values. Threshold analysis and the comparison of optical density within the Western blot data was generated using the Image-J software and before all data was transferred to Microsoft Excel.

## Chapter 3: Results

### 3.1 Uptake and Release of FGF-2 by HMSCs

The uptake and release of FGF-2 by HMSCs was investigated using ELISA and was completed as optimisation work, in order to formulate a successful method for measuring the uptake and release of drugs by HMSCs. Initially a standard curve was produced (Figure 7) and then samples were analysed against this standard data. Uptake, release and residual levels of FGF-2 were calculated (Figure 8). Total uptake percentage of FGF-2 varied from 66-72% throughout all treatment concentrations, with residual percentages showing similar variation from 88-96% of total uptake amount. The release values varied more significantly were 5ng/ml, 10ng/ml 15ng/ml and 20ng/ml were calculated at 4%, 5%, 6.5% and 12% respectively. This data shows that the HMSCs were not only able to uptake FGF-2 but also that the release volume increased in a direct relationship with the treatment volumes. However it also important to note that the HMSCs only released 4-12% of the total uptake volume, meaning that the majority of the drug was either



processed or retained by the cells.

**Figure 7: The correlation of FGF-2 concentration and absorbance at 490nm.** The Standard curve was produced from the standards provided within the ELISA for FGF-2 analysis.

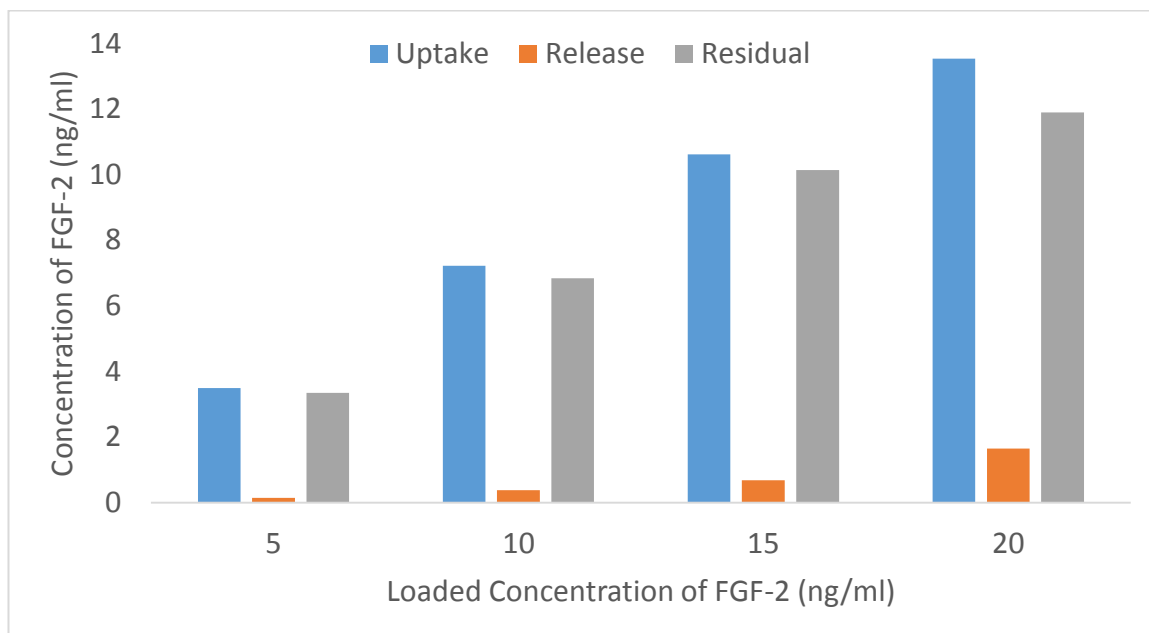


**Figure 8: The uptake, release and residual amount of FGF-2 in HMSCs when treated with varying concentrations (5-20ng) over a period of 48 hours.** The data was generated from cell media samples collected at the time of treatment (0 hours), 24 and 48 hours. The samples were then processed in triplicates by ELISA and compared to the standard curve in Figure 7. *n*=1.

### 3.2 Uptake and Release of p5 by HMSCs

#### 3.2.1 ELISA Analysis of the Uptake and Release of p5 by HMSCs

As an initial optimisation, the uptake and release levels of biotinylated p5 by HMSCs was analysed using a colorimetric HABA reagent ELISA. Although a standard curve was produced using this assay (figure 9), no consistent data was observed. Further optimisation work was then conducted using a fluorescent-based ELISA assay and two standard curves were produced, using the commercial provided standards and a serial dilution of p5 in PBS (figures 10 and 11). Using the standard curve in figure 11, cell lysates were analysed from untreated and p5 (2.5µg/ml) treated HMSCs. From the generated data (figure 12) it was observed level of biotin increased within the treated cells and when compared with the untreated samples there was an increase of approximately 3pg/cell, indicating that the cells were effectively able to uptake the p5. A separate standard curve was then produced by a serial dilution of p5 using cell media but no significant correlation was observed and therefore no reliable data could be produced to estimate the release of p5 by HMSCs (figure 13).

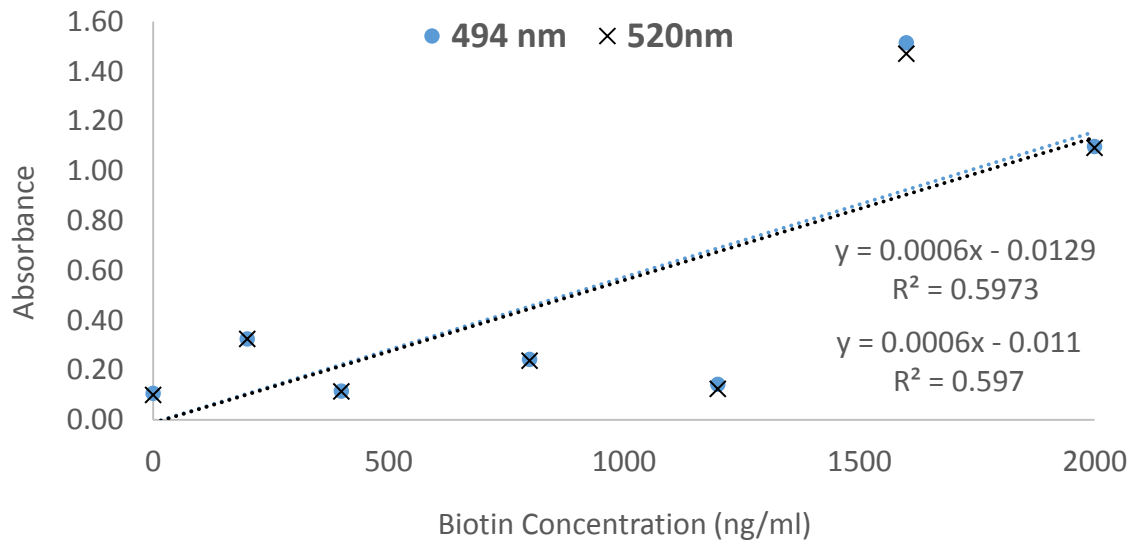


**Figure 9: The correlation of biotin concentration and absorbance at both 494nm and 520nm.** The HABA reagent was used to develop a colour change dependant on biotin to generate the standards. The standard curve was then produced at both 494 and 520nm.

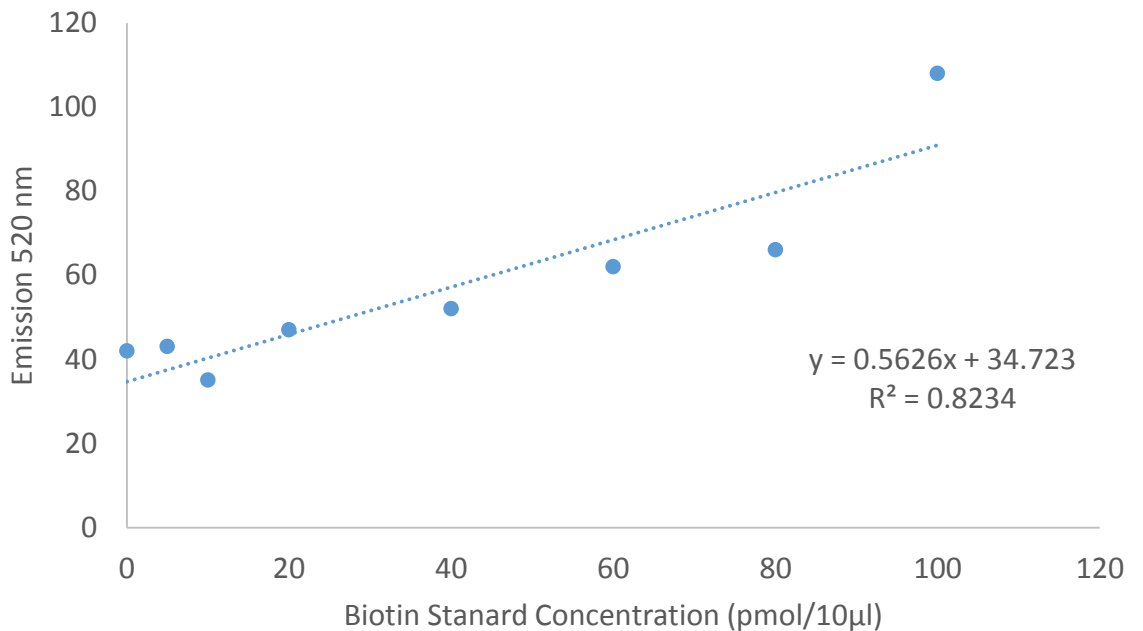


**Figure 10: Commercial Biotinylated p5 standard curve.** The correlation between biotin concentration and emission at 520nm. Standards produced from provided standards in the ELISA.

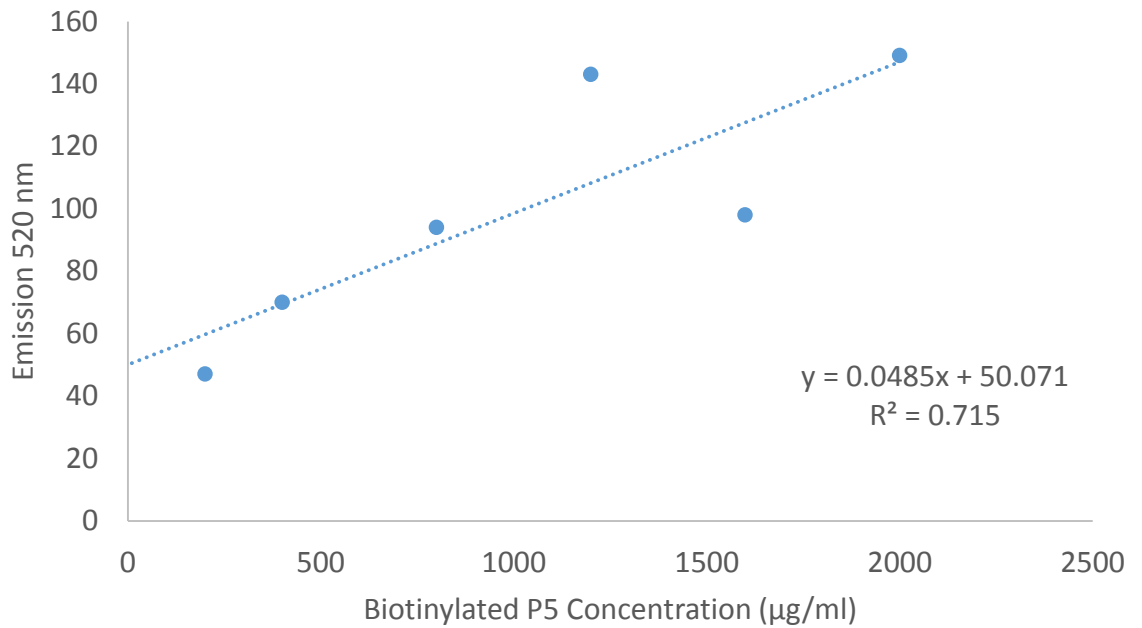


**Figure 11: Biotinylated p5 standard curve.** The correlation between biotinylated p5 and emission at 520nm. The p5 standards were produced in PBS and analysed using the ELISA. A positive correlation was observed.

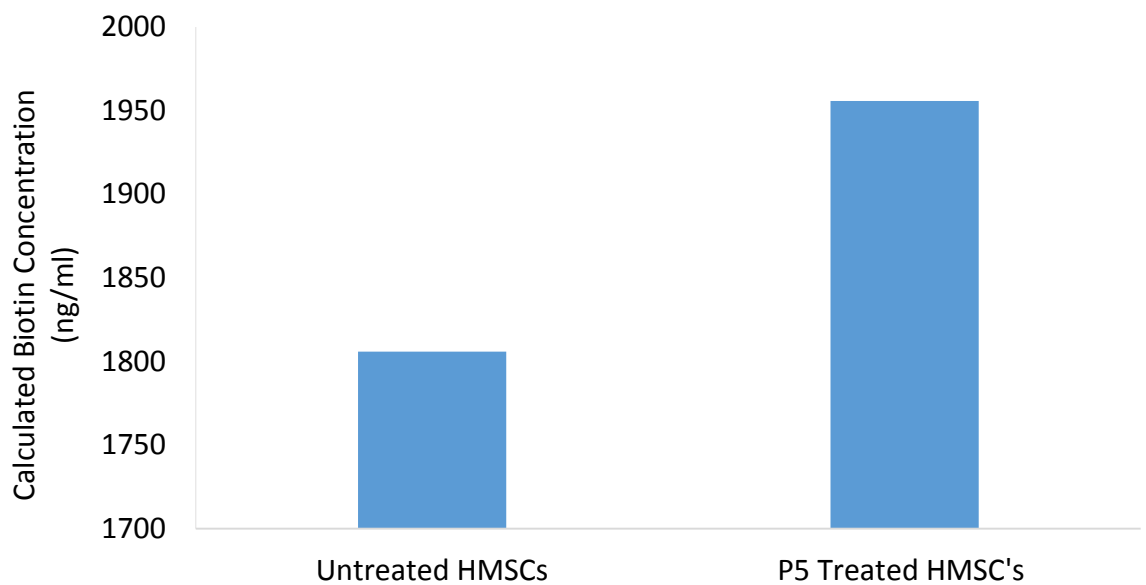


**Figure 12: Uptake of p5 by HMSCs.** Lysates produced of HMSCs comparing uptake of p5 (2.5µg/ml) in treated and untreated cells over 24 hours. This data was produced using the standard curve in figure 11. Analysis of this data, shows that the biotin concentration varied from 3.9pg/cell in treated cells compared with 3.6pg/cell in untreated cells. This was calculated by dividing the total calculated concentration by the total cell numbers.  $n=1$ .

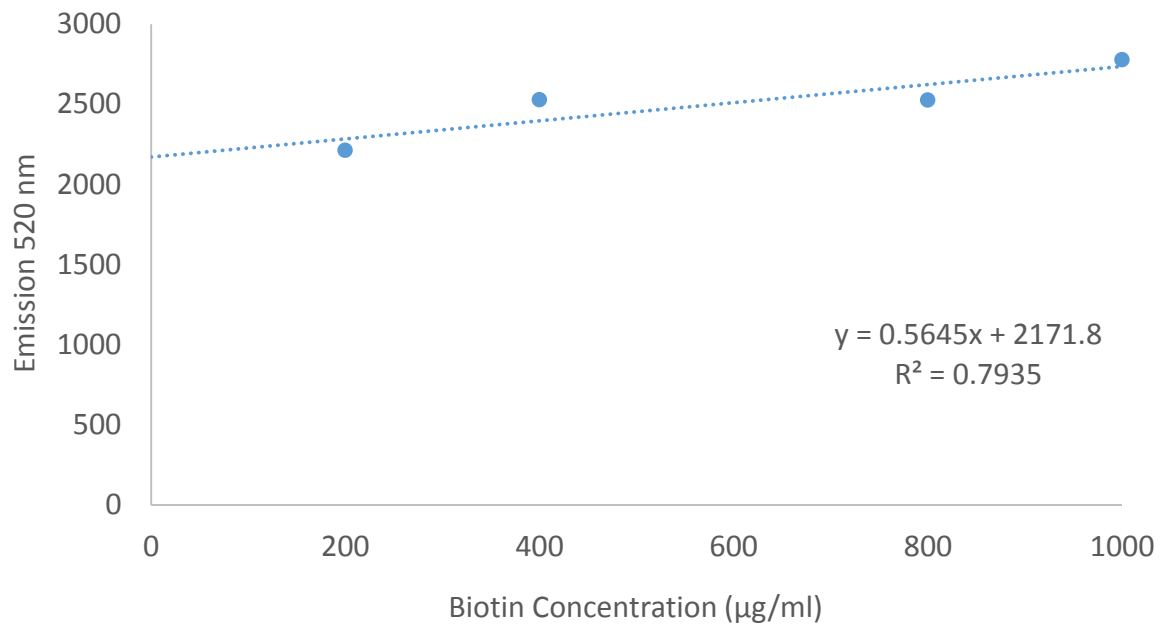


**Figure 13: Biotinylated p5 standard curve.** The correlation of biotin concentration and emission at 520nm. Standards were generated in cell media and fluorescence was generated using the ELISA. No significant correlation was observed.

### 3.2.2 Immuno-fluorescent Analysis of p5 Internalisation by HMSCs

The internalisation of p5 by HMSCs was analysed by fluorescent microscopy. Initially HMSCs were treated with 2.5µg/ml of biotinylated p5 before fixation and staining with anti-fluorescein antibody (figure 14). Accumulation of p5 (green) was shown to be internalised and localised perinuclear within the cells. HMSCs were then treated again with 2.5µg/ml of biotinylated p5 but were fixed at 4, 8, 24 and 48 hour intervals before staining with anti-fluorescein antibody (figure 15). There was an observed increase of p5 (green) internalisation at 48 hours when compared with the negative controls, although through observation alone it cannot be determined whether there is any difference between the 24 and 48 hour time points. As the significance between the timed treatments was difficult to distinguish by microscopy alone, the images were then analysed using Image-J to generate quantitative data (Figure 16). It is clearly visible from the data that the uptake of p5 by HMSCs increased over the 48 hour period.

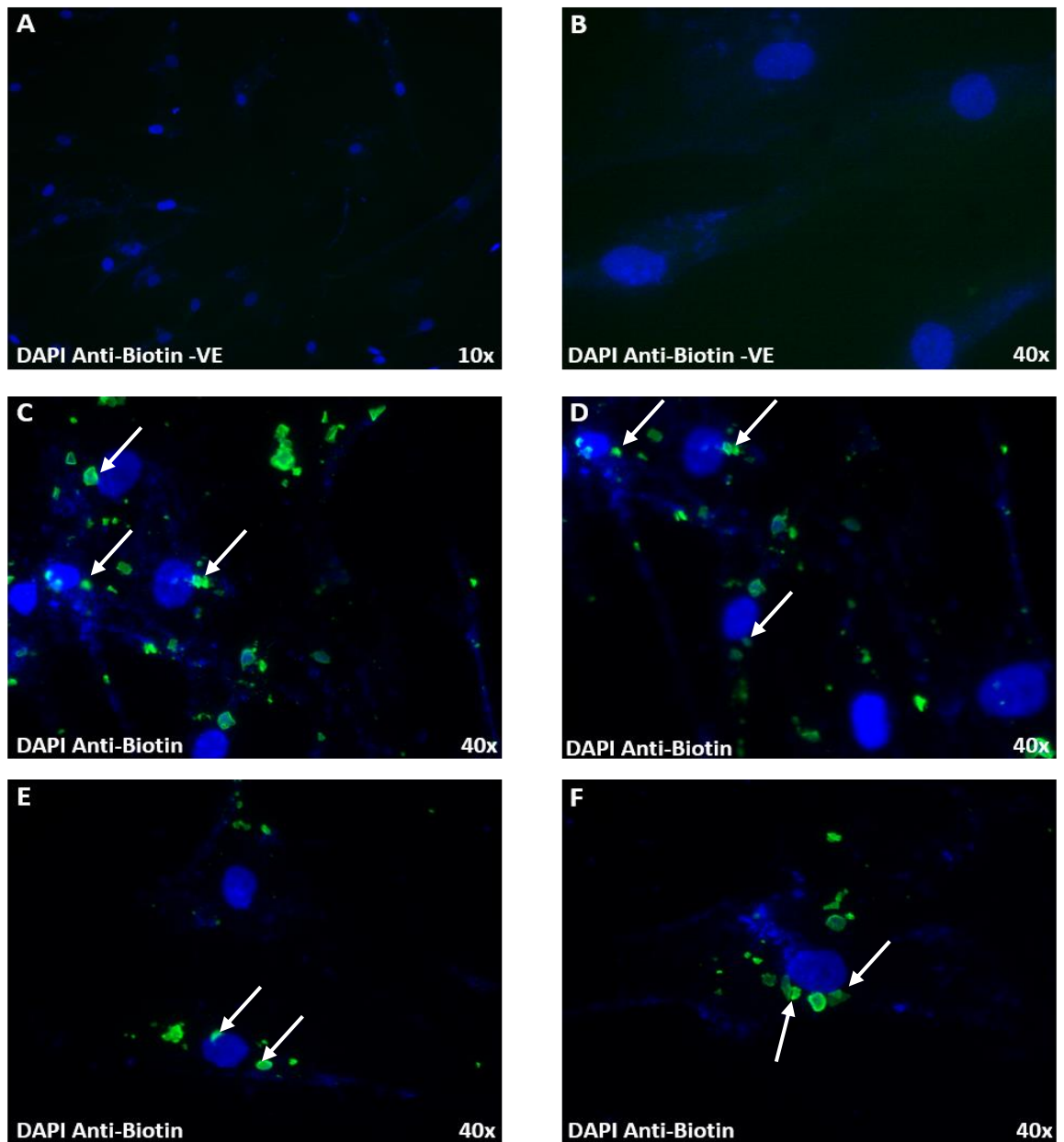


**Figure 14: Internalisation of p5 by HMSC analysed using fluorescent microscopy.** HMSCs were fixed, then treated with both DAPI (blue) and Anti-Fluorescein antibody (green). A and B are negative controls. C-F were treated with biotinylated p5 at 2.5 µg/ml for 24 hours before fixation. White arrows indicate regions of internalised p5.

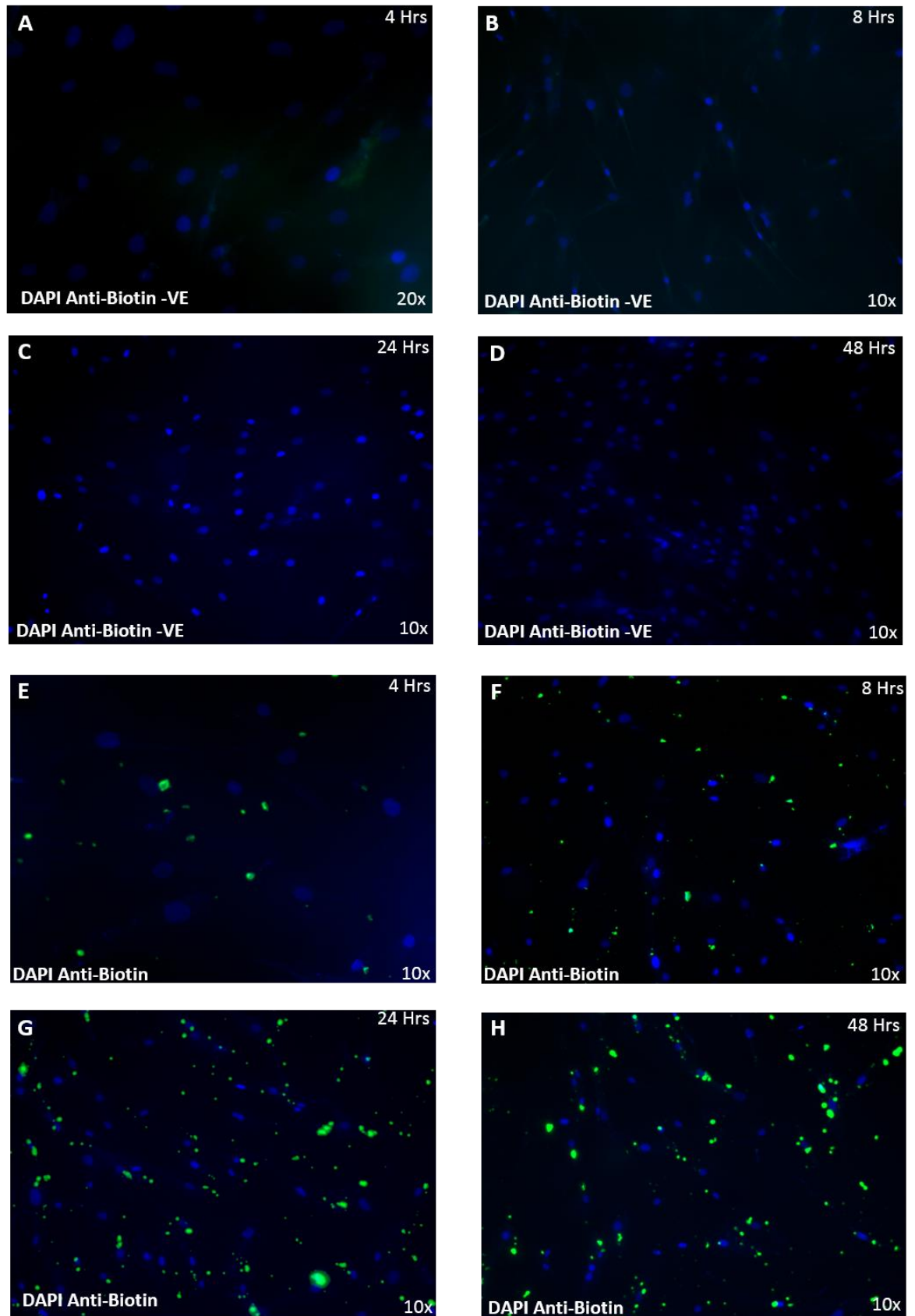


**Figure 15: Analysis of timed p5 treatment using fluorescent microscopy.** Internalisation of p5 at various time points over 48 hours was analysed.  $1 \times 10^5$  HMSCs were fixed at 4, 8, 24 and 48 hours after treatment and then treated with both DAPI (blue) and Anti-Fluorescein antibody (green). A-D are negative controls at all time points. E-H were all treated with biotinylated p5 at 2.5  $\mu\text{g}/\text{ml}$ . The amount of p5 (green) was shown to increase over the 48 hour time period.

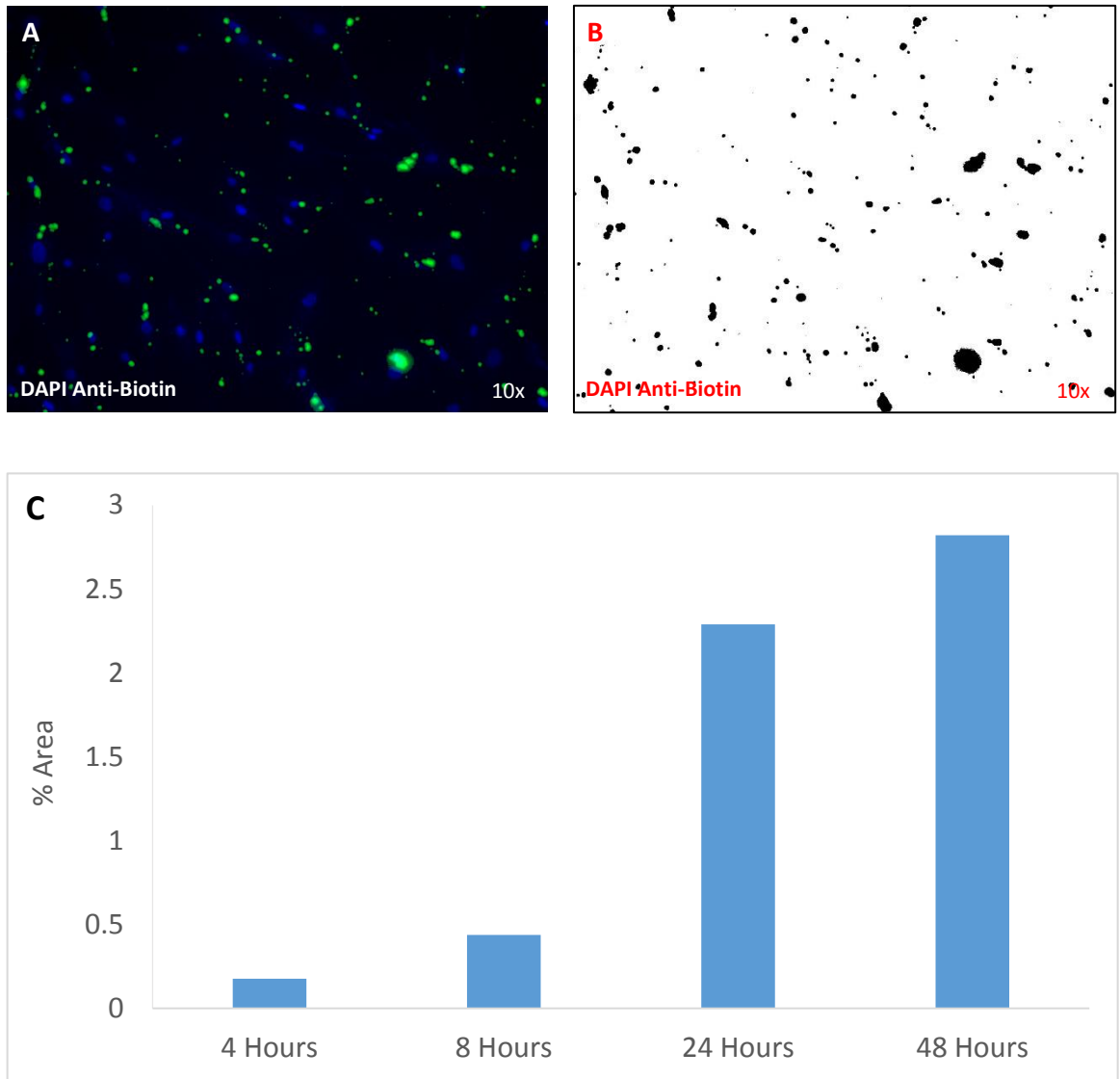


**Figure 16: Threshold analysis of p5 uptake by HMSCs.** Each time point image was acquired by fluorescent microscopy (A) and the threshold values were identified using Image-J (B). The statistical data presented is the percentage threshold area and was produced using Image-J. *n=1*.

### 3.2.3 Analysis of p5 Using HPLC-MS/MS

For quantification with an increased sensitivity, p5 was studied using the application of HPLC-MS/MS. Initially p5 was identified after HPLC in solvent using MS and then a product ion was formed using MS/MS (figure 17). Due to the sample being slightly unstable, the p5 degrades under storage conditions but the area and magnitude of the target peaks make it an effective method for p5 identification within samples.

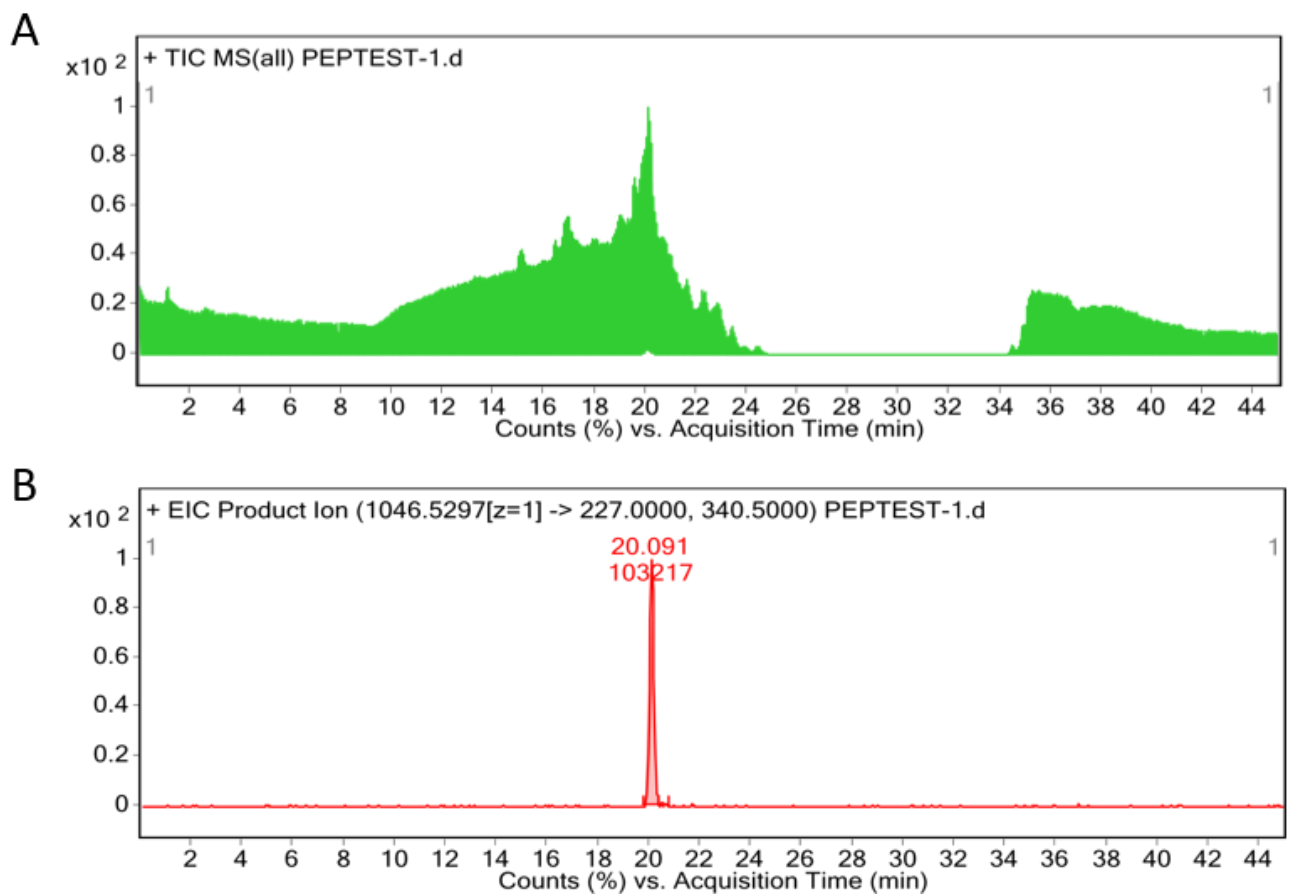
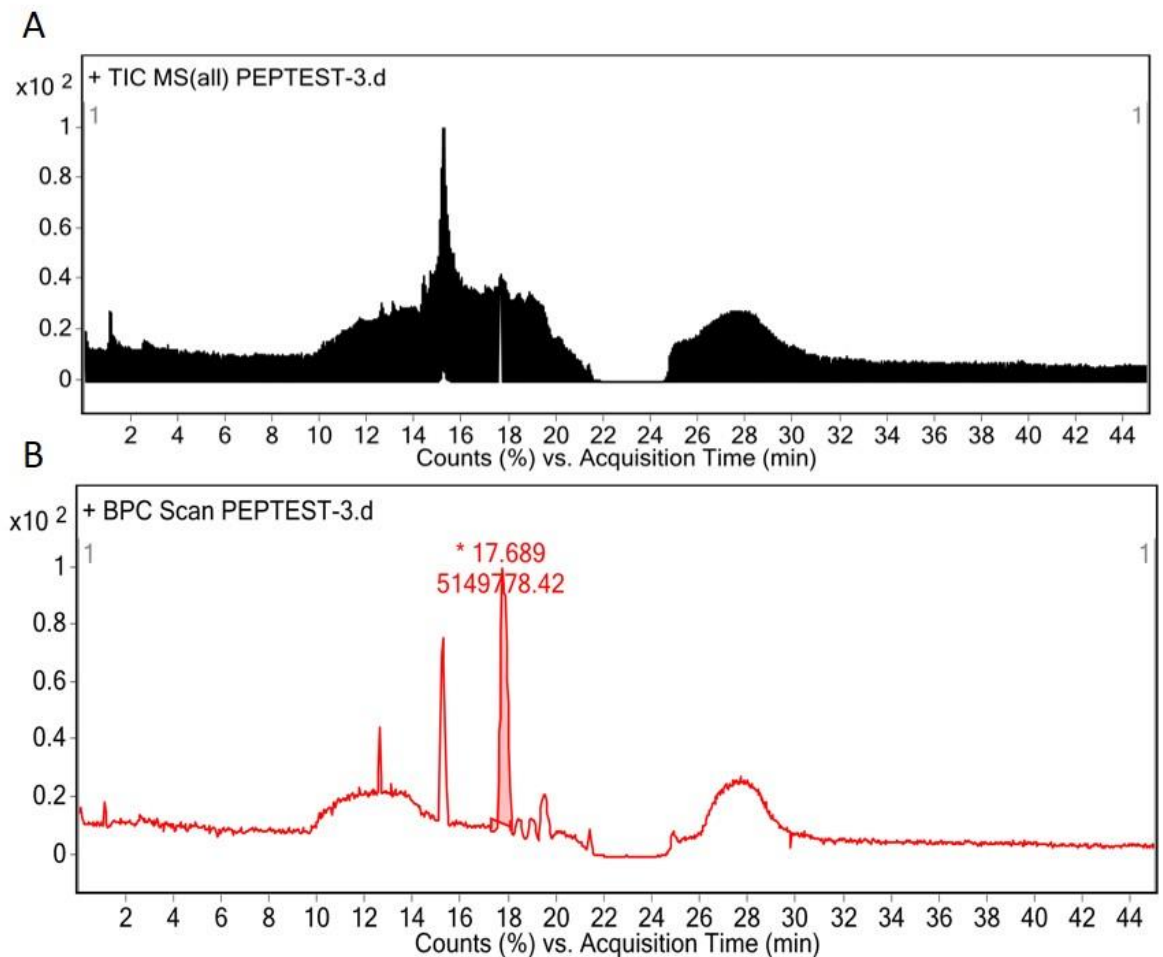


**Figure 17: HPLC-MS/MS of p5.** A: Total ion chromatogram showing summed intensity across the range of masses scanned. B: Extracted-ion chromatogram displaying product ions of the p5 peptide.

The p5 peptide was then extracted using c18 solid phase extraction cartridges after serial dilution in cell media. These samples were then ran through the MS/MS to identify whether p5 was successfully extracted from the cell media and that there was a high enough recovery after the extraction process. Figure 18 shows total ion and base peak chromatograms of extracted p5 with figure 19 showing MS/MS product ion generated from this sample. Although the sample did contain some impurities, the magnitude of the peaks from both chromatograms is significant enough to identify the p5. This data is then confirmed by MS/MS as it has generated the correct



fragment ions for the molecule.

**Figure 18: HPLC-MS/MS of p5 extracted from cell media.** A: Total ion chromatogram showing summed intensity across the range of masses scanned. B: Base peak chromatogram, showing the most intense peak from the scan.

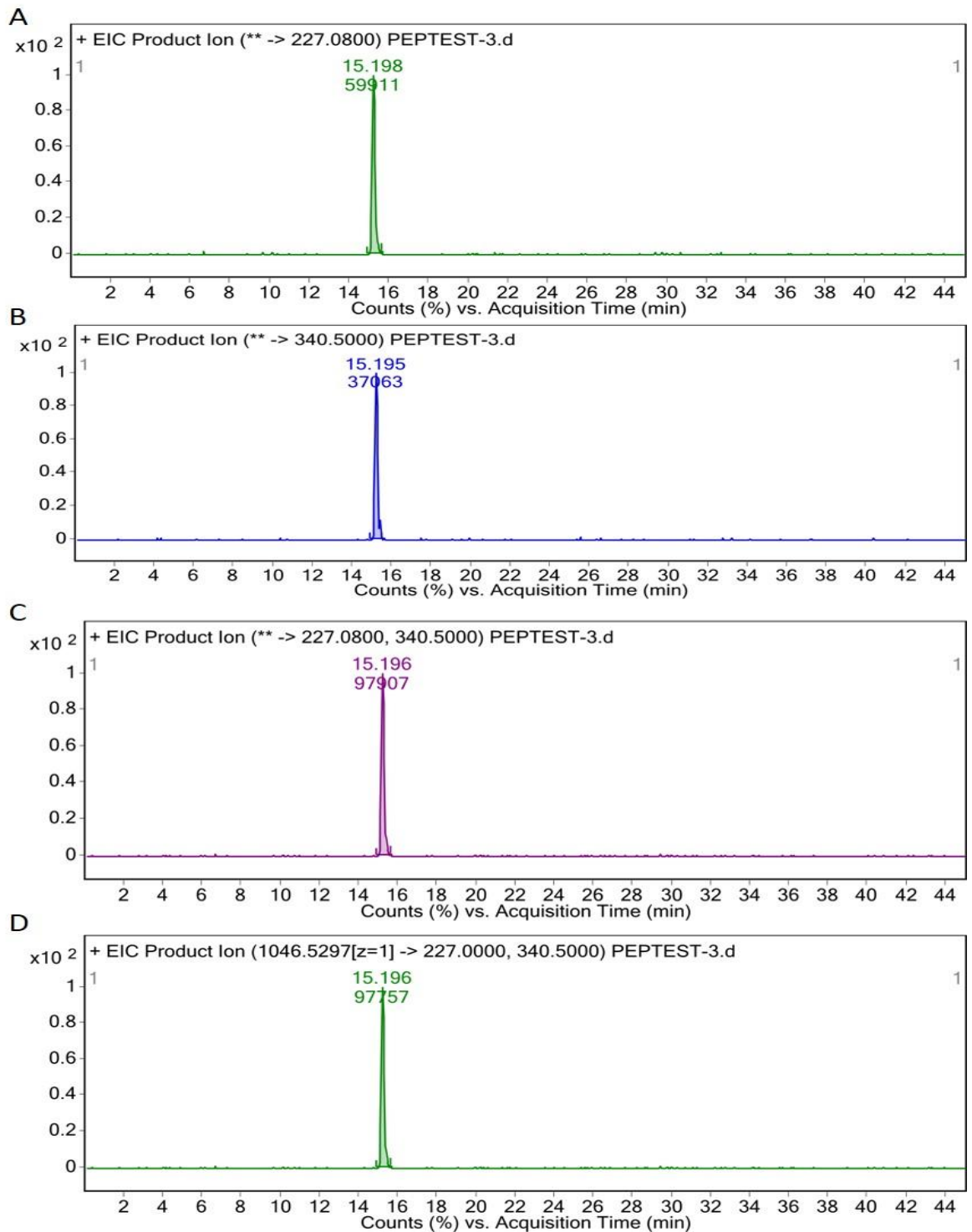


**Figure 19: Extracted-ion chromatograms of p5 extracted from cell media.** A: Intensity of the Product ion at 227.0800 kDa. B: Intensity of the product ion at 340.5000 kDa. C: Intensity of product ions 227.0800 and 340.5000 combined. D: Intensity of product ions at 227.0000, 340.5000, including the product ion at 1046.5297

### 3.3 *In vitro* Activity of p5 in an Experimental Apoptotic Model

The level of p5 activity was measured *in vitro* by using CaCl<sub>2</sub> to induce apoptosis, as an experimental model and the activation levels of certain proteins was recorded using Western blotting. Initially, to activate hyper-phosphorylation and apoptosis, HBMECs were treated 5mM of CaCl<sub>2</sub> for 30 minutes and the levels of ERK, pERK and active caspase 3 activation were observed in cells treated with CaCl<sub>2</sub> alone, or CaCl<sub>2</sub> and p5 compared to the untreated controls (figure 20). Under the 30 minute CaCl<sub>2</sub> treatment, no activation of pERK or active caspase 3 was observed, whereas there was equal levels of activation of ERK throughout all the conditions. The developed band showing  $\alpha$ -tubulin activation also confirms equal loading.

Due to the lack of observed expression of active caspase 3 and pERK, the CaCl<sub>2</sub> treatment time was reduced to 10 minutes and separate samples generated from cells treated with FGF-2 (10ng/ml) were introduced as a positive control. Under these conditions, the expression levels of pERK, ERK, pCdk5, pAKT, and active caspase 3 are shown (figure 21). Within this figure, expression of pERK appears to be most prominent within the FGF-2 treated cells, with reducing levels of expression in untreated, CaCl<sub>2</sub> treated and CaCl<sub>2</sub> and p5 treated cells respectively. Levels of pCdk5 expression however appear to be present within the positive control and CaCl<sub>2</sub> treated cells but is reduced with p5 treatment and not expressed in the control. There was also no observed expression of pAKT or active caspase 3 in any of the parameters and  $\alpha$ -tubulin shows equal loading control. When the expression of ERK, pERK and pCDK5 was compared within the treatment parameters, it is clear that there is a reduction of expression within cells treated with p5 compared to both FGF-2 and CaCl<sub>2</sub>.

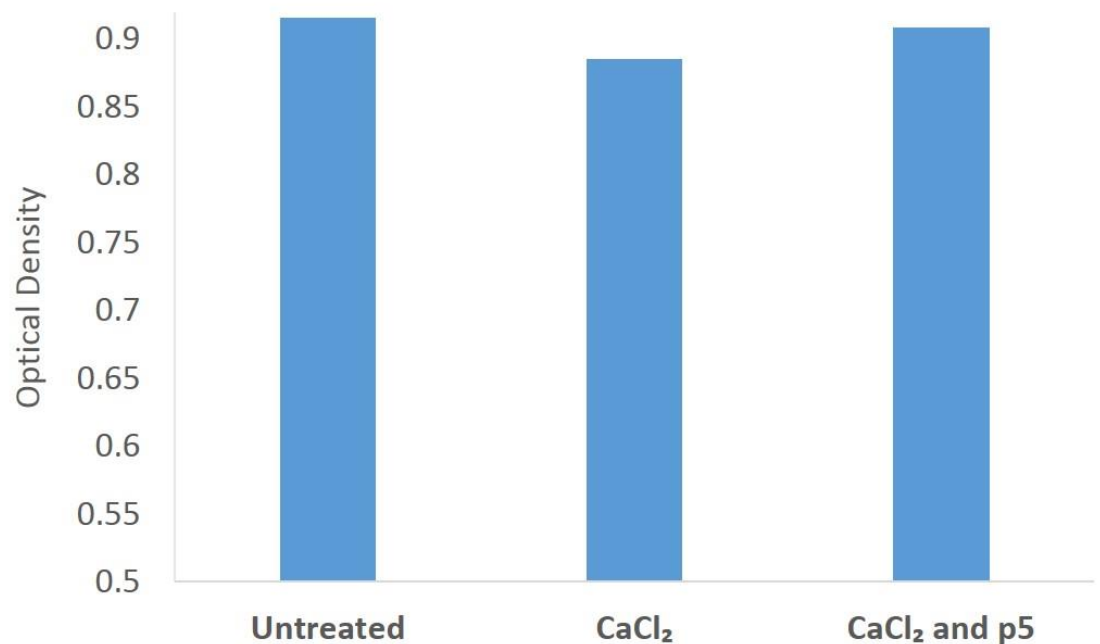
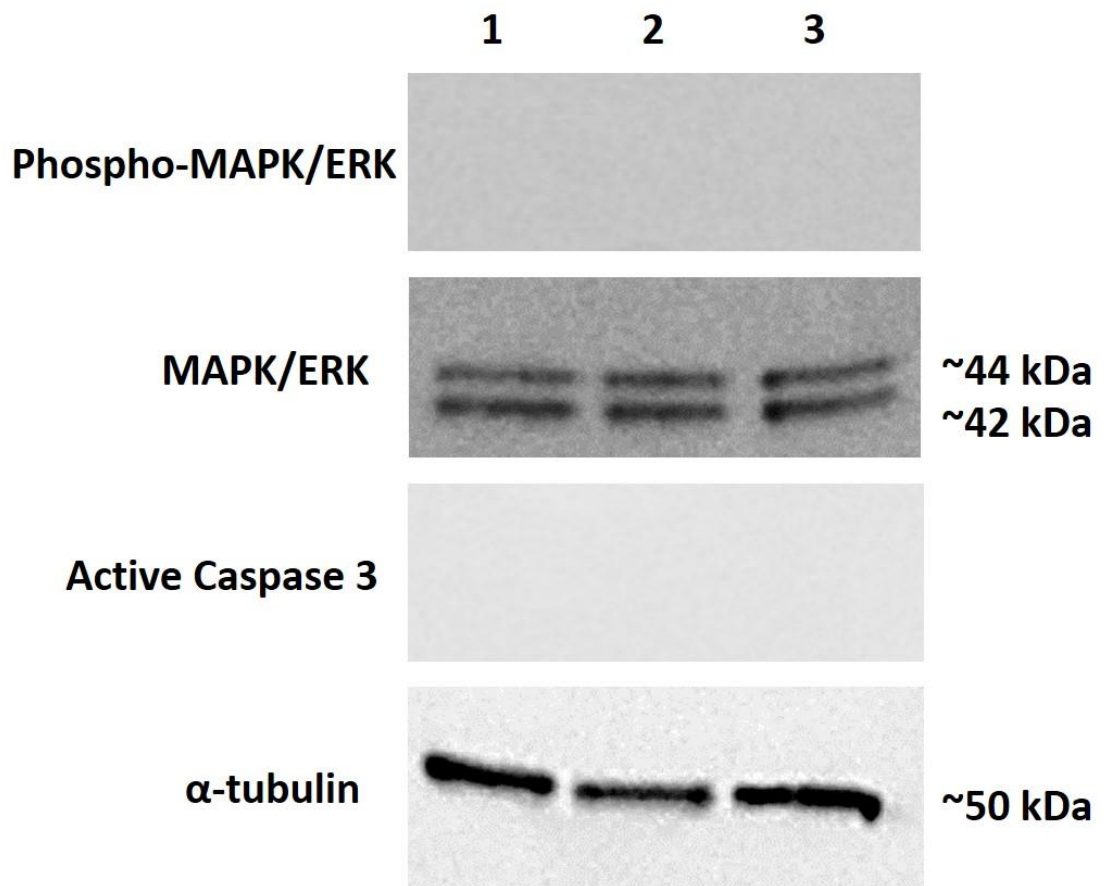


**Figure 20: Analysis of 30 minute CaCl<sub>2</sub> and p5 treatment of HMSCs by Western blot.** Lane 1, untreated cells; lane 2, cells treated with 5mM CaCl<sub>2</sub>; Lane 3, Cells treated with 5 mM CaCl<sub>2</sub> and p5 (2.5 μg/ml). There are clear bands at 44 and 42 kDa showing activation of MAPK/ERK 1 and MAPK/ERK 2 respectively. α-tubulin was used as a loading control. Analysis of optical density compared to α-tubulin, shows similar activation of ERK throughout all conditions. *n*=1.

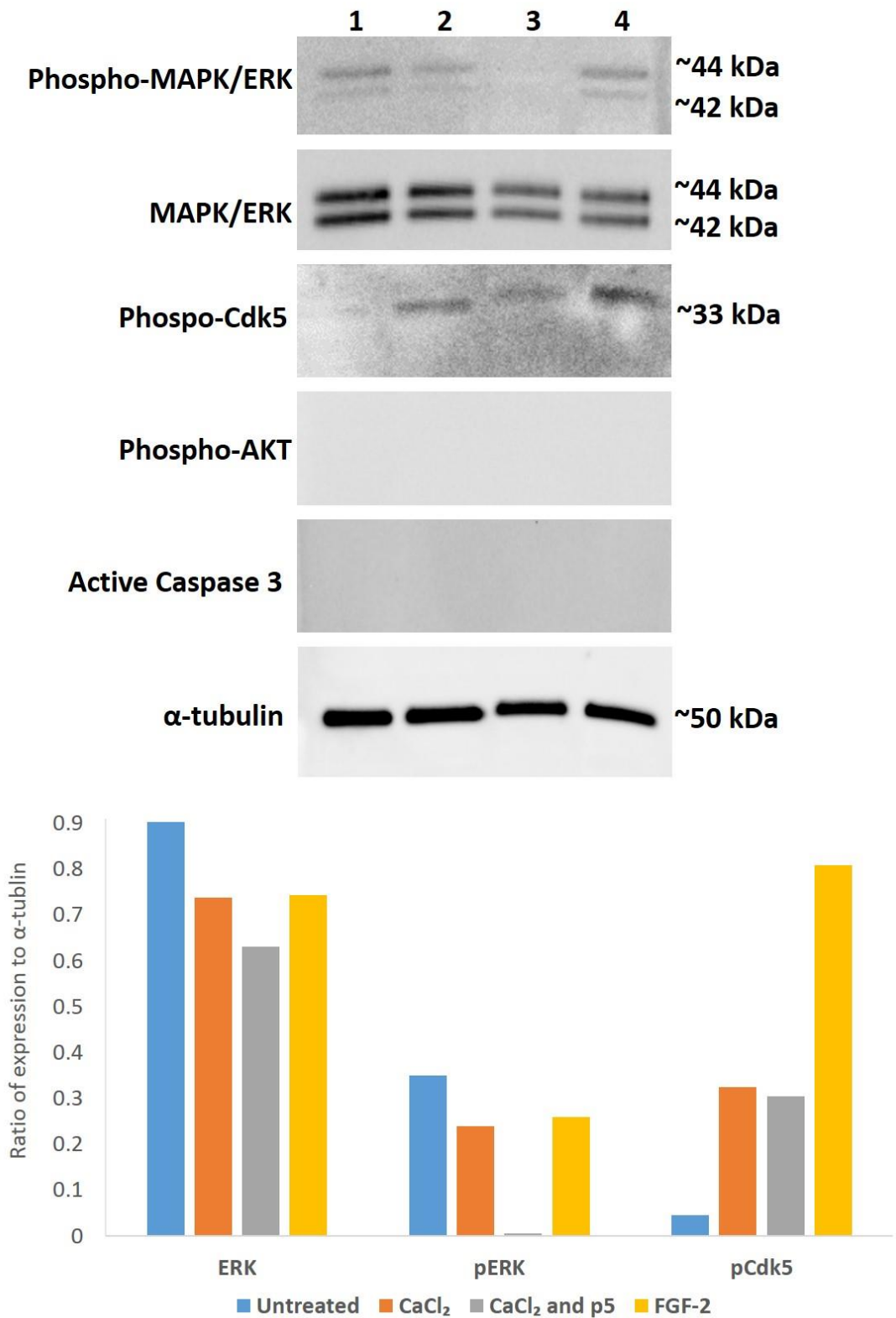


**Figure 21: Analysis of 10 minute CaCl<sub>2</sub> and p5 treatment of HMSCs by Western blot.** Lane 1, untreated cells ; lane 2, cells treated with 5mM CaCl<sub>2</sub>; Lane 3, cells treated with 5 mM CaCl<sub>2</sub> and p5 (2.5  $\mu$ g/ml); Lane 4, cells treated with FGF-2 (10 ng/ml). There is expression of pMAPK/ERK, total MAPK/ERK and phohpo-Cdk5. No expression of pAKT or active caspase 3 was observed and  $\alpha$ -tubulin was used as a loading control. *n*=1.

### 3.3 Cellular internalisation of Superparamagnetic Iron Oxide Nanoparticles

#### 3.3.1 Internalisation of SPIOs by Bovine Aortic Endothelial Cells

As an optimisation stage and in order not to waste precious HMSCs, BAECs were treated with biotin functionalised nanoparticles at 40µg/ml for 1 hour before they were fixed and treated with anti-fluorescein. When these images were investigated using fluorescent microscopy, internalised SPIOs were clearly visible within the cells (figure 22).

#### 3.3.2 Internalisation of Biotin Functionalised SPIOs by Human Mesenchymal Stem Cells

After the successful results with BAECs, the methodology was then transferred to HMSCs. Again, HMSCs were treated with biotin functionalised nanoparticles at 40µg/ml for 1 hour before they were fixed and treated with anti-fluorescein. When these images were captured using fluorescent microscopy, internalised SPIOs were clearly visible within the cells compared to the control images (figure 23).

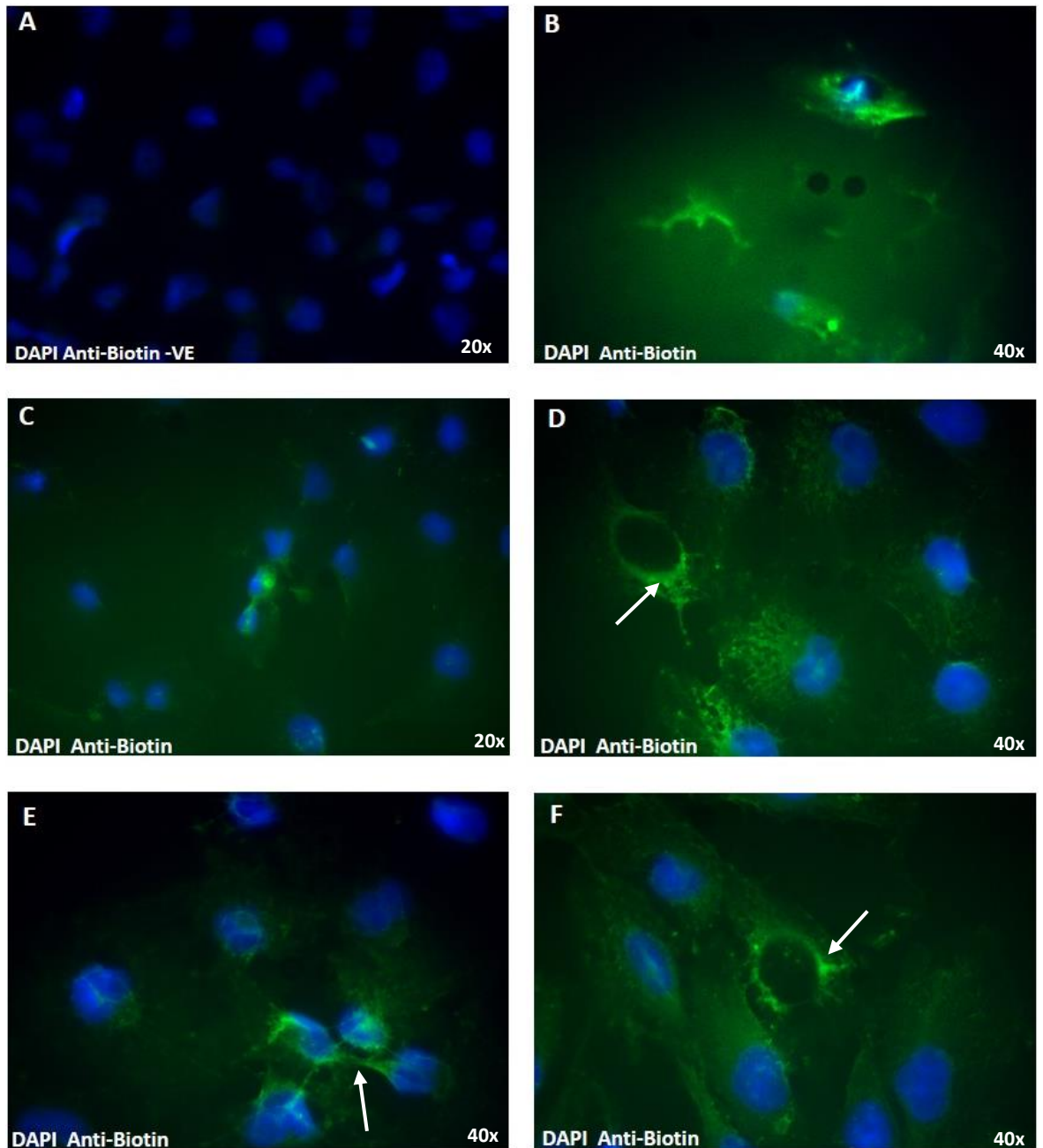


**Figure 22: Internalisation of biotin functionalised SPIOs by BAECs was analysed using fluorescent microscopy.** BAECs were treated with SPIOs at  $40\mu\text{g/ml}$  for 1 hour, fixed and then treated with both DAPI (blue) and Anti-Fluorescein antibody (green). A shows an untreated, negative controls. B-F show treated cells. These images suggest that the SPIOs are located throughout the cytoplasm but the white arrows indicate concentrated regions of staining that could indicate either areas of highly concentrated SPIOs or areas of non-specific fluorescence.

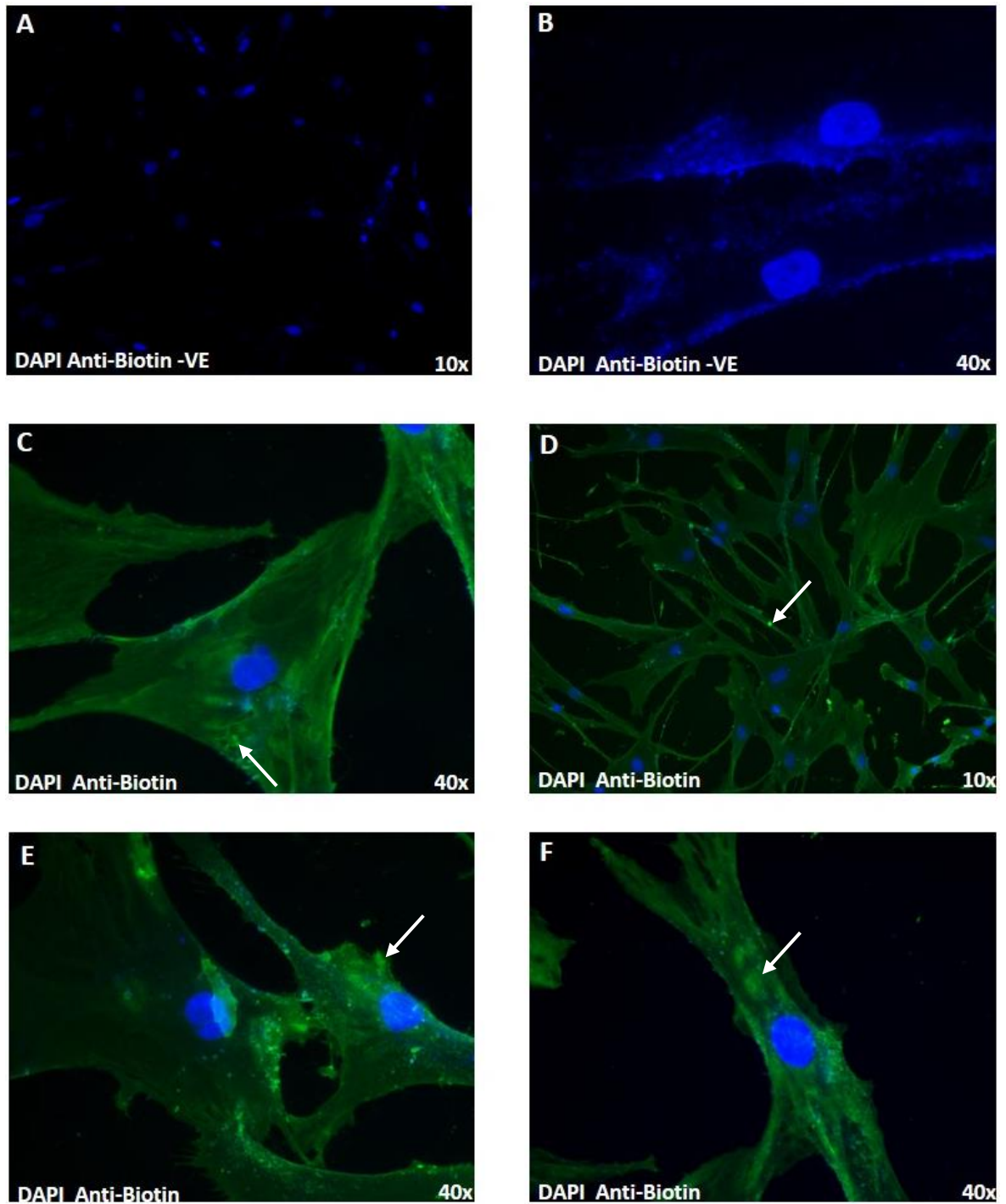


**Figure 23: Internalisation of biotin functionalised SPIOs by HMSCs was analysed using fluorescent microscopy.** HMSCs were treated with SPIOs at 40  $\mu\text{g}/\text{ml}$  for 1 hour, fixed and then treated with both DAPI (blue) and Anti-Fluorescein antibody (green). A and B show negative controls. C-F show treated cells. These images suggest that as with BAECs, the SPIOs are located throughout the cytoplasm but the white arrows indicate concentrated regions of staining that could indicate either areas of highly concentrated SPIOs or areas of non-specific fluorescence.

### 3.3.3 Internalisation of PEG Functionalised SPIOs by Human Mesenchymal Stem Cells

It was next investigated whether the HMSCs would be able to internalise PEG functionalised SPIOs as well as those coated in biotin. To explore this, HMSCs were treated with PEG functionalised SPIOs at 20µg/ml for 1 hour before they were fixed and stained with Prussian blue (Figure 24). Although the stain was successful, under observation by microscopy, there was no visual differences between the control and treated cells.

#### 3.3.3.1 Threshold analysis

Due to there been no observable difference between the control and treated cells when stained with Prussian blue, 5 random fields of view were selected using the bright-field microscope and analysed depending on their threshold. This was to determine if, statistically, there was any difference between the controls and treated cells. The threshold analysis was completed using Image-J shown in figure 25. There was no significant difference between control and SPIOs treated cells.

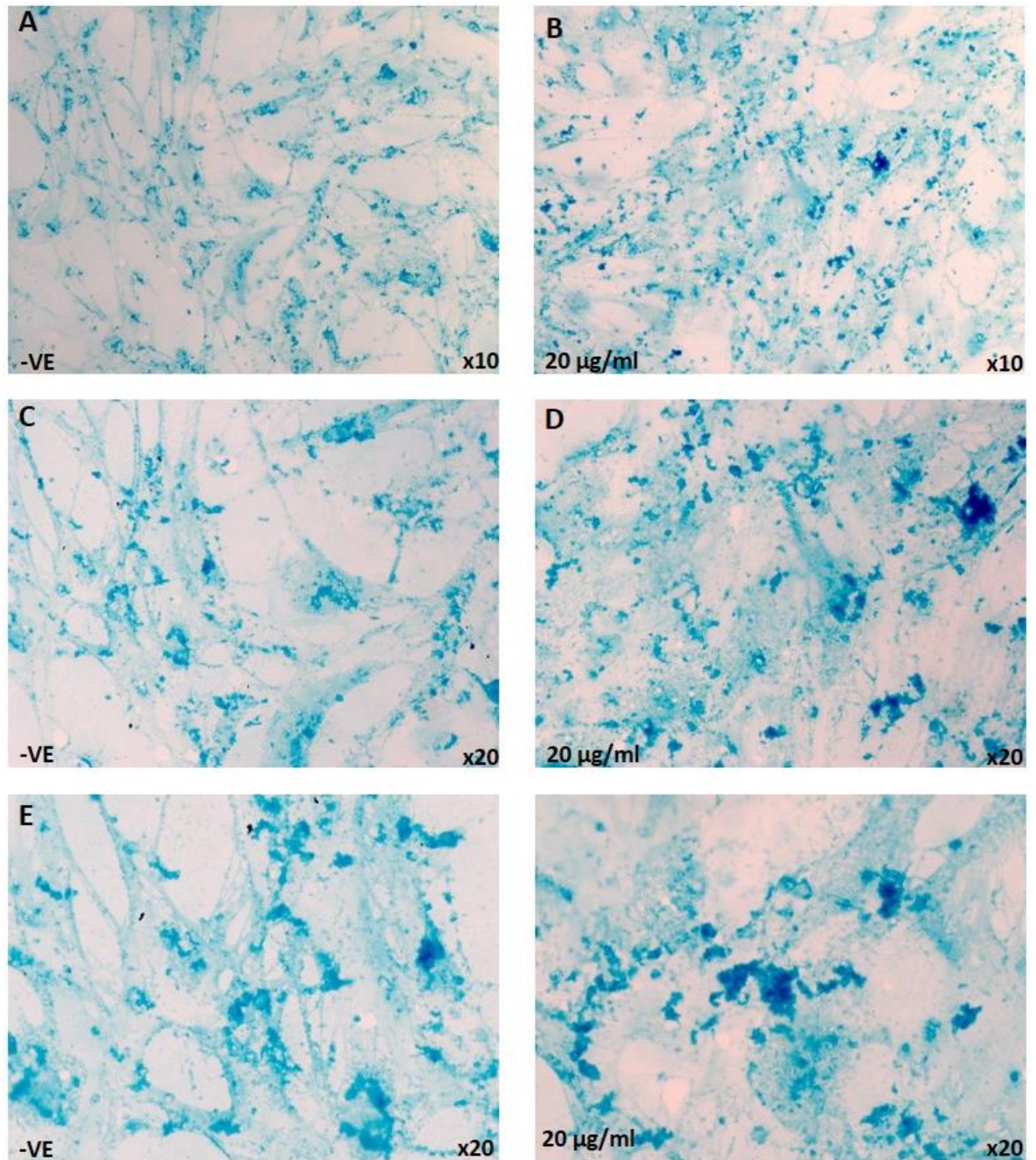


**Figure 24: Internalisation of PEG functionalised SPIOs was analysed using bright-field microscopy.** HMSCs were treated with SPIOs at 20 µg/ml for 1 hour, fixed and then stained with 5% Prussian blue. A, C and E show negative controls. B, D and F show treated cells.

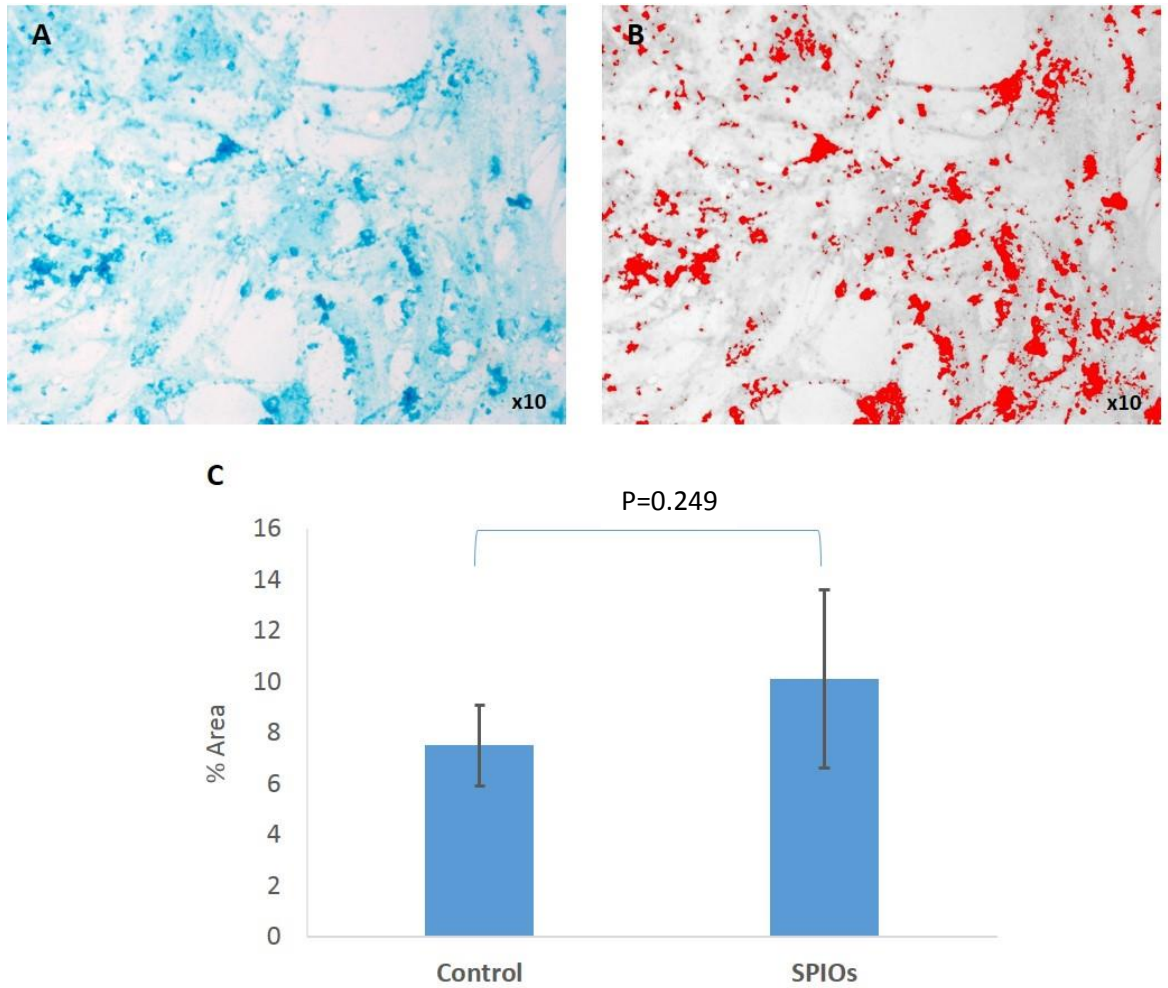


**Figure 25: Threshold analysis of Prussian blue staining.** 5 random fields of view for each slide were selected using bright-field microscopy (A) and the threshold values were identified using Image-J (B). The statistical data presented is the mean percentage threshold area  $\pm$ SEM.  $n=1$ .

### 3.4 HMSC Transwell Migration Assay

#### 3.4.1 Chemotactic Migration

In order to explore the migratory potential of HMSCs and to generate positive control data, HMSCs were initially analysed using a chemotactic transwell migration assay. Figure 26 shows successful migration of HMSCs using both complete media and complete media containing FGF-2 (20ng/ml) as a chemotactic agent.

#### 3.4.2 Magnetic Facilitated HMSC Transwell Migration

$5 \times 10^5$  HMSCs were treated with PEG functionalised SPIOs at concentrations of 20, 40 and  $100 \mu\text{g/ml}$  before been transferred into the transwell. The cells were then incubated for 22 hours in a static magnetic field before staining with 0.5% crystal violet (Figure 27). Due to the amount of migratory cells, no significant difference was observed between any of the parameters or the control. This experiment was the repeated with untreated cells as a negative control and HMSCs treated with PEG functionalised SPIOs at  $20 \mu\text{g/ml}$  (Figure 28). There was again no significant difference between the control and the treated cells. Due to the large amount of migratory cells in the previous two experiments, a reduction in transferred cells number was used to distinguish between treated and control cells.  $2 \times 10^5$  HMSC were transferred to the transwell and again, incubated within a magnetic field for 22 hours (figure 29). Although fewer cells were observed to migrate there was no significant difference between control and treated HMSCs.

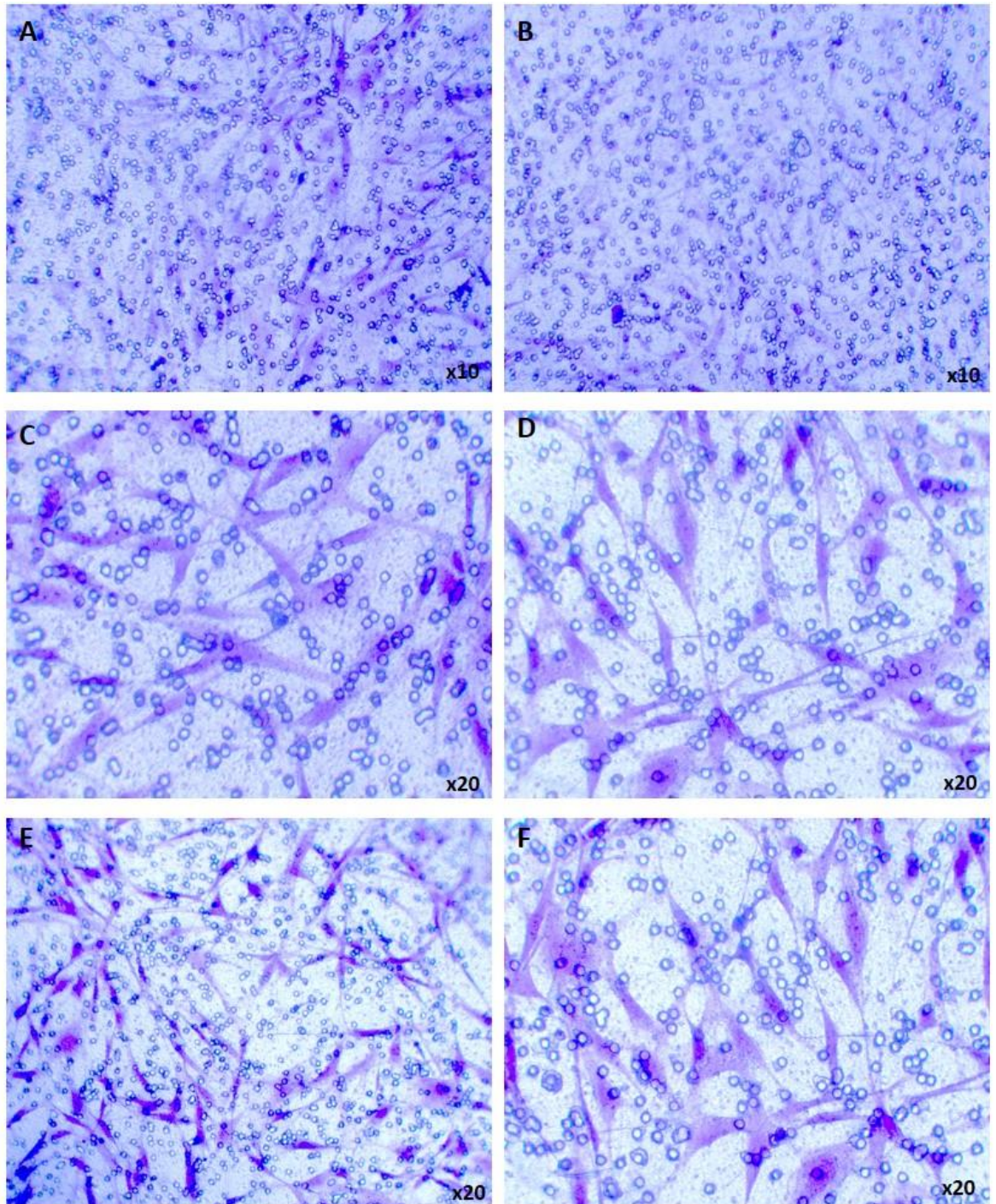


**Figure 26: Chemotactic migration of  $5 \times 10^5$  HMSCs through PET-membrane.** A, C and E show HMSCs exposed to complete media as a chemotactic agent. B, D and F show HMSCs exposed both complete media and FGF-2 (20 ng/ml) as a chemotactic agent. All inserts were stained with 0.5% crystal violet and images were taken with a bright field microscope. This data was generated in order to determine whether the HMSCs could migrate through the membrane, for this reason no negative control was used.

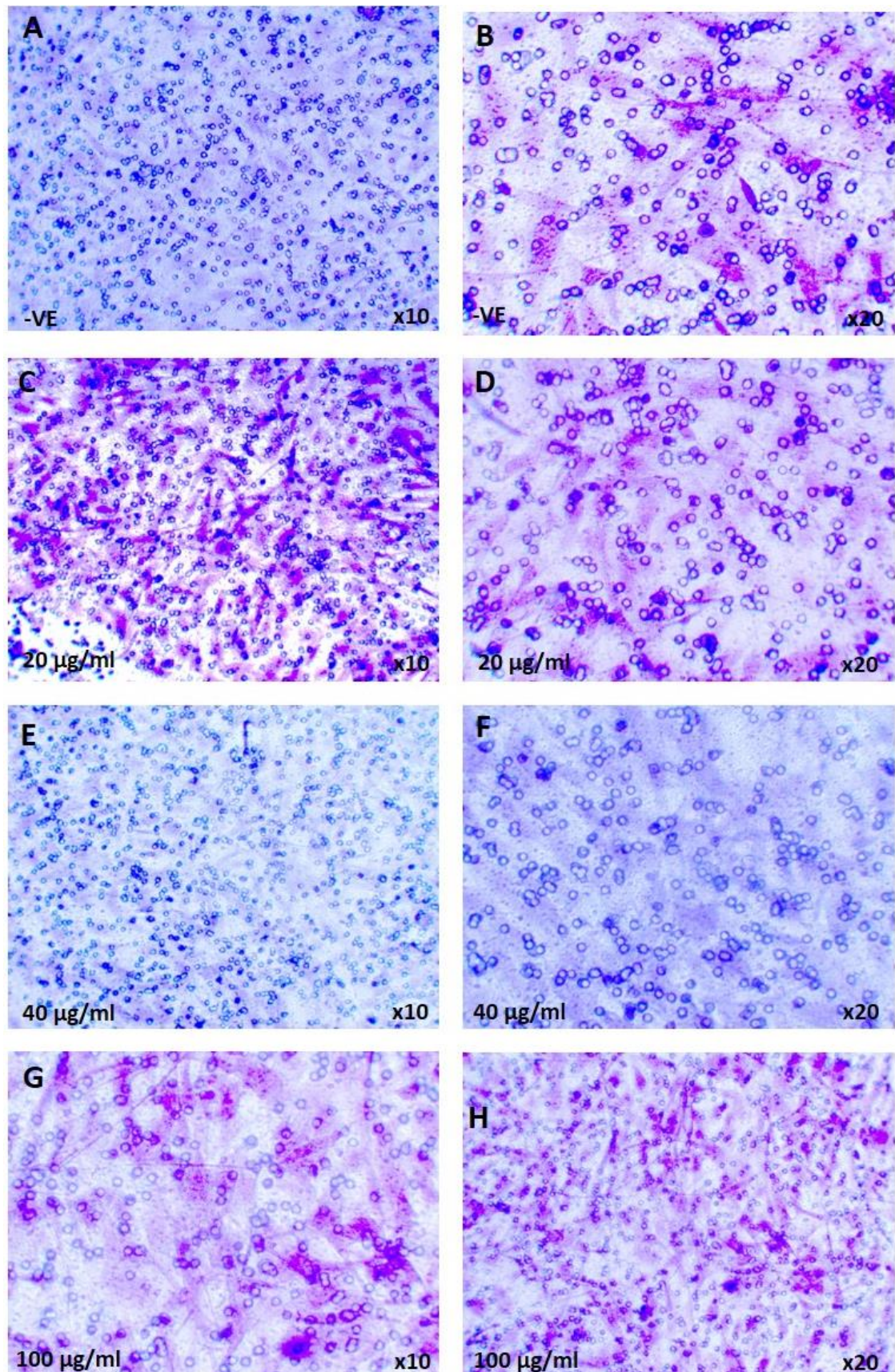


**Figure 27: Magnetic facilitated migration of  $5 \times 10^5$  HMSCs through PET-membrane.** A and B show HMSCs only as a negative control. C-H show HMSCs treated with SPIO primed cell media at 20, 40 and 100  $\mu\text{g/ml}$  before cells were transferred. All inserts were incubated under a magnetic field before they were stained with 0.5% crystal violet and images were taken with a bright field microscope.

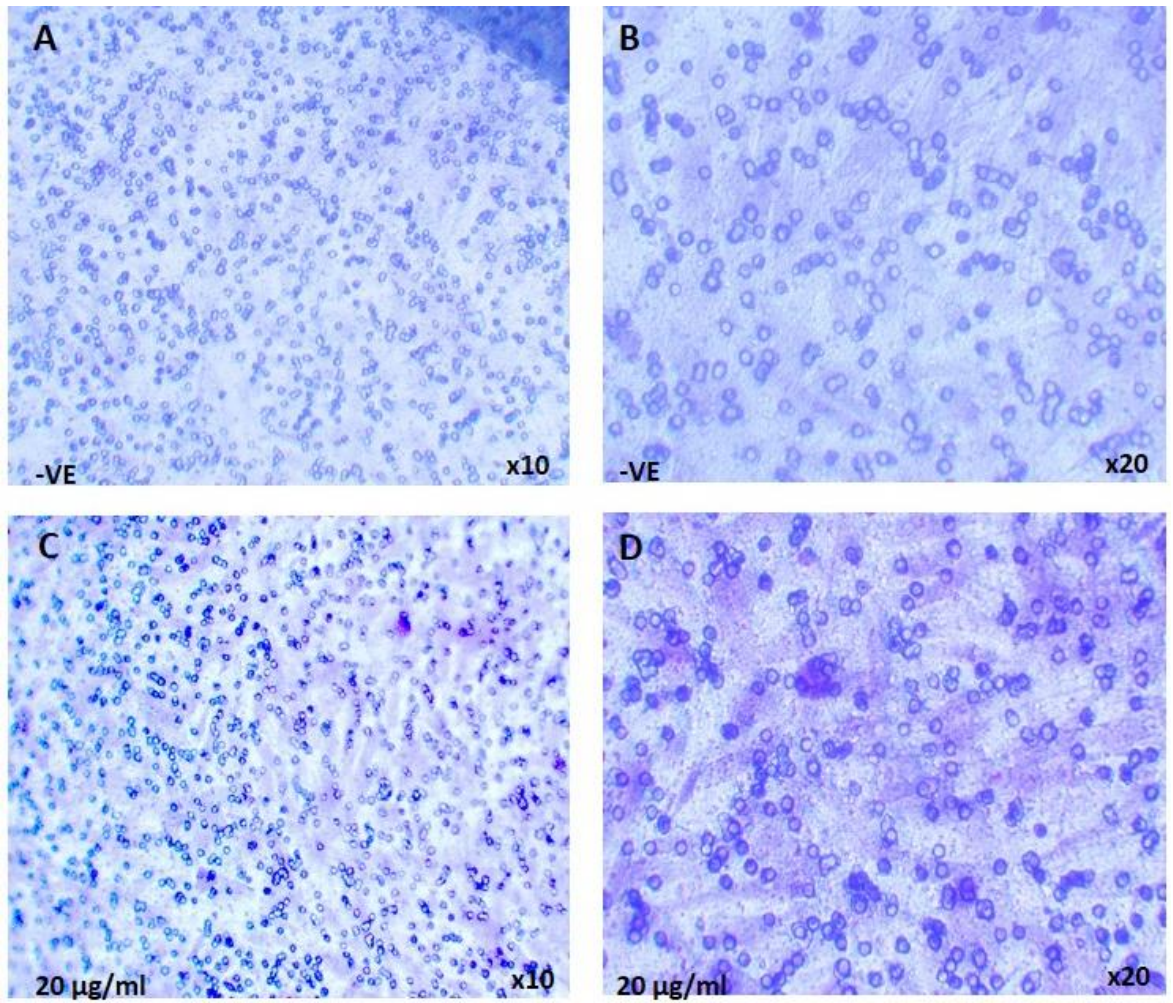


**Figure 28: Magnetic facilitated migration of  $5 \times 10^5$  HMSCs through PET-membrane.** A and B show HMSCs only as a negative control. C and D show HMSCs treated with SPIO primed cell media at 20 µg/ml before cells were transferred. All inserts were stained with 0.5% crystal violet and images were taken with a bright field microscope.

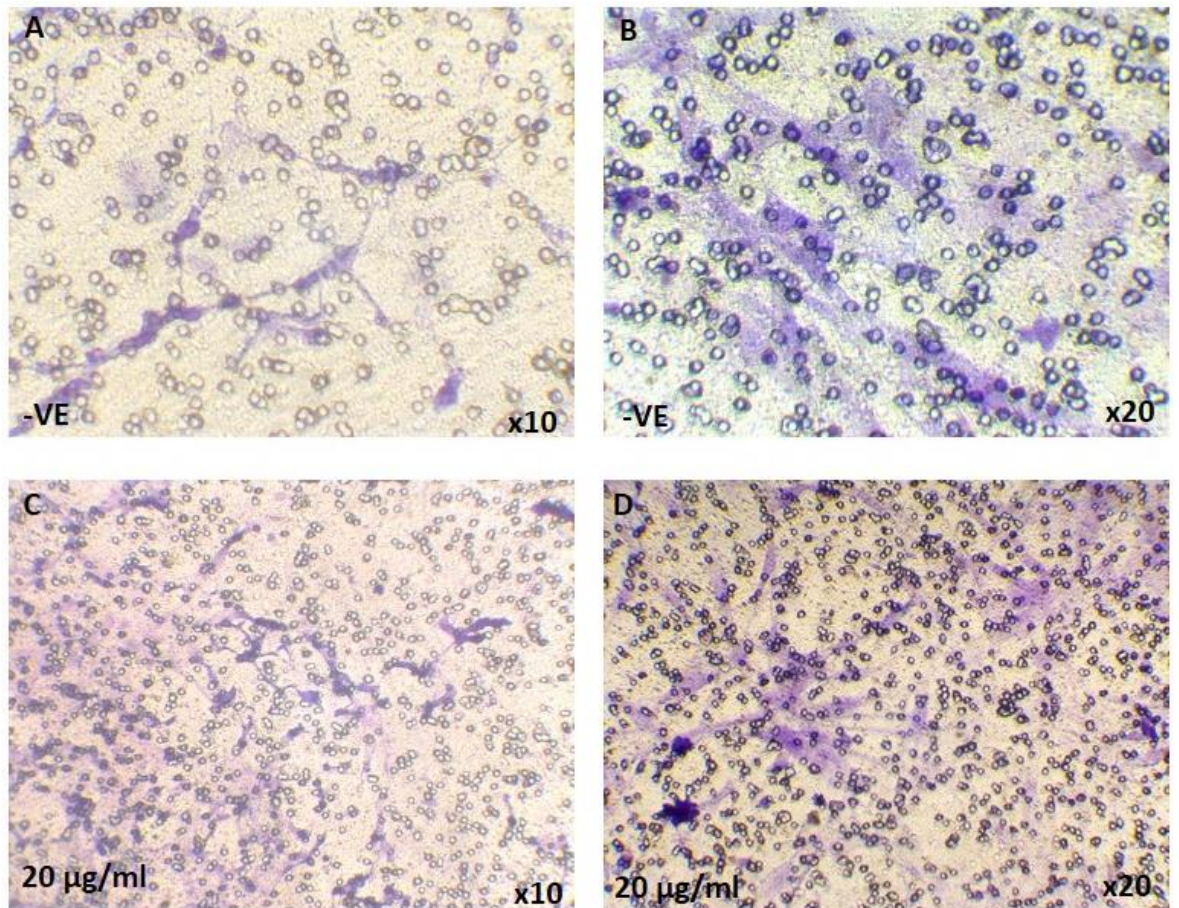


**Figure 29: Magnetic facilitated migration of  $2 \times 10^5$  HMSCs through PET-membrane.** A and B show HMSCs only as a negative control. C and D show HMSCs treated with SPIO primed cell media at 20  $\mu\text{g}/\text{ml}$  before cells were transferred. All inserts were stained with 0.5% crystal violet and images were taken with a bright field microscope.

## Chapter 4: Discussion

### 4.1 Uptake and Release of FGF-2 by Human Mesenchymal Stem Cells

FGF-2 was selected as a possible therapeutic agent, because of its potential for the reduction of apoptosis and promotion of recovery within stroke patients (Shin, *et al.*, 2006). When the uptake and release of FGF-2 by HMSCs was analysed using ELISA it was observed that the cells were not only able to uptake the drug but also to release it over a 48 hour period. This uptake and release mechanism was expected, however, when compared to other work, the uptake and residual data is much higher and the release volume was much lower than expected (Pessina, *et al.*, 2011). It was also observed that the release rates increased dependant on the treatment concentration.

One reason that the recorded data may vary from published data is that at the time of this study there is no published data that shows the uptake and release of FGF-2 by stem cells, so there is no direct comparison available. It is also important to note that due to time constraints and difficulties with initially developing substantial HMSCs cultures, this experiment was only performed once. In order to generate more reliable data, the experiment should have been repeated in at least triplicates in order to generate data with statistical significance and to remove any errors in the experimental method. There is also some doubt with the reliability of the methodology as the purchased ELISA only has a reported sensitivity of 0.07pg/ml whereas the largest recorded release volume was 1.65ng/ml meaning that the methodological errors could be significant. It is also possible that the FGF-2 is processed by HMSCs rather than being contained in vesicles and then released, as it has previously been shown have *in vivo* effects on MSCs by enhancing growth rates and increasing expression of mRNA (Ito, *et al.*, 2007).

## 4.2 Uptake and Release of p5 by Human Mesenchymal Stem Cells

This area of the project investigated the therapeutic potential of p5 that had been proposed within earlier research of the peptide CIP (Zheng, *et al.*, 2002) and how this potential could be applied to a novel stem cell delivery method. Initially there were some difficulties in developing an effective methodology for quantifying the amount of p5 that was up-taken and then released by HMSCs from the loaded cell media. The ELISA based methodology was based on the fact that due to the p5 being biotinylated, the recorded concentration of biotin was directly representative of the concentration of p5. However, when this quantification method was attempted with both a colourimetric based and a fluorescence based ELISA, the only standards that produced a significant standard curve were either the commercial provided standards or p5 standards in PBS. When p5 standards were produced in HMSC media, no data was generated using the HABA colour-metric reagent, the value of the standards did not differ from the blank control samples. Although data was generated using the fluorescence based ELISA, the constructed standard curve was not linear. However, using this fluorescence based ELISA, uptake of p5 was observed in lysates produced for HMSCs that were treated using the p5 loaded cell media when compared to the p5 standards produced in PBS. It was recorded that treated cells contained 1.96µg/ml of biotin (3.9pg/cell) compared to 1.8µg/ml (3.6pg/cell) in the control. Not only is this uptake volume much higher than expected when compared to similar work with HMSCs (Pessina, *et al.*, 2011) but there is also very little difference between the treated and the control cells, the opposite of what was expected. One possibility that could explain the interference with the ELISA based analysis and the observed amount of biotin in the control samples, is the levels of endogenous biotin and the levels of biotin present in the cell media. Biotin is a vitamin that is widely distributed throughout mammalian tissues and the levels of endogenous biotin or biotinylated proteins form a major drawback of the biotin-avidin conjugate detection system (Wood & Warnke, 1981 and Ahmed, *et al.*, 2014). Not only this but biotin has also been shown to be a required ingredient in cell culture medium (Dakshinamurti, *et al.*, 1985) and as an example, 13µg/l is added to IMDM (Sigma-Aldrich) which is a major component to the HMSC cell media.

These factors must have an effect on the results and may explain why the ELISA's were unable to generate reliable standard curves as well as possibly explaining why levels of biotin were also observed within the blank control samples. Due to these variations in endogenous levels of biotin and the concentrations of biotin that are present within the HMSC culture media, it is doubtful that any figures produced by the biotin-avidin ELISA could hold a reliable significance.

Further development was therefore needed into order to explore whether p5 could, at a basic level, be internalised by the HMSCs from the loaded culture medium. This was conducted using fluorescence microscopy and it was observed that not only was the p5 internalised by the cells but also that uptake of p5 increased over a 48 hour period. From micrographs, it is clearly visible that the p5 has been engulfed by the cells and it appears that it localised within the cytoplasm, more specifically, in vesicles within the perinuclear regions of the cytoplasm, which would agree with Baglio, *et al.*, 2012 who describes how MSCs can uptake extracellular molecules using vesicles. When comparing the timed treatment, it is visually apparent that there is an increase in p5 concentration over the 48 hour time period and when the micrographs were reviewed using threshold analysis there is an 2.64% or 15-fold increase from 4 to 48 hours. This uptake of p5 by HMSCs is similar to previously published work that has shown that the anti-cancer drug, paclitaxel, is internalised by HMSCs over a 48 hour period and that the drug accumulates within the perinuclear regions and localises within the golgi apparatus and golgi derived vesicles (Pessina, *et al.*, 2011).

Further work was also focussed on developing an accurate assay for quantifying the uptake and release of p5 by HMSCs by developing work by Pessina, *et al.*, 2011, who used HPLC analysis to detect drugs contained within cell media. However using HPLC alone cannot detect samples accurately with a nanogram range but by combining HPLC with tandem mass spectrometry (HPLC-MS/MS) this can be achieved. HPLC-MS/MS is regularly applied to the drug development industry as a tool for both identification and quantification (Lee & Kerns, 1999) and has also been shown to identify peptides from biological samples (Hernández-Ledesma, *et al.*, 2005). Using a trial and error method of different solvents and mass spectrometry parameters, p5 was able to be

identified using HPLC-MS/MS, when diluted directly into methanol. This provided evidence that the p5 peptide could not only be detected using this method and the peak generated in the chromatographs was significant enough, to provide reliable and definite data. This methodology was then coupled with solid phase extraction, that is used to purify samples before HPLC analysis and can be used to isolate analytes from various matrices including cell lysates and plasma (Räbina, *et al.*, 2001 and Halde, *et al.*, 2011). Using this combined method p5 was also detected after extraction from cell culture media, again with enough significance to confidently conclude p5 is present within the sample and there is a high enough concentration for further analysis. Although this method can accurately detect p5 from cell culture media, there were numerous drawbacks reaching this stage. The methodology itself is very time consuming and due to minor fluctuations within the machine and recovery rates from the extraction method, it is debatable whether this method could be applied to a large amount of samples. This current study also failed to generate any standards or to produce quantifiable data but this was solely due to time constraints of the project.

#### 4.3 Effects of p5 in Apoptotic Stroke Model

If p5 was to be applied as a stroke therapeutic agent, its effectiveness of reducing cellular apoptosis and efficiency of inhibiting Cdk5-p25 hyperactivity would be the major determining factors. In order to investigate p5 activity, the activation of certain proteins associated with apoptosis including phosphorylated Cdk5 were investigated by using  $\text{CaCl}_2$  to induce phosphorylation and apoptosis. The activation of the target proteins selected have all been shown within the apoptotic pathway; pAKT (Walsh, *et al.*, 2009), active caspase 3 (Wu, *et al.*, 2000), pERK (Cagnol & Chambard, 2010) and phosphorylated Cdk5 which is a key mediator in both cell survival and cell death (Cheung & Ip, 2004). Cells were initially treated with 5mM of  $\text{CaCl}_2$  for either 10 or 30 minutes and various levels of protein activation were observed. Under the 30 minute treatment there was equal activation of ERK within all the parameters and no activation of pERK or active caspase 3 was observed. This data suggests that no distinguishable levels of apoptosis was

initiated by the 30 minute  $\text{CaCl}_2$  treatment and due to this fact, cells treated with 10ng/ml of FGF-2 were introduced as a positive control. Under the 10 minute treatment there was varied activation of ERK, pERK and pCdk5 observed. Activation of ERK, appears to be relatively equal throughout all of the treatments and although the developed bands for pERK are faint, there is a definite reduction in activation under the p5 treatment compared with  $\text{CaCl}_2$ , control and FGF-2 treatments which was confirmed by analysing the optical density using Image-J. The developed bands for pCdk5 are also predominantly faint but there is a reduction in protein activation in lane 3 where cells were treated with p5 compared to both FGF-2 and  $\text{CaCl}_2$  treatments, which was again, confirmed by analysing the optical densities using Image-J. Despite these recorded levels of protein activation, there was no observed activation for either pAKT or active caspase 3, producing slightly contrasting results.

In consideration, it would be expected that under both the 10 and 30 minute treatment, phosphorylation and apoptosis would be observed, due to previous findings by Kusakawa, *et al.*, 2000, meaning that, hypothetically, there should be very little difference within the results. This however does not agree with the findings of this study. The evidence collected suggests that  $\text{CaCl}_2$  treatment may increase the level of ERK and Cdk5 phosphorylation but does not induce the caspase 3 or the phosphorylation of pAKT pathway. The levels of phosphorylation produced by this method were also less than expected, meaning that further optimisation work using different  $\text{CaCl}_2$  concentrations and treatment times, may generate data that is more relevant to the apoptosis seen within ischemic attack. It may also be probable that the molarity of the treatment was too high or the treatment times were too long meaning that the acidity of the  $\text{CaCl}_2$  could be denaturing the proteins rather than just inducing apoptosis. It is also important to note, that the phosphorylated proteins investigated, do occur under normal homeostasis as apoptosis is required for normal development throughout multicellular organisms (Somani, *et al.*, 2010), so from the evidence provided it cannot be concluded that the recorded phosphorylation levels are from induced apoptosis alone. It can be said however that from the data shown there is a reduction in pCdk5 expression within the p5 treated cells agreeing with previous work by Zheng,

*et al.*, 2010, that showed a reduction of pCdk5 activity in apoptotic HEK293 cells and cortical neurons.

#### 4.4 Internalisation of SPIOs by Bovine Aortic Endothelial Cells

Although for this project, bovine aortic endothelial cells hold no therapeutic potential, this preliminary work was important to generate a reliable method without wasting precious cultures of HMSCs. Previous work has shown that endothelial cells provide a very similar platform to HMSCs as they are able not only to uptake SPIOs but are also able to be manipulated by using a magnetic field (Kenzaoui, *et al.*, 2012 and Wu, *et al.*, 2013). The micrographs distinctly show that nanoparticles have been absorbed by the BAECs and that they are localised within the cellular cytoplasm. These findings also agree with previous work that has shown a similar dispersion of internalised nanoparticles after human aortic endothelial cells were treated with SPIO loaded culture medium (Ge, *et al.*, 2013).

#### 4.5 Internalisation of SPIOs by Human Mesenchymal Stem Cells

Due to the success of loading BAECs, progress was made towards effectively labelling HMSCs. As previously stated internalisation of SPIOs by HMSCs has been analysed by immuno-histology and used as an MRI contrast agent for a number of years (Ikegame, *et al.*, 2014), with the aim of this section of work being to effectively label HMSCs with two varieties of SPIOs. Immunofluorescent analysis of biotin functionalised SPIOs has shown that, similar to the BAECs, the HMSCs are able to absorb the nanoparticles and then disperse them throughout the cytoplasm. Similar results were generated previously using fluorescent microscopy by (Jasmin, *et al.*, 2001) when HMSCs were successfully labelled using dextran functionalised nanoparticles. In contrast, the analysis of PEG functionalised SPIOs by immunohistochemistry has not produced any significant findings. The micrographs show very little visual difference between the treated cells and the control samples and when the images were quantified, it was confirmed that there was no significant difference in the staining. These results also contradict recent other work that not only shows prussian blue as

a standard stain for iron oxide nanoparticles but also that internalisation of PEG functionalised nanoparticles can be visualised using this protocol (Andreas, *et al.*, 2012 and Tatiana T Sibov, 2014). There are multiple factors that could have effected this methodology but it is more than likely that there is either a major issue with the protocol such as the nanoparticles are not correctly coated and the HMSCs cannot absorb them or that the HMSCs themselves are highly rich in iron masking the nanoparticle staining. This method could also have required a further wash stage in order to remove any nonspecific binding, explaining why such similar results were observed.

#### 4.6 Magnetic Facilitated Human Mesenchymal Stem Cell Migration

The aim of this final section of the project, was to exploit the magnetic properties of the nanoparticles in order to facilitate the migration of HMSCs, with the aspirations of this technique being applied to the infarct regions of stroke, of which similar work has been shown in spinal cord injuries (Vaněček, *et al.*, 2012). To explore the migratory properties of HMSCs, a transwell chamber assay was used with various conditions including negative and positive controls. The main issue that surrounded this area of work is that the same level of migration was observed in all the experimental conditions including both positive and negative controls. In an attempt to overcome these issues, the experiment was initially repeated before being repeated again with a reduced number of seeded cells. Despite these efforts there was still no observable difference between any of the experimental conditions. One probable reason behind this may be that the HMSCs are naturally highly migratory and therefore, under any normal growth conditions would migrate through the membrane. However MSCs are only usually shown to migrate to target tissue that contain sites of stress or inflammation (Tomchuck, *et al.*, 2008) so further experimentation would be needed before any conclusions could be drawn.

## 4.6 Future Work

For this work to be applied as a therapeutic option for stroke, there are many further steps that would need to be taken. In summary, this project only contains preliminary work that has potential implications within this field but there are certain steps that could be taken to develop this work into a much broader and in-depth study. It is also important to note, that due to time constraints, costings and limited reagents, some of the experiments contained within this thesis were only completed once ( $n=1$ ). In general, a much thorough investigation surrounding this subject area could have been formulated with greater  $n$  numbers.

Initially it would be essential to formulate a method that can accurately detect the uptake and release of drugs by HMSCs. The most likely method that could be used to generate a reliable assay would be quantification by HPLC-MS/MS. To do this however, it would be necessary to generate two sets of standards in order to calculate the recovery values from the extraction process and develop the use of an internal standard to quantify how accurate the generated data would be. Once a successful method is developed, it may also be possible to simply apply it to other drugs, in order to investigate whether HMSCs can be used as a multiple drug delivery system.

There are many other drugs or potential targets that could also be applied as a combinational therapy and prime target example would be vascular endothelial growth factor (VEGF). VEGF is a pro-angiogenic growth factor that has been extensively studied within various ischemic diseases as it is not only able to facilitate blood flow recovery in ischemic regions of the brain but also exhibits neuroprotective qualities and promotes neuronal growth (Rhim, *et al.*, 2013). If the uptake and release of multiple drugs could then be quantified individually, it would also provide the opportunity to explore the potential of whether HMSCs could uptake and release multiple drugs and how effective various combinations of drugs are at promoting ischemic recovery.

Further work would also be needed in order to develop data surrounding how effective HMSC delivery of p5 is and whether dose concentration is a contributing factor in comparison with findings by Zheng, *et al.*, 2010 and Tan, *et al.*, 2015) who have shown effective promotion of

neuroprotection in both *in vivo* and *in vitro* studies. One way in which this could be completed, would be to take the primed cell media, after varying treatment concentrations, that the HMSCs have released the p5 into and use this as a parameter within the induced apoptosis model. This methodology would then explore whether p5 released by HMSCs is as effective as p5 applied directly to the *in vitro* study, similar to work done by Pessina, A. *et al.*, 2011 and Pessina, A. *et al.*, 2013. At this stage it would also be important to use multiple effective apoptosis models such as hypoxic incubation in order to ensure that p5 does not only protect against the CaCl<sub>2</sub> treatment. Future work within this study area may also benefit from using flow cytometry and a combination of apoptosis markers such as caspases or nuclear apoptosis assays in order to generate quantifiable data with statistical significance. Similar work has shown that flow cytometry can not only quantify levels of ischemia (Olano, *et al.*, 1996) but has also been shown to provide evidence of protection against ischemia (Widiapradja, *et al.*, 2014).

Multiple areas of research are also exploring the applications of SPIOs and how they can be applied to various disease pathologies, the full potential of SPIOs however is still unknown. From the work contained within this project, it would be beneficial to repeat the histochemical analysis to determine whether HMSCs can effectively uptake PEG coated SPIOs. This may be as simple as repeating the experiment with fresh reagents as there may have been issues with the nanoparticles or staining because previous work has shown that MSCs can effectively uptake PEG coated SPIOs (Wang, *et al.*, 2010 and Bull, *et al.*, 2014). The studies mentioned, however only contain work with bone marrow derived stem cells whereas this study predominantly used adipose derived stem cells, so there may be a variance in uptake of nanoparticles dependant on the lineage of the stem cells, which may provide an interesting focus for further work. It may also prove useful to quantify the loading efficiency through further threshold and statistical analysis of both PEG and Biotin functionalised SPIOs. More data about the internalisation of SPIOs could also be generated by the use of magnetic resonance imaging that has already been shown not only to successfully image nanoparticles contained with MSCs but also to track the cells within *in vivo* models (Andreas, *et al.*, 2012).

Further development would also be needed to produce model for measuring the levels of migration, facilitated by static magnetic field after HMSCs are loaded with SPIOs. This development may come from adaptations of the transwell migration assay featured in this project. Initially it would be essential to investigate different incubation parameters, such as growth factors or increased serum starvation, so that the cells are still healthy but no migration is observed within the negative controls. Further work would then be need to show that under these new conditions, HMSCs are still able to migrate under chemotactic factors in order to generate positive controls before magnetic facilitated migration could be explored. There is also the possibility of developing a new methodology by adapting wound healing models (figure 30) such as cell depletion assays or cell exclusion assays, when cells are encouraged to migrate into areas void of cells (Vedula, *et al.*, 2013).

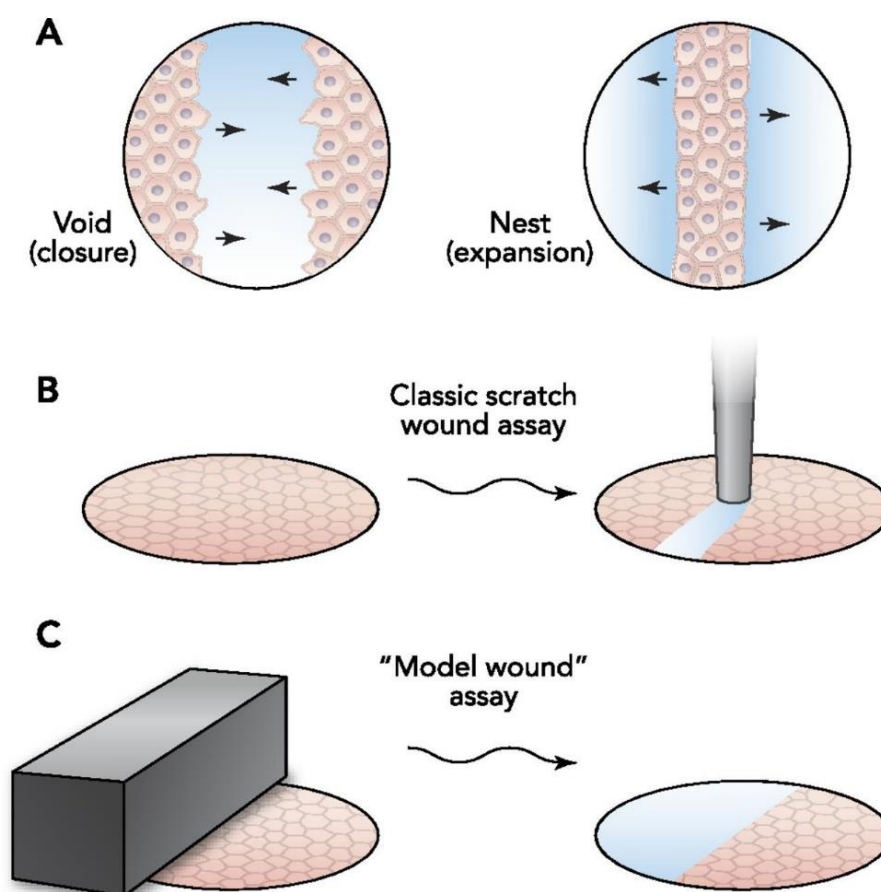


**Figure 30: Wound Healing Models.** A, arrows show various directions of cell migration, dependant on the location of the cell void. B shows a scratch assay where cells are scraped away to for a void. C shows a cell exclusion assay, where a barrier is used to create a cell void before being removed. (Vedula, *et al.*, 2013).

Another possibility for migration assays is the use of matrigel, which is by definition, a gelatinous protein mixture that allows cells to be cultured and observed within a 3D matrix. Matrigel migration/invasion assay have been used to show the migration multiple cell types such as cancer cells, pericytes and macrophages (Tigges, *et al.*, 2008 and Benton, *et al.*, 2011). As with the wound healing models, there is a possibility that this could be applied to magnetic facilitated migration of the HMSCs, proving a more in-depth understanding of this facilitated migration.

Pilot work conducted within this thesis opens the possibility to theorise, how this work and the conceivable future work could be applied to develop a possible stroke therapy. Once the uptake and release of drugs by stem cells is quantified, it is a probable hypothesis, that this drug delivery method could be applied to animal models where, for example it has already been shown that p5 promotes both neuroprotection and neurodegeneration (Sundaram, *et al.*, 2013 and Tan, *et al.*, 2015). It may also be possible to combine this drug delivery method, with targeted SPIO loaded HMSC that has also been shown to increase migration efficiency of HMSCs *in vivo* (Vaněček, *et al.*, 2012).

It is also important to note that the work contained within this thesis, may also benefit from current and future developments in genetically modified stem cells. This area of current research investigates the possibility of modifying the genetics of stem cells, for example through adenoviral transduction, to either force the expression of therapeutic genes or increase the natural production of therapeutic agents (Rhim, *et al.*, 2013). Recent work has shown that this genetic manipulation of MSCs can be used to increase the expression of vascular endothelial growth factor, placental growth factor and neurotrophic factor that provide either neuroprotection or promote angiogenesis and myogenesis after ischemic injury (Nomura, *et al.*, 2005, Liu, *et al.*, 2006 and Gao, *et al.*, 2007).



## 4.7 Conclusions

The work contained within this thesis has highlighted the potential of HMSCs as an applied therapy for stroke. The investigations into exploring whether HMSCs have the potential to uptake and release drugs and as to whether this process can be quantified has provided multiple answers but in turn has developed even more questions. From the data generated it can be concluded that HMSCs can uptake p5 and FGF-2 when exposed to the drug *in vitro* but from this study no significant quantification method could be developed without further experimentation. It was also found that p5 provides some protective characteristics when applied to this experimental apoptotic model, with observed reductions in both pCdk5 and pERK. This experimental model however would also require further development in order to accurately depict the full range of *in vitro* or *in vivo* activity of p5 when applied to areas of induced apoptosis or ischemia. The most promising area of this section of the study is the developments towards a successful methodology for the quantification of drug uptake and release by HMSCs by HPLC-MS/MS. If this methodology could be finalised, the possible applications in the development of stem cells as a drug delivery would be extremely significant.

This collection of work has also provided insights to the uptake of SPIOs by HMSCs and whether this can be used to facilitate cellular migration. The microscopic analysis of the internalisation of SPIOs provided evidence that, within this study, only nanoparticles coated with biotin were able to be visualised after absorption by the HMSCs. Further experimentation however may bring to light the potential of various types of functionalised nanoparticles and the possible differences in cellular uptakes dependant on the SPIO coating. The data that was produced using the transwell migration assay also highlighted, despite varying experimental incubation conditions that HMSCs are naturally highly migratory and with certain modifications to the assay, this work could be used to develop targeted cellular migration.

In conclusion HMSCs provide a highly attractive option for the treatment of stroke due to their many natural characteristics and their potential to be applied as a combinational therapy. The successful delivery of drugs such as p5 and FGF-2 combined with a SPIO targeting method is likely

to exert therapeutic benefits for both neuroprotection and neuro-regeneration after ischemic stroke. However, from the pilot work completed within this study, the future applications of this combinational therapy can only be speculated, but regardless of this fact, the study can provide an insight into the huge potential of HMSCs and there possible applications towards the development of stroke therapies.

## References

- Abbott, J. N., and Friedman, A. (2012). Overview and introduction: The blood–brain barrier in health and disease. *Epilepsia*, 53(6), 1-6.
- Abbott, N. J., Ronnback, L., and Hansson, E. (2006). Astrocyte–endothelial interactions at the blood–brain barrier. *Nature Reviews Neuroscience*, 7, 41-53.
- Ahmed, R., Spikings, E., Zhou, S., Thompsett, A., and Zhang, T. (2014). Pre-hybridisation: an efficient way of suppressing endogenous biotin-binding activity inherent to biotin-streptavidin detection system. *Journal of Immunological Methods*, 406, 143-7.
- Aleynik, A., Gernavage, K. M., Mourad, Y. S., Sherman, L. S., Liu, K., Gubenko, Y. A., and Rameshwar, P. (2014). Stem cell delivery of therapies for brain disorders. *Clinical and Translational Medicine*, 3(24).
- Amin, N. D., Albers, W and Pant H, C. (2002) Cyclin-dependent kinase 5 (cdk5) activation requires interaction with three domains of p35. *Journal of Neuroscience Research*, 67, 354–362
- Andreas, K., Georgieva, R., Ladwig, M., Mueller, S., Notter, M., Sittinger, M., and Ringe, J. (2012). Highly efficient magnetic stem cell labeling with citrate-coated superparamagnetic iron oxide nanoparticles for MRI tracking. *Biomaterials*, 33(18), 4515-25.
- Andreas, K., Georgieva, R., Ladwig, M., Mueller, S., Notter, M., Sittinger, M., and Ringe, J. (2012). Highly efficient magnetic stem cell labeling with citrate-coated superparamagnetic iron oxide nanoparticles for MRI tracking. *Biomaterial*, 33(18), 4515-25.
- Avraham, Y., Davidi, N., Lassri, V., Vorobiev, L., Kabesa, M., Dayan, M., Chernoguz, D., Berry, E., Leker, R. R. (2011). Leptin induces neuroprotection neurogenesis and angiogenesis after stroke. *Current Neurovascular Research*, 4(8), 313-322.
- Avraham, Y., Dayan, M., Lassri, V., Vorobiev, L., Davidi, N., Chernoguz, D., Berry, E., Leker, R. R. (2013). Delayed leptin administration after stroke induces neurogenesis and angiogenesis. *Journal of Neuroscience Research*, 2(91), 187-195.
- Baglio, S. R., Pegtel, D. M., and Baldini, N. (2012). Mesenchymal stem cell secreted vesicles provide novel opportunities in (stem) cell-free therapy. *Frontiers in Physiology*, 6(3), 359.
- Balami, J. S., Chen, R. L., Grunwald, I. Q., and Buchan, A. M. (2011). Neurological complications of acute ischaemic stroke. *The Lancet Neurology*, 6(13), 1474-4422.
- Banerjee, S., and Bhat, M. A. (2007). Neuron-Glial Interactions in Blood-Brain Barrier Formation. *Annual Review of Neuroscience*, 30, 235-258.

- Benakis, C., Garcia-Bonilla, L., Ladecola, C., and Anrather, J. (2014). The role of microglia and myeloid immune cells in acute cerebral ischemia. *Frontiers in Cellular Neuroscience*, *8*, 461.
- Benton, G., Kleinman, H. K., George, J., and Arnaoutova, I. (2011). Multiple uses of basement membrane-like matrix (BME/Matrigel) in vitro and in vivo with cancer cells. *International Journal of Cancer*, *128*(8), 1751-1757.
- Birbrair, A., Zhang, T., Wang, Z., Messi, M. L., Olson, J. D., Mintz, A., and Delbono, O. (2014). Type-2 pericytes participate in normal and tumoral angiogenesis. *American Journal of Cell Physiology*, *1*(307), c25-c38.
- Bosutti, A., Qi, J., Pennucci, R., Bolton, D., Matou, S., Ali, K., Tsai, L. H., Krupinski, J., Petcu, E. B., Montaner, J., Baradie, R. A., Caccuri, F., Caruso, A., Alessandri, G., Kumar, S., Rodriguez, C., Martinez-Gonzalez, J., and Slevin, M. (2013). Targeting p35/Cdk5 signalling via CIP-peptide promotes angiogenesis in hypoxia. *PLoS One*, *9*(8), 1371.
- Brouns, R., and De Deyn, P. P. (2009). The complexity of neurobiological processes in acute ischemic stroke. *Clinical Neurology and Neurosurgery*, *111*(6), 483-495.
- Bull, B., Madani, S. Y., Sheth, R., Seifalain, A., Green, M., and Sheifalian, A. M. (2014). Stem Cell Tracking Using Iron Oxide Nanoparticles. *International Journal of Nanomedicine*, *9*(1), 1641-1653.
- Bull, E., Madani, S. Y., Sheth, R., Seifalian, A., Green, M., and Seifalian, A. M. (2014). Stem cell tracking using iron oxide nanoparticles. *Stem cell tracking using iron oxide nanoparticles*, *9*(1), 1641-1653.
- Cagnol, S., and Chambard, J. (2010). ERK and cell death: mechanisms of ERK-induced cell death--apoptosis, autophagy and senescence. *The FEBS Journal*, *1*(227), 2-21.
- Chao, M. V. (2000). Trophic Factors: An Evolutionary Cul-de-Sac or Door Into Higher Neuronal Function? *Journal of Neuroscience Research*(59), 353-355.
- Chen, X., Huang, T., Zhang, J., Song, J., Chen, L., and Zhu, Y. (2008). Involvement of calpain and p25 of CDK5 pathway in ginsenoside Rb1's attenuation of  $\beta$ -amyloid peptide<sub>25-35</sub>-induced tau hyperphosphorylation in cortical neurons. *Brain Research*, *1200*, 99-106.
- Cheung, Z. H., and Ip, N. P. (2004). Cdk5: Mediator of neuronal death and survival. *Neuroscience Letters*, *361*(1), 47-51.
- Chopp, M., and Li, Y. (2002). Treatment of neural injury with marrow stromal cells. *The Lancet Neurology*, *1*(2), 92-100.

- Dakshinamurti, K., Chalifour, L., and Bhullar, R. P. (1985). Requirement for biotin and the function of biotin in cells in culture. *Annals of the New York Academy of Sciences*, 447, 38-55.
- Detante, O., Moisan, A., Dimastromatteo, J., Richard, M. J., Riou, L., Grillon, E., Barbier, E., Desruet, M. D., De Fraipont, F., Segebarth, C., Jaillard, A., Hommel, M., Ghezzi, C., and Remy, C. (2009). Intravenous administration of <sup>99m</sup>Tc-HMPAO-labeled human mesenchymal stem cells after stroke: in vivo imaging and biodistribution. *Cell Transplantation*, 18(12), 1369-79.
- Detante, O., Valable, S., de Fraipont, F., Grillon, E., Barbier, E. L., Moisan, A., Arnaud, J., Moriscot, C., Segebarth, C., Hommel, M., Remy, C., and Richard, M. J. (2012). Magnetic resonance imaging and fluorescence labeling of clinical-grade mesenchymal stem cells without impacting their phenotype: study in a rat model of stroke. *Stem Cells Translational Medicine*, 1(4), 333-41.
- Dewey, H. M., Thift, A. G., Mihalopoulos, C., and Carter, R. (2001). Cost of stroke in Australia from a societal perspective: results from the North East Melbourne Stroke Incidence Study (NEMESIS). *Stroke*, 32(10), 2409-16.
- Dhavan, R., and Tsai, J. H. (2001). A decade of CDK5. *Nature Reviews Molecular Cell Biology*, 2, 749-759.
- Dirnagl, U., Iadecola, C., and Moskowitz, M. A. (1999). Pathobiology of ischaemic stroke: an integrated view. *Trends Neurosci*, 22, 391-397.
- Donnan, G. A., Fisher, M., Macleod, M., and Davis, S. (2008). Stroke. *Lancet*, 1612-23.
- El Haj, A. J., Glossop, J. R., Sura, H. S., Lees, M. R., Hu, B., Wolbank, S., Van Griensven, M., Redl, H., and Dobson, J. (2015). An in vitro model of mesenchymal stem cell targeting using magnetic particle labelling. *Journal of Tissue Engineering and Regenerative Medicine*, 1(6), 724-733.
- Fabbro, D., Ruetz, S., Buchdunger, E., Cowan-Jacob, S. W., Fendrich, G., Liebetanz, J., Mestan, J., O'Reilly, T., Traxler, P., Chaudhuri, B., Fretz, H., Zimmermann, J., Meyer, T., Caravatti, G., Furet, P., and Manley, P. W. (2002). Protein kinases as targets for anticancer agents: from inhibitors to useful drugs. *Pharmacology and Therapeutics*, 2(93), 79-98.
- Faustino, J. V., Wang, X., Johnson, C. E., Klivanov, A., Derugin, N., and Wendland, M. F. (2011). Microglial cells contribute to endogenous brain defenses after acute neonatal focal stroke. *Journal of Neuroscience*, 31(36), 12992-13001.

- Font, M. A., Arboix, A., and Krupinski, J. (2010). Angiogenesis, Neurogenesis and Neuroplasticity in Ischemic Stroke. *Current Cardiology Reviews*(6), 238-244.
- Friedenstein, A. J., Gorskaja, J. F., and Kulagina, N. N. (1976). Fibroblast precursors in normal and irradiated mouse hematopoietic organs. *Experimental Hematology*, 4(5), 267-274.
- Gao, F., He, T., Wang, H., Yu, S., Yi, D., Liu, W., and Cai, Z. (2007). A promising strategy for the treatment of ischemic heart disease: Mesenchymal stem cell-mediated vascular endothelial growth factor gene transfer in rats. *The Canadian Journal of Cardiology*, 23(11), 891-8.
- Ge, G., Wu, H., Xiong, F., Zhang, Y., Guo, Z., Bian, Z., and Yang, D. (2013). The cytotoxicity evaluation of magnetic iron oxide nanoparticles on human aortic endothelial cells. *Nanoscale Research Letters*, 7(8), 215.
- Gelderblom, M., Leyboldt, F., Steinbach, K., Behrens, D., Choe, C. U., Siler, D. A., Arumugam, T. V., Orthey, E., Gerloff, C., Tolosa, E., and Magnus, T. (2009). Temporal and spatial dynamics of cerebral immune cell accumulation in stroke. *Stroke*, 5(40), 1849-57.
- Geschwind, D. H. (2003). Tau Phosphorylation, Tangles, and Neurodegeneration: The Chicken or the Egg? *Neuron*, 40(3), 457-460.
- Goldstein, L. B. (2007). Acute ischemic stroke treatment in 2007. *Circulation*, 116(13), 1504-1514.
- Gonzalez, M., and Bernad, A. (2012). Characteristics of adult stem cell. *Advances in Experimental Medicine and Biology*, 741, 103-120.
- Greenburg, D. A. (1998). Angiogenesis and Stroke. *Drug News and Perspectives*, 5(11), 265-270.
- Halde, S., Mungantiwar, A., and Chintamaneni, M. (2011). Simple, Precise and Accurate HPLC Method of Analysis for Nevirapine Suspension from Human Plasma. *Indian Journal of Pharmaceutical Sciences*, 4(73), 416-421.
- Hankey, G., Jamrozik, K., Broadhurst, R. J., Forbes, S., Burvill, P. W., Anderson, C. S., and Stewart-Wynne, E. (1998). Long-term risk of first recurrent stroke in the Perth Community Stroke Study. *Stroke*, 29(12), 2491-500.
- Hankey, G., Jamrozik, K., Broadhurst, R. J., Forbes, S., Burvill, P. W., Anderson, C. S., and Stewart-Wynne, E. G. (2000). Five-year survival after first-ever stroke and related prognostic factors in the Perth Community Stroke Study. *Stroke*, 9(31), 2080-2086.

- Hernández-Ledesma, B., Dávalos, A., Bartolomé, B., and Amigo, L. (2005). Preparation of antioxidant enzymatic hydrolysates from alpha-lactalbumin and beta-lactoglobulin. Identification of active peptides by HPLC-MS/MS. *Journal of Agricultural and Food Chemistry*, 3(53), 588-93.
- Hisanaga, S., and Saito, T. (2003). The regulation of cyclin-dependent kinase 5 activity through the metabolism of p35 or p39 Cdk5 activator. *Neuro-Signals*, 4(12), 221-9.
- Hossmann, K. A. (1994). Viability thresholds and the penumbra of focal ischemia. *Annals of Neurology*, 36(4), 557-565.
- Hu, X., Zhang, M., Leak, R. K., Gan, Y., Li, P., Gao, Y., and Chen, J. (2012). Delivery of neurotherapeutics across the blood brain barrier in stroke. *Current Pharmaceutical Design*, 18(25), 3704-3720.
- Ikegame, Y., Yamashita, K., Hayashi, S., Mizuno, H., Tawada, M., You, F., Yamada, K., Tanaka, Y., Egashira, Y., Nakashima, S., Yoshimura, S., and Iwama, T. (2011). Comparison of mesenchymal stem cells from adipose tissue and bone marrow for ischemic stroke therapy. *Cytotherapy*, 13(6), 675-685.
- Ikegame, Y., Yamashita, K., Nakashima, S., Nomura, Y., Yonezawa, S., Asano, Y., Shinoda, J., Hara, H., and Iwama, T. (2014). Fate of graft cells: what should be clarified for development of mesenchymal stem cell therapy for ischemic stroke? *Frontiers in Cellular Neuroscience*, 8(322), 1-8.
- Ito, T., Sawada, R., Fujiwara, Y., Seyama, Y., and Tsuchiya, T. (2007). FGF-2 suppresses cellular senescence of human mesenchymal stem cells by down-regulation of TGF- $\beta$ 2. *Biochemical and Biophysical Research Communications*, 359(1), 108-114.
- Jasmin, Torres, A. L., Nunes, H. M., Passipieri, J. A., Jelicks, L. A., Gasparetto, E. L., Spray, D. C., Campos de Carvalho, A. C., and Mendez-Otero, R. (2001). Optimized labeling of bone marrow mesenchymal cells with superparamagnetic iron oxide nanoparticles and in vivo visualization by magnetic resonance imaging. *Journal of Nanobiotechnology*, 9(4), 9-12.
- Jin, R., Yang, G. J., and Li, G. H. (2010). Inflammatory mechanisms in ischemic stroke: role of inflammatory cells. *Journal of Leukocyte Biology*, 87, 779-89.
- Kenzaoui, B. H., Bernasconi, C. C., Hofmann, H., and Juillerat-Jeanneret, L. (2012). Evaluation of uptake and transport of ultrasmall superparamagnetic iron oxide nanoparticles by human brain-derived endothelial cells. *Nanomedicine*, 7(1), 39-53.

- Kesavapany, S., Amin, N., Zheng, Y. L., Nijhara, R., Jaffe, H., Sihag, R., Gutkind, J. S., Takahashi, S., Kulkarni, A., Grant, P., and Pant, H. C. (2004) p35/cyclin-dependent kinase 5 phosphorylation of ras guanine nucleotide releasing factor 2 (RasGRF2) mediates Rac-dependent extracellular signal-regulated kinase 1/2 activity, altering RasGRF2 and microtubule-associated protein 1b distribution in neurons. *Journal of Neuroscience*, *24*, 4421–4431.
- Ko, J., Humbert, S., Bronson, R. T., Takahashi, S., Kulkarni, A. B., Li, E., and Tsai, L. H. (2001). p35 and p39 are essential for cyclin-dependent kinase 5 function during neurodevelopment. *The Journal of Neuroscience*, *21*(17), 6758-71.
- Krupinski, J., Issa, R., Bunjy, T., Slevin, M., Kumar, P., and Kumar, S. K. (1997). A Putative Role for Platelet-Derived Growth Factor in Angiogenesis and Neuroprotection After Ischemic Stroke in Humans. *Stroke*, *3*(28), 564-573.
- Kurozumi, K., Nakamura, K., Tamiya, T., Kawano, Y., Ishii, K., Kobune, M., Hirai, S., Uchida, H., Sasaki, K., Ito, Y., Kato, K., Honmou, O., Houkin, K., Date, I., and Hamada, H. (2005). Mesenchymal stem cells that produce neurotrophic factors reduce ischemic damage in the rat middle cerebral artery occlusion model. *Molecular Therapy*, *11*(1), 96-104.
- Kusakawa, G. I., Saito, T., Onuki, R., Ishiguro, K., Kishimoto, T., and Hisanaga, S. I. (2000). Calpain-dependent proteolytic cleavage of the p35 cyclin-dependent kinase 5 activator to p25. *Journal of Biological Chemistry*, *275*(22), 17166-17172.
- Landázuri, N., Tong, S., Suo, J., Joseph, G., Weiss, D., Sutcliffe, D. J., Giddens, D. P., Bao, G., and Taylor, W. R. (2013). Magnetic targeting of human mesenchymal stem cells with internalized superparamagnetic iron oxide nanoparticles. *Small*, *23*(9), 4017-26.
- Lee, M. S., and Kerns, E. H. (1999). LC/MS applications in drug development. *Mass Spectrometry Reviews*, *18*(3-4), 187-279.
- Lee, T., Jenner, R., Boyer, L., Guenther, M., Levine, S., Kumar, R. M., Chevalier, B., Johnstone, S. E., Cole, M. F., Isono, K., Koseki, H., Fuchikami, T., Abe, K., Murray, H. L., Zucker, J. P., Yuan, B., Bell, G. W., Herbolsheimer, E., Hannett, N. M., and Sun, K. (2006). Control of developmental regulators by Polycomb in human embryonic stem cells. *Cell*, *125*(2), 301-13.
- Liu, H., Honmou, O., Harada, K., Nakamura, K., Houkin, K., Hamada, H., and Kocsis, J. D. (2006). Neuroprotection by PlGF gene-modified human mesenchymal stem cells after cerebral ischaemia. *Brain*, *129*(10), 2734-45.

- Lobsien, D., Dreyer, A. Y., Stroh, A., Boltze, J., and Hoffmann, K. (2013). Imaging of VSOP Labeled Stem Cells in Agrose Phantoms with Susceptibility Weighted and T2\* Weighted MR Imaging at 3T: Determination of the Detection Limit. *PLoS*, 8(5).
- Luo, Y. (2011). Cell-Based Therapy for Stroke. *Journal of Neural Transmission*, 118(1), 61-74.
- Mattson, M. P., Duan, W., Pedersen, W. A., and Culmsee, C. (2001). Neurodegenerative disorders and ischemic brain diseases. *Apoptosis*, 69(6), 69-81.
- Menicanin, D., Bartold, P. M., Zannettino, A. C., and Gronthos, S. (2009). Genomic profiling of mesenchymal stem cells. *Stem Cell Reviews*, 5(1), 36-50.
- Morgan, d. O. (1997). CYCLIN-DEPENDENT KINASES: Engines, Clocks, and Microprocessors. *Annual Review of Cell and Developmental Biology*, 13, 261-291.
- Nomura, T., Honmou, O., Harada, K., Houkin, K., Hamada, H., and Kocsis, J. D. (2005). I.V. infusion of brain-derived neurotrophic factor gene-modified human mesenchymal stem cells protects against injury in a cerebral ischemia model in adult rat. *Neuroscience*, 136(1), 161-9.
- Olano, J. P., Wolf, D., Keherly, M., and Gelman, B. B. (1996). Quantifying apoptosis in banked human brains using flow cytometry. *Journal of Neuropathology and Experimental Neurology*, 55(11), 1164-1172.
- Oshima, S., Kamei, N., Nakasa, T., Yasunaga, Y., and Ochi, M. (2014). Enhancement of muscle repair using human mesenchymal stem cells with a magnetic targeting system in a subchronic muscle injury model. *Journal of Orthopaedic Science*, 3(19), 478-88.
- Paglini, G., and Caceres, A. (2001). The role of the Cdk5-p35 kinase in neuronal development. *European Journal of Chemistry*, 268(6), 1528-1533.
- Patrick, G. N., Zukerberg, L., Nikolic, M., de la Monte, S., Dikkes, P., and Tsai, L. (1999). Conversion of p35 to p25 deregulates Cdk5 activity and promotes neurodegeneration. *Nature*, 9(402), 615-22.
- Pessina, A., Bonomi, A., Valentina, C., Invemici, G., Navone, S., Cavicchini, L., Sisto, F., Ferrari, M., Ciusani, E., Crovace, A., Falchetti, M. L., Zicari, S., Caruso, A., Navone, S., Marfia, G., Benetti, A., Ceccarelli, P., Parati, E., and Alessandri, G. (2011). Mesenchymal Stromal Cells Primed with Paclitaxel Provide a New Approach for Cancer Therapy. *PLOS One*, 6(12).
- Pessina, A., Coccè, V., Pascucci, L., Bonomi, A., Cavicchini, L., Sisto, F., Ferrari, M., Vigano, L., Locatelli, A., Ciusani, E., Cappelletti, G., Cartelli, D., Caruso, A., Parati, E., Marfia, G., Pallini, R., Falchetti, M. L., and Alessandri, G. (2013). Mesenchymal stromal cells primed with

- Paclitaxel attract and kill leukaemia cells, inhibit angiogenesis and improve survival of leukaemia-bearing mice. *British Journal of Haematology*, 6(106), 766-78.
- Preynat-Seauve, O., and Krause, K. H. (2011). Stem cell sources for regenerative medicine: the immunological point of view. *Seminars in Immunopathology*, 33(6), 519-24.
- Quittet, M. S., Touzani, O., Sindji, L., Cayon, J., Fillesoye, F., Toutain, J., Divoux, D., Marteau, L., Lecocq, M., Roussel, S., Montero-Menei, C. N., and Bernaudin, M. (2015). Effects of mesenchymal stem cell therapy, in association with pharmacologically active microcarriers releasing VEGF, in an ischaemic stroke model in the rat. *Acta Biomaterialia*(15), 77-88.
- Räbina, J., Mäki, M., Savilahti, E. M., Järvinen, N., Penttilä, L., and Renkonen, R. (2001). Analysis of nucleotide sugars from cell lysates by ion-pair solid-phase extraction and reversed-phase high-performance liquid chromatography. *Glycoconjugate Journal*, 18(10), 799-805.
- Rhim, T., Lee, D. Y., and Lee, M. (2013). Drug delivery systems for the treatment of ischemic stroke. *Pharmaceutical Research*, 30(10), 2429-44.
- Rhim, T., Lee, D. Y., and Lee, M. (2013). Drug Delivery Systems for the Treatment of Ischemic Stroke. *Pharmaceutical Research*, 30, 2429-2444.
- Riegler, J., Liew, A., Hynes, S. O., Ortega, D., O'Brien, T., Day, R. M., Richards, T., Sharif, F., Pankhurst, Q. A., and Lythgoe, M. F. (2013). Superparamagnetic iron oxide nanoparticle targeting of MSCs in vascular injury. *Biomaterials*, 8(34), 1987-94.
- Saqqur, M., Tsivgoulis, G., Molina, C. A., Demchuk, A. M., Siddiqui, M., and Alvarez-Sabín, J. (2008). Symptomatic intracerebral hemorrhage and recanalization after IV rt-PA: a multicenter study. *Neurology*, 71, 1304-1312.
- Shi, L. L., Yang, W. N., Chen, X. L., Zhang, J. S., Yang, P. B., Hu, X. D., Han, H., Qian, Y. H., and Liu, Y. (2012). The protective effects of tanshinone IIA on neurotoxicity induced by  $\beta$ -amyloid protein through calpain and the p35/Cdk5 pathway in primary cortical neurons. *Neurochemistry International*, 61(2), 227-235.
- Shin, H. K., Dunn, A. K., Jones, P. B., Boas, D. A., Moskowitz, M. A., and Ayata, C. (2006). Vasoconstrictive neurovascular coupling during focal ischemic depolarizations. *Journal of Cerebral Blood Flow and Metabolism*, 8(26), 1018-1030.
- Sims, N. R., and Muyderman, H. (2010). Mitochondria, oxidative metabolism and cell death in stroke. *Biochimica et Biophysica Acta (BBA) - Molecular Basis of Disease*, 1802(1), 80-91.

- Sinden, J. D., and Muir, K. W. (2012). Stem cells in stroke treatment: the promise and the challenges. *International Journal of Stroke*, 7(5), 426-434.
- Sisto, F., Bonomi, A., Cavicchini, L., Coccè, V., Scaltrito, M. M., Bondiolotti, G., Alessandri, G., Parati, E., and Pessina, A. (2014). Human mesenchymal stromal cells can uptake and release ciprofloxacin, acquiring in vitro anti-bacterial activity. *Cytotherapy*, 2(16), 181-90.
- Slevin, M., Kumar, P., Gaffney, J., Kumar, S., and Krupinski, J. (2006). Can angiogenesis be exploited to improve stroke outcome? Mechanisms and therapeutic potential. *Clinical Science*, 3(111), 171-183.
- Somani, R., Kalantri, P., and Kadam, V. (2010). Apoptosis: Concept, mechanisms and clinical implications. *Pharmaceutical Reviews*, 8(2), 116-124.
- Sridhar, J., Akula, N., and Pattabiraman, N. (2006). Selectivity and Potency of Cyclin-dependent Kinase Inhibitors. *The AAPS Journal*, 8(1), 204-21.
- Sundaram, J. R., Poore, C. P., Sulaimi, N. H., Pareek, T., Asad, A. B., Rajkumar, R., Cheong, W. F., Wenk, M. R., Dawe, G. S., Chuang, K. H., Pant, H. C., and Kesavapany, S. (2013). Specific inhibition of p25/Cdk5 activity by the Cdk5 inhibitory peptide reduces neurodegeneration in vivo. *The Journal of Neuroscience*, 33(1), 334-343.
- Taiyoun, R., Dong, Y. L., and Minhyung, L. (2013). Drug Delivery Systems for the Treatment of Ischemic Stroke. *Pharmaceutical Research*, 30(10), 2429-2444.
- Tan, X., Chen, Y., Li, J., Li, X., Miao, Z., Xin, N., Zhu, J., Ge, W., Feng, Y., and Xu, X. (2015). The inhibition of Cdk5 activity after hypoxia/ischemia injury reduces infarct size and promotes functional recovery in neonatal rats. *Neuroscience*(290), 552-60.
- Tatiana, T. and Sibov, L. (2014). Umbilical cord mesenchymal stem cells labeled with multimodal iron oxide nanoparticles with fluorescent and magnetic properties: application for in vivo cell tracking. *International Journal of Nanomedicine*, 9, 337-350.
- Thored, P., Arvidsson, A., Cacci, E., Ahlenius, H., Kallur, T., Darsalia, V., Ekdahl, C. T., Kokaia, Z., and Lindvall, O. (2006). Persistent production of neurons from adult brain stem cells during recovery after stroke. *Stem Cells*, 24(3), 739-47.
- Tigges, U., Hyer, E. G., Scharf, J., and Stallcup, W. B. (2008). FGF2-dependent neovascularization of subcutaneous Matrigel plugs is initiated by bone marrow-derived pericytes and macrophages. *Development*, 135(3), 523-32.

- Tomchuck, S. L., Zvezdaryk, K. J., Coffelt, S. B., Waterman, R. S., Danka, E. S., and Scandurro, A. B. (2008). Toll-like receptors on human mesenchymal stem cells drive their migration and immunomodulating responses. *Stem Cells*, 26(1), 99-107.
- Tsai, L. K., Wang, Z., Munasinghe, J., Leng, Y., Leeds, P., and Chuang, D. M. (2011). Mesenchymal stem cells primed with valproate and lithium robustly migrate to infarcted regions and facilitate recovery in a stroke model. *Stroke*, 10(42), 2932-9.
- Uyttenboogaart, M., De Keyser, J., and Luijckx, G. (2009). Thrombolysis for acute ischemic stroke. *Current Topics in Medicinal Chemistry*, 7, 229-42.
- Vaněček, V., Zablotskii, V., Forostyak, S., Růžička, J., Herynek, V., Babič, M., Jendelová, P., Kubinová, S., Dejneka, A., and Syková, E. (2012). Highly efficient magnetic targeting of mesenchymal stem cells in spinal cord injury. *International Journal of Nanomedicine*, 7, 3719-3730.
- Vasconcelos-dos-Santos, A., Rosado-de-Castro, P. H., Lopes de Souza, S. A., da Costa Silva, J., Ramos, A. B., Rodriguez de Freitas, G., Barbosa da Fonseca, L. M., Gutfilen, B., and Mendez-Otero, R. (2012). Intravenous and intra-arterial administration of bone marrow mononuclear cells after focal cerebral ischemia: Is there a difference in biodistribution and efficacy? *Stem Cell Research*, 9(1), 1-8.
- Vassalli, J. D., Sappino, A. P., and Belin, D. (1991). The plasminogen activator/plasmin system. *The Journal of Clinical Investigation*, 88, 1067-1072.
- Vedula, S. R., Ravasio, A., Lim, C. T., and Ladoux, B. (2013). Collective cell migration: a mechanistic perspective. *Physiology*, 28(6), 370-379.
- Verdaguer, E., Alvira, D., Jiménez, A., Rimbau, V., Camins, A., and Pallàs, M. (2005). Inhibition of the cdk5/MEF2 pathway is involved in the antiapoptotic properties of calpain inhibitors in cerebellar neurons. *British Journal of Pharmacology*, 145(8), 1103-1111.
- Walsh, S., Gill, C., O'Neill, A., Fitzpatrick, J. M., and Watson, R. W. (2009). Hypoxia increases normal prostate epithelial cell resistance to receptor-mediated apoptosis via AKT activation. *International Journal of Cancer*, 124(8), 1871-1878.
- Wang, Y., Quercy-Jouvet, T. W., Li, A., Chak, C., Xuan, S., Shi, L., Wang, D., Lee, S., Leung, P., Lau, C. B. S., Fung, K., and Leung, K. C. (2010). Efficacy and durability in direct labeling of mesenchymal stem cells using ultrasmall superparamagnetic iron oxide nanoparticles with organosilica, dextran, and peg coatings. *Materials*, 4(4), 703-715.

- Weinstein, J. S., Varallyay, C. G., Dosa, E., Gahramanov, S., Hamilton, B., Rooney, W. D., Muldoon, L. L., and Neuwelt, E. A. (2009). Superparamagnetic iron oxide nanoparticles: diagnostic magnetic resonance imaging and potential therapeutic applications in neurooncology and central nervous system inflammatory pathologies, a review. *Journal of Cerebral Blood Flow and Metabolism*, 1(30), 15-35.
- Weishaupt, J. H., Neusch, C., and Bahr, M. (2003). Cyclin-dependent kinase 5 (CDK5) and neuronal cell death. *Cell and Tissue Research*, 312(8), 1-8.
- Weissleder, R., Elizondo, G., Wittenberg, J., Rabito, C. A., Bengele, H. H., and Josephson, L. (1990). Ultrasmall superparamagnetic iron oxide: characterization of a new class of contrast agents for MR imaging. *Radiology*, 175(2), 489-93.
- White, H., Simes, R. J., Anderson, N. E., Hankey, G. J., Watson, J. D., Hunt, D., Colquhoun, D. M., Glasziou, P., MacMahon, S., Kirby, A. C., West, M. J., and Tonkin, A. M. (2000). Pravastatin therapy and the risk of stroke. *New England Journal of Medicine*, 343(5), 317-26.
- Widiapradja, A., Santro, T., Basta, M., Sobey, C. G., Manzanero, S., and Arumugam, T. V. (2014). Intravenous immunoglobulin (IVIg) provides protection against endothelial cell dysfunction and death in ischemic stroke. *Experimental and Translational Stroke Medicine*, 6(7), 1-6.
- Wood, G. S., and Warnke, R. (1981). Suppression of endogenous avidin-binding activity in tissues and its relevance to biotin-avidin detection systems. *Journal of Histochemistry and Cytochemistry*, 29(10), 1196-1204.
- Woodruff, T. M., Thundyil, J., Tang, S., Sobey, C. G., Taylor, S. M., and Arumugam, T. V. (2011). Pathophysiology, treatment, and animal and cellular models of human ischemic stroke. *Molecular Neurodegeneration*, 11(6).
- Wu, M., Lu, L. X., Sun, X., Du, F., and Bi, Y. (2013). Comparison between dextran-coated superparamagnetic iron oxide nanoparticles and magnetoliposome on rabbit corneal endothelial cells labeling. *Advanced Materials Research*, 652, 234-240.
- Wu, W., Lee, W. L., Wu, Y. Y., Chen, D., Liu, T. J., Jang, A., Sharma, P. M., and Wang, P. H. (2000). Expression of constitutively active phosphatidylinositol 3-kinase inhibits activation of caspase 3 and apoptosis of cardiac muscle cells. *Journal of Biological Chemistry*, 275(51), 40113-9.
- Xing, C., Arai, K., Lo, E. H., and Hommel, M. (2012). Pathophysiologic cascades in ischemic stroke. *International Journal of Stroke*, 5(7), 378-385.

- Yanai, A., Häfeli, U. O., Metcalfe, A. L., Soema, P., Addo, L., Gregory-Evans, C. Y., Po, K., Shan, X., Moritz, O. L., and Gregory-Evans, K. (2012). Focused magnetic stem cell targeting to the retina using superparamagnetic iron oxide nanoparticles. *Cell Transplantation*, *6*(21), 1137-48.
- Yin, K. J., Hamblin, M., and Chen, Y. E. (2015). Angiogenesis-regulating microRNAs and ischemic stroke. *Current Vascular Pharmacology*, *13*(3), 352-365.
- Zhang, J., Cicero, S. A., Wang, L., Romito-Digiacomio, R. R., Yang, Y., and Herrup, K. (2008). Nuclear localization of Cdk5 is a key determinant in the postmitotic state of neurons. *PNAS*, *105*(25), 8772-8777.
- Zheng, Y. L., Amin, N. D., Hu, Y. F., Rudrabhatla, P., Shukla, V., Kanungo, J., Kesavapany, S., Grant, P., Albers, W., and Pant, H. C. (2010). A 24-residue peptide (p5), derived from p35, the Cdk5 neuronal activator, specifically inhibits Cdk5-p25 hyperactivity and tau hyperphosphorylation. *The Journal of Biological Chemistry*, *285*(44), 34202-12.
- Zheng, Y. L., Kesavapany, S., Gravell, M., Hamilton, R. S., Schubert, M., Amin, N., Albers, W., Grant, P., and Pant, H. C. (2005). A Cdk5 inhibitory peptide reduces tau hyperphosphorylation and apoptosis in neurons. *The EMBO Journal*, *24*, 209-220.
- Zheng, Y. L., Li, B. S., Amin, N. D., Albers, W., and Pant, H. C. (2002). A peptide derived from cyclin-dependent kinase activator (p35) specifically inhibits Cdk5 activity and phosphorylation of tau protein in transfected cells. *European Journal of Biochemistry*, *269*(18), 4427-4434.
- Zhou, W., Liesz, A., Bauer, H., Sommer, C., Lahrmann, B., Valous, G., Grabe, N., and Veltkamp, R. (2013). Postischemic brain infiltration of leukocyte subpopulations differs among murine permanent and transient focal cerebral ischemia models. *Brain Pathology*, *1*(23), 34-44.

# Appendix 1- HPLC-MS/MS Acquisition Report

## Acquisition Method Report



### Acquisition Method Info

Method Name PEP-04-09-2015-TRY.m  
 Method Path D:\MassHunter\Methods\PEP-04-09-2015-TRY.m  
 Method Description loop method.

#### Device List

HIP Sampler  
 Binary Pump  
 Column Comp.  
 DAD  
 Q-TOF

### TOF/Q-TOF Mass Spectrometer

|                      |              |                         |                  |
|----------------------|--------------|-------------------------|------------------|
| Component Name       | MS Q-TOF     | Component Model         | G6540A           |
| Ion Source           | Dual ESI     | Stop Time (min)         | No Limit/As Pump |
| Can wait for temp.   | Enable       | Fast Polarity           | N/A              |
| MS Abs. threshold    | 200          | MS Rel. threshold(%)    | 0.010            |
| MS/MS Abs. threshold | 5            | MS/MS Rel. threshold(%) | 0.010            |
| Tune File            | AutoTune.tun |                         |                  |

#### Time Segments

| Time Segment # | Start Time (min) | Diverter Valve State | Storage Mode | Ion Mode |
|----------------|------------------|----------------------|--------------|----------|
| 1              |                  | 0 MS                 | Both         | Dual ESI |

#### Time Segment 1

##### Acquisition Mode MS1

|                         |      |
|-------------------------|------|
| Min Range (m/z)         | 60   |
| Max Range (m/z)         | 1700 |
| Scan Rate (spectra/sec) | 1.00 |

##### Source Parameters

| Parameter        | Value |
|------------------|-------|
| Gas Temp (°C)    | 80    |
| Gas Flow (l/min) | 6     |
| Nebulizer (psig) | 15    |

##### Scan Segments

| Scan Seg # | Ion Polarity |
|------------|--------------|
| 1          | Positive     |

#### Scan Segment 1

##### Scan Source Parameters

| Parameter      | Value |
|----------------|-------|
| VCap           | 1500  |
| Fragmentor     | 80    |
| Skimmer1       | 45    |
| OctopoleRFPeak | 750   |

#### ReferenceMasses

|                      |          |
|----------------------|----------|
| Ref Mass Enabled     | Disabled |
| Ref Nebulizer (psig) |          |

#### Chromatograms

| Chrom Type | Label | Offset | Y-Range   |
|------------|-------|--------|-----------|
| TIC        | TIC   | 15     | 100000000 |

Name: **HiP Sampler** Model: **G1367E**

**Auxiliary**

Draw Speed 200.0 µl/min  
 Eject Speed 200.0 µl/min  
 Draw Position Offset 0.0 mm  
 Wait Time After Drawing 0.0 s  
 Sample Flush Out Factor 5.0  
 Vial/Well bottom sensing Yes

**Injection**

Injection Mode Standard injection  
 Injection Volume 10.00 µL

**High throughput**

Automatic Delay Volume Reduction No  
 Overlapped Injection  
 Enable Overlapped Injection No

**Valve Switching**

Valve Movements 0  
 Valve Switch Time 1  
 Switch Time 1 Enabled No  
 Valve Switch Time 2  
 Switch Time 2 Enabled No  
 Valve Switch Time 3  
 Switch Time 3 Enabled No  
 Valve Switch Time 4  
 Switch Time 4 Enabled No

**Stop Time**

Stoptime Mode As pump/No limit

**Post Time**

Posttime Mode Off

Name: **Binary Pump** Model: **G1312B**

Flow 0.300 ml/min  
 Use Solvent Types No  
 Low Pressure Limit 0.00 bar  
 High Pressure Limit 450.00 bar  
 Maximum Flow Gradient 100.000 ml/min<sup>2</sup>

**Stroke A**

Automatic Stroke Calculation A Yes

**Stroke B**

Automatic Stroke Calculation B Yes

**Compress A**

Compressibility Mode A Compressibility Value Set  
 Compressibility A 100 10e-6/bar

**Compress B**

Compressibility Mode B Compressibility Value Set  
 Compressibility B 115 10e-6/bar

**Stop Time**

Stoptime Mode Time set  
 Stoptime 15.00 min

**Post Time**

Posttime Mode Off

**Solvent Composition**

|   | Channel | Solvent 1 | Name 1               | Solvent 2 | Name 2              | Selected | Used | Percent |
|---|---------|-----------|----------------------|-----------|---------------------|----------|------|---------|
| 1 | A       | H2O       | WATER, 0.1% Formic   | H2O       | 50ACN49MEO H1FORMIC | Ch. 2    | Yes  | 100.0 % |
| 2 | B       |           | ACN 0.1% formic acid |           | meoh                | Ch. 1    | No   |         |

**Name:** Column Comp. **Model:** G1316A

**Valve Position** Port 1 -> 2  
**Left Temperature Control**  
**Temperature Control Mode** Temperature Set  
**Temperature** 20.00 °C  
**Enable Analysis Left Temperature**  
**Enable Analysis Left Temperature On** Yes  
**Enable Analysis Left Temperature Value** 0.80 °C  
**Right Temperature Control**  
**Right temperature Control Mode** Combined  
**Enable Analysis Right Temperature**  
**Enable Analysis Right Temperature On** Yes  
**Enable Analysis Right Temperature Value** 0.80 °C  
**Stop Time**  
**Stoptime Mode** As pump/injector  
**Post Time**  
**Posttime Mode** Off

**Name:** DAD **Model:** G1315C

**Peakwidth** >0.10 min (2.0 s response time) (2.5 Hz)  
**Slit** 4 nm  
**UV Lamp Required** No  
**Vis Lamp Required** No  
**Analog Output 1**  
**Analog 1 Zero Offset** 5 %  
**Analog 1 Attenuation** 1000 mAU  
**Analog Output 2**  
**Analog 2 Zero Offset** 5 %  
**Analog 2 Attenuation** 1000 mAU  
**Signals**  
**Prepare Mode**  
**Margin for negative Absorbance** 100 mAU  
**Autobalance**  
**Autobalance Prerun** No  
**Autobalance Postrun** No  
**Spectrum**  
**Spectrum Store** None  
**Stoptime**  
**Stoptime Mode** As pump/injector  
**Posttime**  
**Posttime Mode** Off

**Signals**

**Signal table**

|   | Use Sig. | Signal   |
|---|----------|----------|
| 1 | No       | Signal A |
| 2 | No       | Signal B |
| 3 | No       | Signal C |
| 4 | No       | Signal D |
| 5 | No       | Signal E |
| 6 | No       | Signal F |
| 7 | No       | Signal G |
| 8 | No       | Signal H |